Bid Maintains Cell Viability and Homeostasis by Regulating Mitochondrial Physiology and the DNA Damage Response.

By

Clinton Cody Bertram

Dissertation

Submitted to the Faculty of the

Graduate School of Vanderbilt University

in partial fulfillment of the requirements

for the degree of

DOCTOR OF PHILOSOPHY

in

Cell and Developmental Biology

December, 2015

Nashville, Tennessee

Approved:

Sandra S. Zinkel, M.D., Ph.D.

William P. Tansey, Ph.D.

Matthew J. Tyska, Ph.D.

James G. Patton, Ph.D.

To my parents, Ronald and Margaret, for encouraging my passion for learning

and

To my fiancée, Sarah, for her love and support

ACKNOWLEDGEMENTS

I thank my thesis advisor and mentor, Dr. Sandra Zinkel, for her guidance and her commitment to my training as a scientist. Dr. Zinkel challenged me to think critically, be persistent, and work hard to achieve my goals as a Ph.D. student. I am grateful for the opportunity she gave me to work in her lab and her commitment to my training. I also thank all of the members of my thesis dissertation committee: Dr. William Tansey, Dr. Laura Lee, Dr. James Patton, and Dr. Matthew Tyska. Their feedback provided unique perspective and insight into my project. Their input challenged me to critically evaluate myself both professionally and personally. I am thankful for the time, support, and attention that they committed to my training.

For all of their hard work, I thank my collaborators. I thank Dr. Aurelia Vergeade and her mentor Dr. L. Jackson Roberts II as well as Dr. Olivier Boutaud for sharing their expertise in lipid biology and for performing experiments for cardiolipin studies. I thank Dr. Joshua Fessel, for his assistance in experimental design, usage of his reagents and resources, and for his feedback on the project. I am also grateful to Dr. Fessel for his professional advice; it was a privilege and a pleasure to work with him. I thank Dr. Quinn Wells for his work in the identification of an association between *BID* SNPs and myocardial infarction in human patients. I thank Dr. Jay Jerome for sharing his expertise in electron microscopy and image quantitation. I also thank Dr. Yu Shyr, Dr. Huiyun Wu, and Dr. Heidi Chen for performing statistical analysis of data. Lastly, I thank Dr. Jennifer Pietenpol, Dr. Scott Hiebert, Dr. James West, and Dr. Utpal Davé for their feedback and/or sharing of reagents.

I thank all of the members of the Zinkel laboratory for their numerous contributions to my work and my graduate school experience. In particular, I would like to thank my fellow graduate students in the lab Patrice Wagner and Christi Salisbury-Ruf. Patrice and Christi both

provided valuable feedback on my project and were also great friends and colleagues. Christi also directly contributed to my research by performing and assisting in experiments that became part of my thesis project. I especially thank her for the collection and analysis of images from MPC cell lines via electron microscopy. I thank Consolate Uwimariya and Aubrey Wernick, who both expertly managed the mouse colonies for the Zinkel lab and assisted me in mouse experiments. I also thank Qiong Shi, the Zinkel lab's senior research scientist, for sharing her technical expertise and for maintaining an organized and efficient lab environment. I thank Dr. Yang Liu, a former graduate student in the Zinkel lab; his work laid the framework from which I developed my thesis project. I am sincerely grateful for the friendships I have made in the Zinkel lab. The personal and professional support from my colleagues and co-workers was vital in reaching my goals.

I thank the Department of Cell and Developmental Biology, the Vanderbilt Cell Imaging Shared Resource, and the Vanderbilt Flow Cytometry Shared Resource. In addition, this work would not have been possible without financial support from the Vanderbilt Cellular Biochemical and Molecular Sciences Training Program. This work was supported by 1R01HL088347 & 1I01BX002250 (SSZ), 2P01 GM015431 (LJR), T32 GM08554 (CCB)**,** and by support from the Parker B. Francis Foundation, Entelligence/Actelion Pharmaceuticals, and K08 HL121174 (JPF).

Finally, it is impossible to overstate the importance of my family for my success thus far. My parents provided vital support and understanding as I pursued my goals both up to, and during, my graduate career. Equally important was the role of my fiancée, Dr. Sarah Hainline, in the pursuit of my career goals. I am extremely grateful for her love, support, and understanding during the challenging pursuit of my Ph.D.

TABLE OF CONTENTS

LIST OF TABLES

LIST OF FIGURES

LIST OF ABBREVIATIONS

9-1-1	Rad9-Rad1-Hus1
ADIFAB	Acrylodated intestinal fatty acid binding protein
AIDS	Acquired immunodeficiency syndrome
AIF	Apoptosis inducing factor
ALCAT	Acyl-CoA:lysocardiolipin acyltransferase
ANT	Adenine nucleotide translocator
Apaf-1	Apoptotic protease activating factor-1
ATM	Ataxia telangiectasia mutated (ATM) and ATM and rad-3 related (ATR)
ATR	ATM and rad-3 related
ATRIP	ATR-interacting protein
Bad	Bcl-2-associated death promoter
Bak	Bcl-2 homologous antagonist killer
Bax	Bcl-2-associated X protein
Bcl-2	B cell lymphoma-2
Bcl-w	B cell lymphoma-w
Bcl-xL	B cell lymphoma extra large
BH3	Bcl-2 homology 3 domain
Bid	BH3 interacting domain death agonist
BNip3	Bcl-2/adenovirus E1B 19 kDa protein-interacting protein 3
BrdU	Bromodeoxyuridine
Caspase	Cysteine-dependent aspartate-specific protease
CAD	Caspase activated DNAse

Cdc25	Cell division cycle 25
Cdk	Cyclin dependent kinase
CDP-DAG	Cytidinediphosphate-diacylglycerol
CDS	CDP-DAG synthase
CFU-GM	Colony Forming Unit-Granulocyte, Monocyte
Chk1/2	Checkpoint kinase 1 and 2
CK1/2	Casein kinase 1 and 2
CL	Cardiolipin
CMML	Chronic myelomonocytic leukemia
CS	Cardiolipin synthase
CypD	Cyclophilin D
DDR	DNA damage response
DISC	Death inducing signaling complex
DLCL	Dilysocardiolipin
DOPC	Dioleoylphosphatidylcholine
Drp1	Dynamin-related protein 1
DSB	Double strand break
ELISA	Enzyme Linked Immunosorbent Assay
Erk1/2	Extracellular Signal-Regulated Kinase 1/2
ETC	Electron transport chain
FasL	Fas ligand
FCCP	Carbonyl cyanide 4-(trifluoromethoxy)phenylhydrazone
H2AX	H2A histone family, member X

HA	Hemagglutinin
HIV	Human immunodeficiency virus
HtrA2/Omi	High-temperature-requirement protein A2
HU	Hydroxyurea
IAP	Inhibitor of apoptosis
IAPP	Islet amyloid polypeptide
IL-3	Interleukin-3
IMM	Inner Mitochondrial Membrane;
IMS	Inter-membrane space
iPLA$_2\gamma$	Calcium-independent phospholipase A$_2\gamma$
L_4CL	Tetralinoleoyl cardiolipin
LC/ESI/MS/MS	Liquid Chromatography-Electrospray Ionization Tandem Mass Spectrometry
LO_3CL	Linoleoyl-trioleoylcardiolipin
M_4CL	Tetramyristoylcardiolipin
MBD	Membrane binding domain
Mcl-1	Myeloid cell leukemia 1
Mdc1	Mediator of DNA damage checkpoint protein 1
MEF	Mouse Embryonic Fibroblast
Mfn1	Mitofusin-1
MLCL	Monolyso-cardiolipin
MLCLAT	MLCL acyltransferase
MLKL	Mixed lineage kinase domain-like

MOMP	Mitochondrial outer membrane permeabilization
MPCs	Myeloid Progenitor Cells;
MPTP	Mitochondrial permeability transition pore
Mre11	Meiotic recombination 11 homolog
MRN	Mre11-Rad50-Nbs1
MS	Multiple sclerosis
Mtch2	Mitochondrial carrier homolog 2
mtCK	Mitochondrial creatine kinase
NAO	Nonyl acridine orange
Nbs1	Nijmegen breakage syndrome
NDPK	Nucleoside diphosphate kinase
NOD	Nucleotide-binding and oligomerization domain
NMDA	N-Methyl-D-aspartic acid
OCR	Oxygen Consumption Rate
OMM	Outer mitochondrial membrane
PA	Phosphatidic acid
PCD	Programmed cell death
PG	Phosphatidylglycerol
PG-P	Phosphatidylglycerol phosphate
PGPP	PG-P phosphatase
PGPS	Phosphatidylglycerol phosphate synthase (PGPP)
PI	Propidium iodide;
PiC	Mitochondrial phosphate carrier

PIDD	p53 induced death domain protein
PIKK	Phosphatidylinositol 3-kinase-like protein kinase
Puma	p53 upregulated modulator of apoptosis
RIPK	Receptor interacting protein kinase
RNAi	Ribonucleic acid interference
ROS	Reactive oxygen Species
RPA	Replication protein A
siRNA	Small interfering RNA
Smac/Diablo	Second mitochondria-derived activator of caspases/direct inhibitor of apoptosis (IAP)-binding protein with low pI
SOD1	Superoxide dismutase 1
SSB	Single strand break
ssDNA	Single stranded DNA
Stat5	Signal transducer and activator of transcription 5;
tBID	Truncated Bid
TCA cycle	Tricarboxylic acid cycle
TEM	Transmission electron microscopy
TNF-α	Tumor necrosis factor-α
TNFR1	TNF receptor 1
TOPBP1	Topoisomerase-binding protein 1
TRAIL	TNF-related apoptosis-inducing ligand
VDAC	Voltage dependent anion channel

CHAPTER I

INTRODUCTION

Apoptotic cell death is regulated by members of the Bcl-2 family through modulation of mitochondrial structure and physiology. However, emerging evidence suggests that certain members of the Bcl-2 family can regulate mitochondrial homeostasis in non-apoptotic conditions. Bid, a pro-apoptotic BH3-only member of the Bcl-2 family, has been extensively studied in the context of apoptosis and cellular stress. However, it is undetermined if Bid can impact mitochondria in non-apoptotic conditions, despite evidence that Bid has other non-canonical functions. Indeed, in contrast to its canonical pro-apoptotic function, Bid can promote cell survival by facilitating execution of the DNA damage response during replicative stress (1-5). In the studies presented here, I have used Bid deficient cell lines and mice both to further characterize the role of Bid's function in the DNA damage response and to determine how Bid regulates mitochondria in non-apoptotic contexts. I provide evidence that the localization and phosphorylation of Bid is controlled by the DNA damage to regulate its function during replicative stress. I also reveal a novel pro-survival function for Bid that is distinct from its apoptotic function in which Bid maintains normal mitochondrial structure. Given the dependence of the heart on mitochondrial function, I also investigated the effect of Bid deficiency on the mouse heart during cardiac stress *in vivo* and explored the association between Bid single nucleotide polymorphisms and cardiac diseases in human patients. These studies demonstrate that Bid is cardioprotective during acute cardiac stress and that Bid SNPs are associated with myocardial infarction in humans.

The Bcl-2 Family and Regulation of Programmed Cell Death

Cell Death and Apoptosis

Programmed cell death (PCD) is a critical cellular process that is functionally conserved in all metazoans (6). During embryonic development, PCD is essential in regulating proper tissue and organ architecture by the timely and precise removal of specific cells or cell groups (7). PCD is also required for maintaining cellular homeostasis by elimination of old, damaged, or superfluous cells (8). Furthermore, PCD is critical for eliminating cells that are potentially harmful, such as those infected by a pathogen or showing signs of malignant transformation (8).

Aberrant regulation of PCD has severe biological consequences, highlighting its critical role in maintaining normal physiology. Indeed, many neurodegenerative diseases including Parkinson's disease, Huntington's disease, and Alzheimer's disease are characterized by aberrant cell death of neurons (9-11). Apoptotic cell death is essential for maintaining a normal immune response through multiple mechanisms such as by facilitating T-cell selection, restraining the clonal expansion of immune cells, and by inducing cell death in infected or transformed cells (9). Dysregulation of apoptosis in this context can contribute to autoimmune disorders such as systemic lupus erythematosus (12, 13), rheumatoid arthritis (14), and diabetes mellitus (15). Furthermore, acquired immunodeficiency syndrome (AIDS) is a consequence of T-cell death mediated by human immunodeficiency virus (HIV) infection (16). PCD also contributes to ischemic injury such as during stroke and myocardial infarction (17, 18). As one of the hallmarks of cancer, apoptosis also plays a central role in cancer development and resistance to anti-cancer therapies (19). Table 1-1 highlights multiple pathologies, the type of cell death disruption, and the relevant effects of cell death dysregulation upon disease development/progression. The

contribution of PCD to these and other pathologies makes cell death inhibitors and activators high priority targets for drug development and therapy.

Table 1-1. Pathologies associated with aberrant or deficient cell death.

Pathology	**Cell Death Disruption**	**Effect**
Cancer	Decrease	Resistance of transformed cells to removal by apoptosis (19)
Systemic Lupus Erythematosus	Decrease	Resistance of immune cells to Fas induced apoptosis (12, 13)
Rheumatoid Arthritis	Decrease	Resistance of pro-inflammatory cells to apoptosis (14)
Diabetes mellitus	Increase	Apoptosis of pancreatic β-cells mediated by autoimmunity and other stimuli (e.g. IAPP deposition, cytokines, glucose, and others) (15)
Multiple sclerosis	Decrease/ Increase	Resistance of autoreactive T-cells to apoptosis/Apoptotic cell death of MS lesions (20)
Parkinson's Disease	Increase	Aberrant cell death of neurons induced by α-synuclein (9)
Alzheimer's Disease	Increase	Aberrant apoptosis of neurons induced by amyloid β (10)
Huntington's Disease	Increase	Mutant Huntingtin/BNip3 induced apoptosis of neurons (11)
Amyotrophic lateral sclerosis	Increase	Mutant SOD1 mediated mitochondrial damage and cell death (21)
Status epilepticus	Increase	Seizure induced cell death of neurons (22)
Retinitis pigmentosa	Increase	Aberrant cell death of photoreceptors (23)
AIDS	Increase	HIV induced apoptosis of $CD4^+$ T cells (16)
Liver Disease	Increase	Hepatocyte cell death induced by viral infection, drug/alcohol exposure, autoimmunity, etc. (24)
Ischemia/ reperfusion injury	Increase	Necrotic and apoptotic cell death induced by cerebral or myocardial ischemia/reperfusion (17, 18)

The two most well-characterized forms of PCD are programmed necrosis (or necroptosis) and apoptosis, though other pathways such as autophagic death also exist (25, 26). Although both apoptosis and necrosis ultimately lead to cell death, each is characterized by a distinct morphology, signaling pathway, and progression. Programmed necrosis is characterized by cellular and nuclear swelling, loss of plasma membrane integrity, nonspecific fragmentation of chromosomal DNA, vacuolization of the cytoplasm, and is dependent on both receptor-interacting protein kinases (RIPK) and mixed lineage kinase domain-like protein (MLKL) (27, 28). In contrast, apoptosis is characterized by cellular and nuclear condensation, ordered fragmentation of chromosomal DNA, dependence on caspase activation, and a morphological change referred to as blebbing, in which apoptotic cells fragment into small, membrane bound apoptotic bodies that are later engulfed by phagocytes (27, 29).

To avoid aberrant activation of apoptosis, apoptotic signaling is only initiated upon receiving specific signals from either extrinsic or intrinsic sources. The extrinsic apoptotic pathway is mediated by extracellular death ligands such as tumor necrosis factor-α (TNF-α), Fas ligand (FasL), or TNF-related apoptosis-inducing ligand (TRAIL). Death ligands, secreted by immune cells or neighboring cells during stress, bind to their corresponding death receptors at the plasma membrane of target cells, TNF receptor 1 (TNFR1), Fas, or death receptor 4/5, respectively (6). The cytoplasmic tails of activated death receptors promote the formation of a multi-protein complex called the death inducing signaling complex (DISC), which serves as an activation platform for Caspase-8. Following death receptor activation, extrinsic apoptosis occurs using one of two different signaling pathways depending on cell type (30, 31). Type I cells such as thymocytes undergo apoptosis through a predominantly mitochondria independent manner. In type I cells, large amounts of Caspase-8 are rapidly activated which directly cleaves and

activates Caspase-3 to induce cell death (30, 31). In contrast, type II cells such as hepatocytes are highly dependent on mitochondrial amplification of apoptosis. In type II cells, Caspase-8 activation is less efficient than in type I cells (30, 31). Mitochondrial amplification is achieved through Caspase-8 mediated cleavage and activation of Bid, a potent Bcl-2 homology 3 (BH3)-only protein of the B cell lymphoma-2 (Bcl-2) family (31-33). The cleaved form of Bid, truncated Bid (tBid), mediates mitochondrial amplification of extrinsic apoptosis through activation of the pro-apoptotic Bcl-2 family members, Bcl-2 associated X (Bax) and Bcl-2 homologous antagonist killer (Bak), which in turn mediate mitochondrial outer membrane permeabilization (MOMP) (34). A diagram of the extrinsic apoptotic pathway is presented in Figure 1-1.

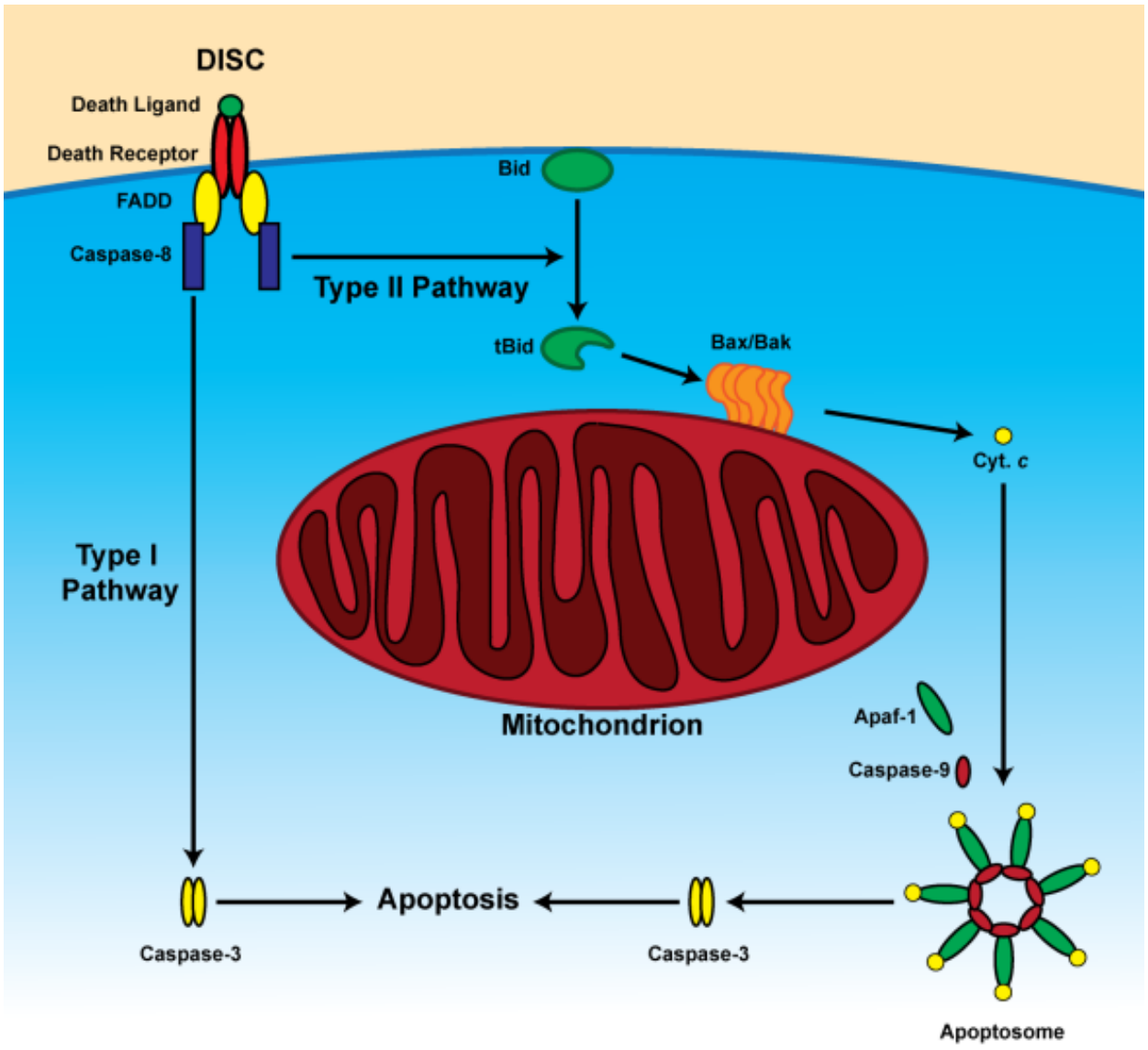

Figure 1-1: The extrinsic apoptotic pathway. Extrinsic apoptosis is activated through binding between a death ligand (Fas, TNF-α, TRAIL) to plasma membrane death receptors (TNFR1, Fas, death receptor 4/5). The cytoplasmic tails of death receptors then recruit Fas-associated protein with death domain (FADD) and procaspase 8 to form the death inducing signaling complex (DISC). The DISC activates Caspase-8 which can directly cleave Caspase-3 in type I cells to induce apoptosis. In type II cells, mitochondrial amplification of apoptotic signaling is required to induce apoptosis. Mitochondrial amplification is achieved through the Caspase-8 mediated cleavage and activation of BH3-only Bid into truncated Bid (tBid), a potent apoptotic activator. tBid activates Bax/Bak mediated MOMP, resulting in Cytochrome *c* release, apoptosome formation, and Caspase-9 and -3 activation. Caspase-3 can also cleave additional Bid molecules, thus resulting in a feed forward amplification loop of apoptotic signaling

Apoptosis can also occur in response to intrinsic apoptotic stimuli such as DNA damage (35), endoplasmic reticulum stress (36), growth factor/cytokine withdrawal (37), and oxidative stress (38). The initiation of intrinsic apoptosis occurs through the activation of a sensor of cellular stress, typically a BH3-only protein (discussed in detail below), which can vary depending on the type of stress (39). Following activation, BH3-only proteins initiate apoptosis by activating the pro-apoptotic Bcl-2 family members Bcl-2 associated X (Bax) and Bcl-2 homologous antagonist killer (Bak). BH3-only proteins activate Bax and Bak either by directly binding Bax/Bak or by binding and inhibiting the anti-apoptotic Bcl-2 family members, such as Bcl-2, Bcl-xL, and Mcl-1. Following activation, Bax and Bak form hetero-oligomers in the OMM that are responsible for mitochondrial outer membrane permeabilization (MOMP).

The mitochondria are essential to the execution of intrinsic apoptosis. MOMP is an irreversible and essential step in the execution of the intrinsic apoptotic pathway which results in the cytosolic release of multiple pro-apoptotic factors from the mitochondrial inter-membrane space (IMS). In particular, the cytosolic release of Cytochrome *c* is important for activation of apoptosis (46). Once released into the cytosol by MOMP, Cytochrome *c* interacts with apoptotic protease activating factor-1 (Apaf-1) and Caspase-9 to form a large, disc shaped multi-protein complex known as the apoptosome. The apoptosome functions as a Caspase-9 activation platform by facilitating the proximity induced dimerization and activation of Caspase-9 (6). Active Caspase-9 cleaves and activates the effector caspase, Caspase-3, which is responsible for the downstream execution of apoptosis. In addition to Cytochrome *c*, second mitochondria-derived activator of caspases/direct inhibitor of apoptosis (IAP)-binding protein with low pI (Smac/Diablo) and high-temperature-requirement protein A2 (HtrA2/Omi) are released from the mitochondria during MOMP to promote apoptosis by binding and preventing the inhibitor of

apoptosis proteins (IAPs) from interacting with and inhibiting caspases (43, 47, 48). Furthermore, apoptosis inducing factor (AIF) and endonuclease G are released from the mitochondria by MOMP and then translocate to the nucleus where they induce fragmentation of genomic DNA and condensation of chromatin (40-42, 49, 50). DNA fragmentation is further facilitated by caspase activated DNAse (CAD) (51). Altogether, these mitochondrial proteins facilitate execution of the intrinsic apoptotic pathway as shown in Figure 1-2.

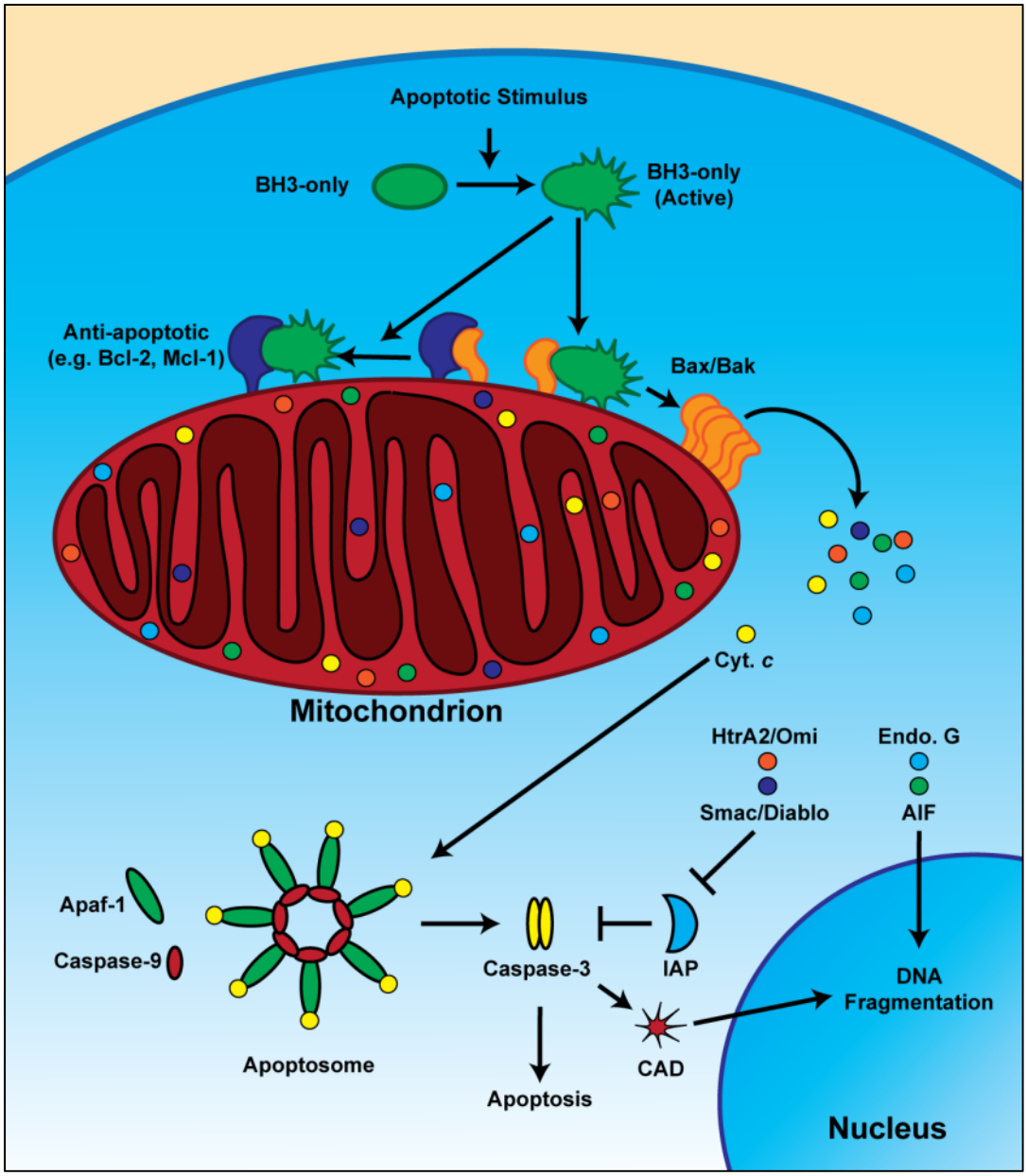

Figure 1-2: The intrinsic apoptotic pathway. BH3-only proteins are upstream sensors of apoptotic stimuli that, upon activation, associate with anti-apoptotic Bcl-2 family members (Bcl-2, Bcl-xL, Mcl-1, etc.) or pro-apoptotic Bax and Bak. BH3 proteins then relieve inhibition of Bax/Bak by binding to anti-apoptotic Bcl-2 proteins and can also directly interact with Bax/Bak to promote their activation and hetero-oligomerization in the OMM. Activated Bax/Bak form a pore that releases Cytochrome *c* (Cyt. *c*), HtrA2/Omi, Smac/Diablo, Endonuclease G (Endo. G), and AIF from the IMS. Cytochrome *c* interacts with Apaf-1 and Procaspase-9 to form the apoptosome resulting in activation of multiple caspases including Caspase-3 which is a major driver of the apoptotic program. HtrA2/Omi and Smac/Diablo inhibit IAPs, ubiquitin ligases that degrade active Caspase-3. Endo.G and AIF as well as the cytoplasmic caspase activated DNAse (CAD) translocate to the nucleus where they regulate chromatin condensation and genomic DNA fragmentation.

.

In addition to Bax/Bak mediated MOMP, the mitochondrial permeability transition pore (MPTP) has also been implicated in mitochondrial apoptosis and necroptosis signaling. Opening of the MPTP leads to loss of membrane potential, inhibition of ATP production, increased reactive oxygen species (ROS) production, and influx of water into the mitochondrial matrix, thus resulting in swelling and rupture of the mitochondria. This mitochondrial damage results in release of pro-apoptotic factors that promotes apoptosis (52). Though separate from Bax/Bak mediated MOMP, the MPTP can, at least in some contexts, also be regulated by Bcl-2 family members including Bax (53-55) and Bcl-2 (56). The MPTP is a multi-protein complex that is localized at mitochondrial contact sites, microdomains where the inner mitochondrial membrane and outer mitochondrial membrane interact (57). The complete molecular composition of the MPTP is unclear but several key components have been identified including adenine nucleotide translocase (ANT), mitochondrial phosphate carrier (PiC), F_OF_1-ATP synthase, voltage dependent anion channel (VDAC), and cyclophilin D (CypD) (58). Opening of the MPTP occurs in response to stimuli such as oxidative stress or high Ca^{2+} concentrations through a mechanism that is not yet fully understood. While the opening of the MPTP can induce cell death, its contribution to apoptosis remains controversial since most cases of apoptotic cell death do not require the MPTP and do not display mitochondrial swelling such as that seen during MPTP opening (59).

While the mitochondria and Bcl-2 family are essential regulators of the upstream events in apoptosis, the downstream execution of apoptosis is primarily mediated by caspases, a family of intracellular cysteine proteases (Cysteine-dependent aspartate-specific proteases) (Fig 1-3A) (60). Although caspases have functions in multiple cellular processes, they are essential for the execution of apoptotic cell death. Apoptotic caspases are zymogens which can be classified as

either initiator caspases or as effector caspases. Following an apoptotic stimulus, initiator caspases such as Caspase-8 and Caspase-9 are recruited to multi-protein complexes known as activation platforms (e.g. the DISC or apoptosome) which facilitate activation of initiator caspases by proximity-induced dimerization (61). Active initiator caspases cleave and activate numerous downstream pro-apoptotic substrates including effector caspases such as Caspase-3 and Caspase-7 (Fig. 1-3B) (62). In contrast, effector caspases exist as constitutive dimers that are activated by their cleavage in an inter-subunit linker sequence (61). Upon cleavage by initiator caspases, effector caspase dimers undergo conformational changes both in the active site loops and the substrate binding groove leading to full activation (Fig. 1-3C). During apoptosis, the caspase cleavage cascade can result in the cleavage of hundreds of different substrates, which can have both gain-of-function and loss-of-function effects on these proteins and their related signaling pathways, resulting in the complex morphological and physiological changes observed during apoptosis (62, 63).

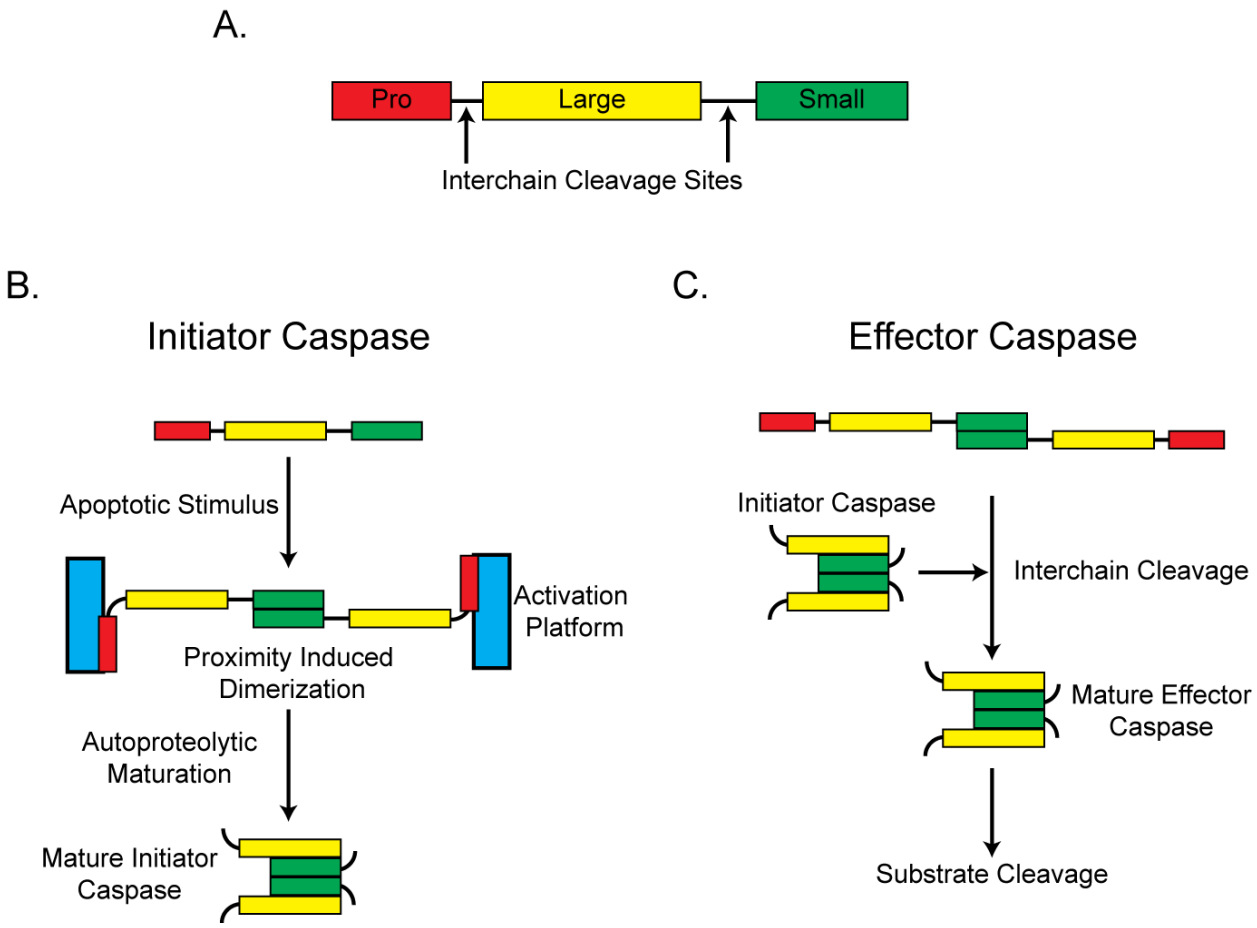

Figure 1-3. Caspase structure and activation mechanisms. A) Caspases are composed of three separate subunits, a pro-domain, a large subunit, and a small subunit. Each subunit is separated by a linker region, each of which contains an inter-chain caspase cleavage site that is cleaved during caspase maturation. B) Initiator caspases exist as monomers in resting cells. During an apoptotic stimulus, activation platforms such as the DISC recruit initiator caspases through their pro-domain. Here the initiator caspases undergo proximity induced dimerization, resulting in activation of protease activity. Autoproteolytic cleavage of the inter-chain linkers results in initiator caspase maturation. C) Effector caspases are constitutive dimers maintained in an inactive state by the inter-subunit linker between the large and small subunits. Activation of effector caspases is mediated by initiator caspases and other upstream proteases such as granzymes. Upon cleavage of the inter-chain linkers, effector caspases undergo a conformational change that activates the catalytic site, allowing cleavage of downstream substrates and effectors (Figure adapted from (60)).

The Bcl-2 Family

Early studies investigating cell fate in *C. elegans* revealed that specific cells always die during development (64). To determine what genes were responsible for regulating this precisely controlled cell death program, H. Robert Horvitz employed a forward genetic screen which identified two genes, *ced-3* and *ced-4,* which are essential for cell death in *C. elegans* (65). While *ced-3* is an ortholog of mammalian caspases, *ced-4* is an ortholog of mammalian Apaf-1. In addition, *ced-9*, an ortholog of mammalian Bcl-2, was later identified and characterized as an inhibitor of cell death (66) while *egl-1*, an ortholog of BH3-only Bcl-2 family members, was identified as a pro-apoptotic gene (67). The identification and characterization of these genes revealed a pathway regulating cell death in *C. elegans* in which EGL-1 blocks CED-9 mediated inhibition of CED-4, leading to activation of CED-3 by CED-4 and subsequent activation of cell death (Fig. 1-4) (6). Thus, the Bcl-2 family is evolutionarily and functionally conserved for the regulation of programmed cell death.

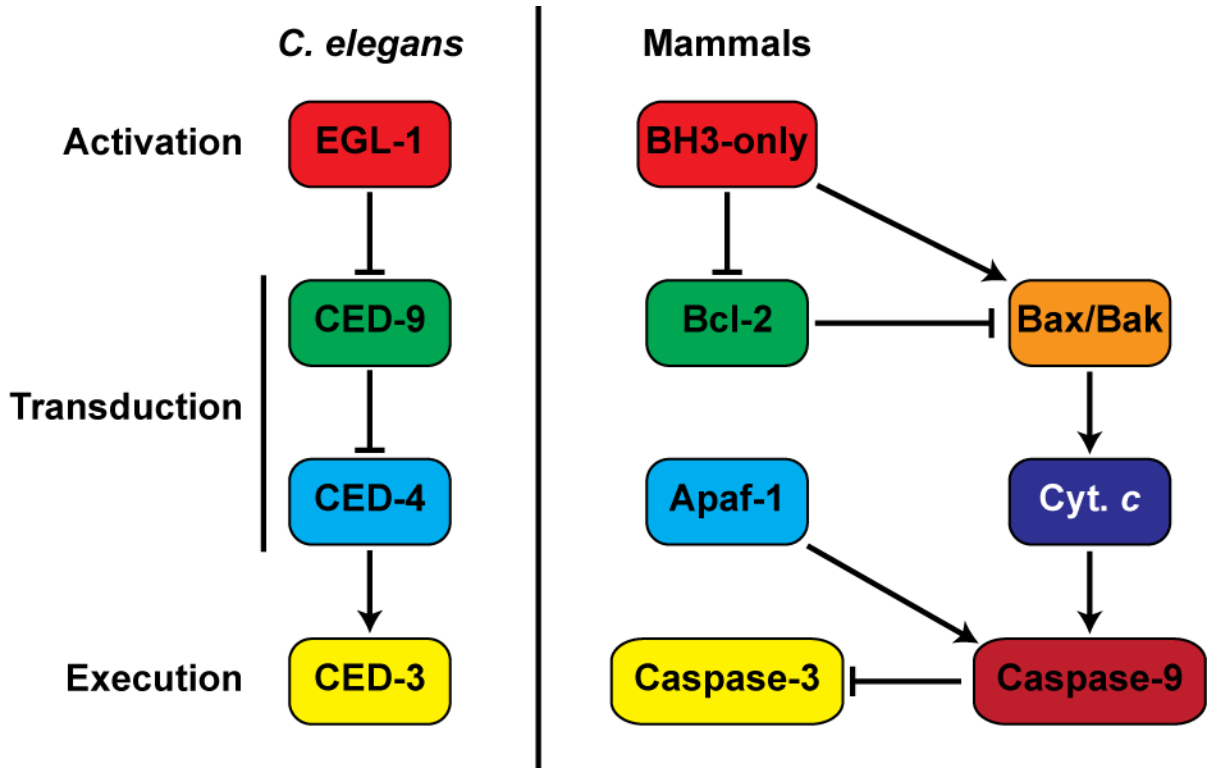

Figure 1-4. Apoptosis regulation in *C. elegans* and mammals. Similar to mammalian cell death regulation, the *C. elegans* BH3-only homolog EGL-1 promotes activation of the apoptotic pathway following an apoptotic stimulus through direct interaction with the Bcl-2 homolog CED-9. However, in contrast to mammalian apoptosis signaling, CED-9 directly binds to CED-4, the *C. elegans* Apaf-1 homolog. This interaction inhibits the ability of CED-4 to associate with and activate the effector caspase homolog CED-3. Activated Egl-1 relieves this inhibition by displacement of CED-4 from CED-9, thus leading to CED-3 activation and execution of apoptotic cell death. Although these genes are evolutionarily conserved between species, one significant difference is the lack of requirement for mitochondrial permeabilization in *C. elegans* for apoptosis execution. Thus, *C. elegans* does not require Cytochrome *c* release and formation of an apoptosome for caspase activation and cell death (Figure adapted from (6)).

In parallel to the studies performed in *C. elegans*, Tsujimoto et al. identified Bcl-2, the founding member of the Bcl-2 family, at the chromosomal breakpoint of the t(14:18) chromosomal translocation in B-cell leukemia and follicular lymphoma cells (68). The t(14:18) translocation resulted in production of a hybrid immunoglobulin heavy chain/Bcl-2 transcript that was proposed to alter expression of Bcl-2 (69). It was later confirmed that Bcl-2 mRNA expression was significantly altered in B-cell lymphoma cells harboring the t(14:18) translocation (70). The t(14:18) transduction in Bcl-2 was later found to facilitate transformation of Eμ-Myc B-cell progenitors and to protect hematopoietic progenitors from cytokine withdrawal induced cell death *in vitro* (71). Bcl-2's pro-survival effect was later confirmed *in vivo* using a transgenic mouse line harboring the t(14:18) transgene (72). The t(14:18) transgenic mice developed a pathology that was similar to follicular lymphoma and conferred a survival advantage on splenocytes isolated from these mice, suggesting that Bcl-2 promoted transformation via promoting cell survival (72). In 1990, Hockenbery et al. determined that Bcl-2 was a mitochondrial membrane protein that blocked apoptotic death, indicating that it facilitated transformation by inhibiting apoptosis (73). In 1993, Bax, a pro-apoptotic protein sharing significant homology with Bcl-2 was identified as a Bcl-2 interacting partner (74). These studies identified a novel protein family that regulated apoptotic cell death through interacting at the mitochondrial membrane.

The Bcl-2 family encompasses numerous proteins with both anti- and pro-apoptotic activity and share homology to the founding member, Bcl-2, in at least one of four conserved domains known as Bcl-2 homology (BH) domains. The Bcl-2 family can be subdivided into the multi-domain, anti-apoptotic members (e.g. Bcl-2, Bcl-xL, Mcl-1, and Bcl-w), the multi-domain, pro-apoptotic members (e.g. Bax and Bak), and the pro-apoptotic BH3-only proteins (e.g. Bid,

Bim, Bad, Puma, and Noxa) (Fig. 1-5) (39). Unlike multi-domain proteins, the BH3-only proteins share only the BH3 domain with other Bcl-2 family members, which is essential for the pro-apoptotic function of these proteins (34). To avoid aberrant apoptotic activation, the Bcl-2 family is regulated through a variety of mechanisms including sub-cellular localization, post translational modification, protein-protein interactions, and modulation of expression levels (39).

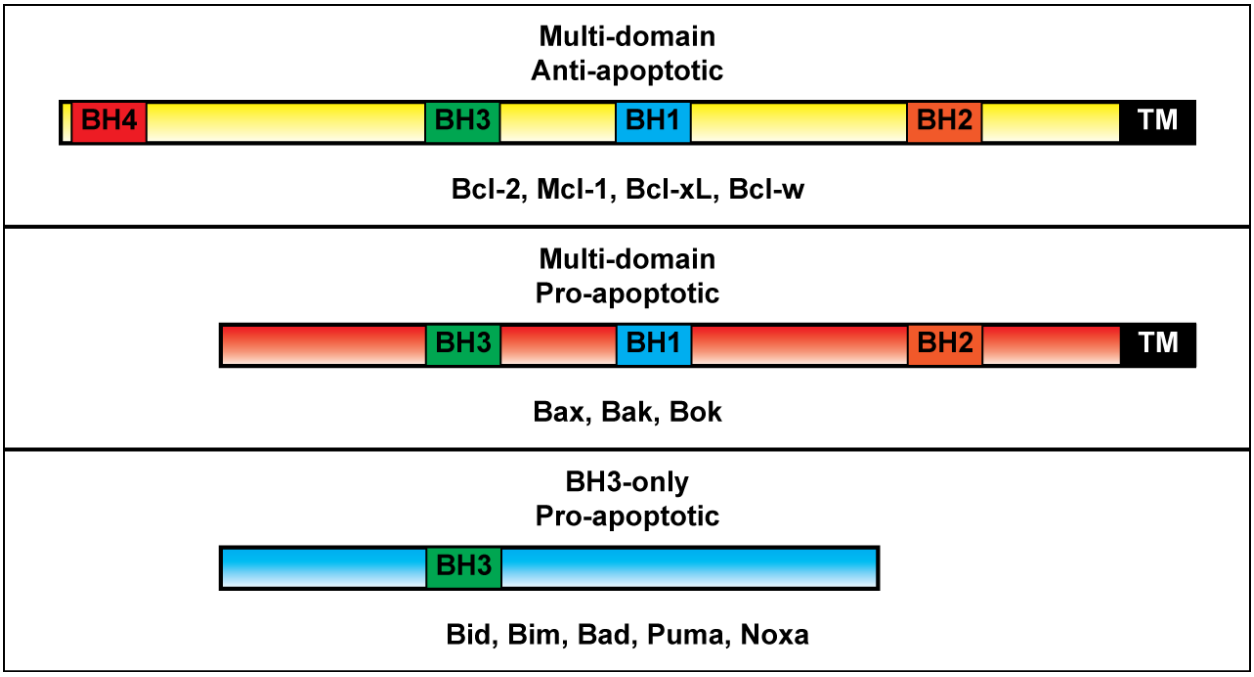

Figure 1-5. Bcl-2 family classification by domain homology and apoptotic function. The Bcl-2 family is subdivided into three different groups depending on their apoptotic function and the number of Bcl-2 homology (BH) domains. Multi-domain, anti-apoptotic Bcl-2 family members generally contain BH domains 1-4 and a c-terminal transmembrane domain. However, some multi-domain, anti-apoptotic members such as Mcl-1 do not include a BH4 domain. Multi-domain, pro-apoptotic Bcl-2 family members harbor BH domains 1-3 and a transmembrane domain. In contrast, BH3-only members of the Bcl-2 family contain the BH3 domain alone, which is critical for their pro-apoptotic function. Some BH3-only proteins, such as Bim, also contain transmembrane domains. BH domains form alpha helical structures which are critical for protein-protein interactions. The BH3 domain of BH3-only proteins binds multi-domain Bcl-2 family proteins through interacting with a hydrophobic cleft formed by the BH1-3 domains (Figure adapted from (39))

The first level of regulation in apoptosis occurs through modulating the activity of BH3-only proteins which function as upstream sensors that selectively respond to cellular stresses or apoptotic stimuli. Different BH3-only proteins display specialization, responding preferentially to specific types of stimuli. Table 1-2 lists several cell death stimuli and their associated BH3-only proteins. Although there is some overlap in the function of BH3-only proteins, the activation of apoptosis is frequently context and tissue specific, thus the contribution of a particular BH3-only protein to apoptosis can vary between different tissues. BH3-only proteins also demonstrate unique mechanisms of activation. For example, Bid is activated through cleavage by active Caspase-8 (32, 33). The pro-apoptotic activity of Bad is primarily regulated through modulating its phosphorylation, which promotes its association with 14-3-3 proteins that inhibit its interaction with other Bcl-2 family members (75, 76). Bim is regulated by transcription, phosphorylation, ubiquitin mediated degradation, and is sequestered to the microtubule associated dynein motor complex through binding to cytoplasmic dynein light chain (77-79). Both Puma and Noxa are regulated by p53 mediated transcription in response to numerous types of cellular stress (80-83). Cytokine dependent phosphorylation has also been shown to regulate Puma stability by promoting ubiquitin mediated degradation (84).

Table 1-2. BH3-only proteins and associated cell death stimuli.

BH3-only protein	Cell death stimulus	Mechanisms of regulation	References
Bid	Death receptor signaling	Cleavage, phosphorylation, and localization	(32, 33, 85, 86)
Bad	Growth factor and cytokine withdrawal	Phosphorylation, protein-protein interaction	(75, 76)
Bim	Cell detachment, growth factor withdrawal, and cytokine withdrawal	Phosphorylation, transcription, degradation	(77-79)
Puma	DNA damage, growth factor withdrawal, and cytokine withdrawal	Transcription, phosphorylation, degradation	(80, 81, 84)
Noxa	DNA damage, hypoxia, cytokine withdrawal	Transcription	(87-89)

The primary function of the Bcl-2 family in apoptosis is to regulate MOMP which is directly regulated by the activation of Bax/Bak on the OMM (39). Thus, Bax and Bak are the essential gatekeepers of apoptotic signaling and their activation must be regulated to maintain cell viability. Though Bax and Bak are similar in structure and function, Bak and Bax display differences in their mechanism of activation. For example, Bak is an integral membrane protein constitutively localized to the OMM while Bax exists as a soluble monomer either in the cytosol or peripherally associated with the OMM. During apoptosis, active BH3 only proteins bind Bax and induce conformational changes that facilitate its insertion into the OMM (90). Upon activation by BH3-only proteins, Bax and Bak hetero-oligomerize in the OMM and form a pore that permeabilizes the OMM and allows the release of Cytochrome *c* from the intermembrane space. While Bax and Bak have several specific functions, they are functionally redundant for pore formation and apoptosis in most cases (91). However, cells deficient for both Bax and Bak

are completely resistant to apoptotic cell death, indicating that the presence of either Bax or Bak is necessary for apoptosis.

The anti-apoptotic Bcl-2 family members confer an additional layer of regulation to prevent aberrant activation of Bax/Bak. Anti-apoptotic Bcl-2 family proteins prevent Bax/Bak activation through both direct and indirect mechanisms. By directly binding to Bax/Bak, anti-apoptotic proteins inhibit the oligomerization of Bax/Bak and thus block MOMP and apoptosis (90). In addition, the anti-apoptotic proteins can bind and sequester BH3-only proteins, preventing them from activating Bax/Bak. This interaction has two consequences. While the anti-apoptotic proteins inhibit BH3-only proteins, the BH3-only proteins also inhibit the ability of anti-apoptotic proteins to bind and sequester Bax/Bak. This interaction, referred to as mutual sequestration, thus has a two-fold effect of blocking activation of Bax/Bak but also sensitizes Bax/Bak for activation by additional BH3-only proteins. The consequence of this phenomenon is that the relative concentration and the interactions of pro-and anti-apoptotic Bcl-2 family members contributes to the sensitivity of mitochondria to MOMP and apoptosis (92). However, it is important to keep in mind that the concentration of Bcl-2 family members is not the only factor in determining whether a cell will undergo apoptosis since Bcl-2 family members are also dynamically regulated through other mechanisms as described above.

The interactions between Bcl-2 family proteins are central to their role in regulating MOMP and apoptosis. These interactions are largely mediated by the alpha helical BH domains. Specifically, a hydrophobic cleft formed by the BH1, BH2, and BH3 domains of multi-domain Bcl-2 family members binds the BH3 domain of binding partners (39). Importantly, Bcl-2 family proteins display specificity in their affinity for one another. This difference in affinity determines how apoptosis is regulated by the Bcl-2 family and is particularly critical for how BH3-only

proteins regulate the activation of Bax/Bak. The specificities of the BH3-only proteins to other Bcl-2 family members led to their classification into subgroups designated as activators or sensitizers (93, 94). Activator BH3-only proteins Bid, Bim, and Puma are unique in that they directly interact with and activate Bax/Bak and can also bind and inhibit all of the anti-apoptotic Bcl-2 family proteins (e.g. Bcl-2, Bcl-w, Bcl-xL, and Mcl-1) (93, 95-97). In contrast, sensitizer BH3-only proteins, such as Bad and Noxa, are unable to directly induce Bax/Bak activation (93, 95, 98). Instead, sensitizers promote apoptosis through the inhibition of anti-apoptotic proteins, thus decreasing the threshold for activation of Bax/Bak by activator BH3-only proteins (Fig. 1-6A). Sensitizer BH3-only proteins also show specificity to anti-apoptotic proteins. For example, Bad is only able to bind and inhibit the anti-apoptotic proteins Bcl-2, Bcl-w, and Bcl-xL but it cannot bind to Mcl-1 or to Bax/Bak (95). In contrast, Noxa is only able to bind to Mcl-1 (12, 98) (Fig 1-6B). While sensitizer BH3-only proteins are limited to acting only as sensitizers, activators can also function as sensitizers through binding anti-apoptotic proteins (90). Altogether, the nature of activator BH3-only proteins suggests that they are required for activation of Bax/Bak-mediated MOMP. Consistent with this hypothesis, deletion of Bid, Bim, and Puma prevents the induction of apoptosis to diverse apoptotic stimuli and results in developmental defects similar to mice with genetic deletion of Bax and Bak (91, 99). Thus, activator BH3-only proteins are required for activation of Bax/Bak mediated apoptosis.

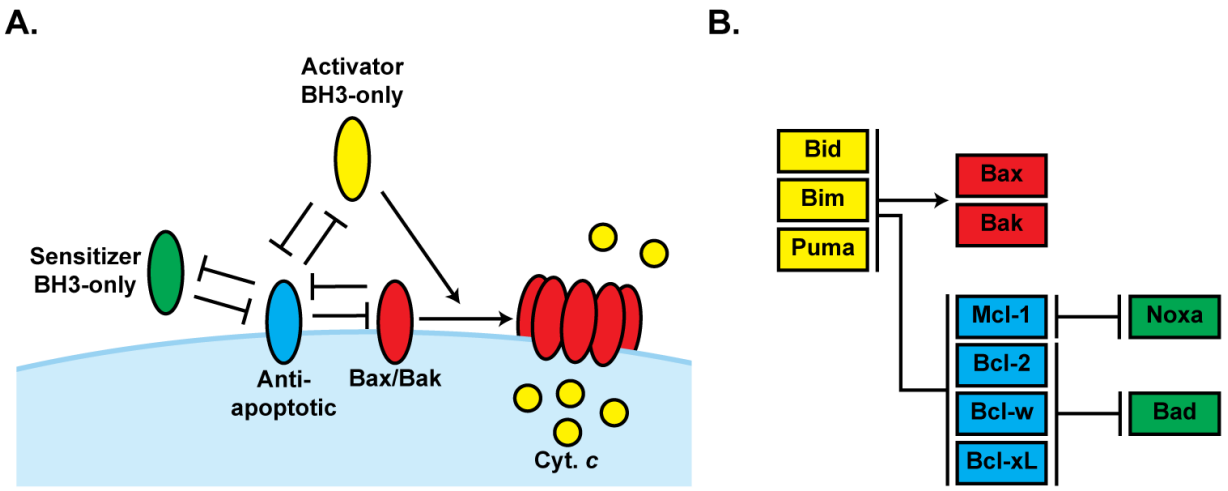

Figure 1-6. Mechanism of apoptotic regulation by activator and sensitizer BH3-only proteins. A) BH3-only proteins are functionally classified based on their affinity for different Bcl-2 family members. Sensitizer BH3-only proteins are limited to interactions with anti-apoptotic Bcl-2 proteins, thus promoting apoptosis by relieving inhibition of Bax/Bak by anti-apoptotic proteins. Activator BH3-only proteins can interact with both the anti-apoptotic Bcl-2 family members and Bax/Bak, thus they promote Bax/Bak activation through direct activation as well as sensitization. The interactions between pro-apoptotic and anti-apoptotic Bcl-2 family members results in mutual inhibition since it sequesters both interacting partners from binding other molecules. Mutual sequestration in the Bcl-2 family results in a highly dynamic system that determines sensitivity to Bax/Bak activation, MOMP, and Cytochrome *c* release. Thus, apoptotic activation is dependent on an apoptotic threshold that is determined by the relative concentrations of pro-and anti-apoptotic proteins. B) Activator BH3-only proteins (Yellow) Bid, Bim, and Puma can bind to all anti-apoptotic Bcl-2 family members (Blue) as well as to both Bax and Bak (Red). In contrast, sensitizer BH3-only proteins (Green) such as Bad and Noxa are limited to binding specific anti-apoptotic members. Noxa binds to Mcl-1 alone while Bad binds to Bcl-2, Bcl-w, and Bcl-xL but not to Mcl-1 (Figure adapted from (100))

Accumulating evidence indicates that Bcl-2 family members have numerous alternative functions that are distinct from their canonical roles in apoptosis (Table 1-3). For example, cytosolic Bax promotes mitochondrial fusion through interacting with mitofusin-1 (Mfn1) and is required for homeostasis of normal mitochondrial dynamics (101, 102). In addition, Bcl-xL interacts with ATP synthase to regulate the efficiency of oxidative phosphorylation by inhibiting proton leakage across the IMM (103-105). Furthermore, a splice variant of Mcl-1 localizes to the mitochondrial matrix and is critical for maintaining IMM structure, mitochondrial dynamics, and respiration (106). Multiple Bcl-2 family members including Bcl-2, Bcl-xL, and Bax are found at the ER membrane where they regulate Ca^{2+} signaling and release to the mitochondria in a manner that is independent of their apoptotic function (107).

BH3 only proteins have also been shown to have alternative functions. For example, Bid plays a pro-survival role by regulating the response to genotoxic stress (1-5). Bid is also able to regulate the innate immune response by interacting with components of the nucleotide-binding and oligomerization domain (NOD) signaling pathway (108). In addition, Bad exhibits a pro-survival function in certain contexts such as in Sindbis virus and N-Methyl-D-aspartic acid (NMDA)-induced neuronal cell death (109). Bad also regulates glucokinase and maintains homeostatic control of glucose metabolism and insulin secretion (110, 111). Furthermore, Noxa facilitates cell survival through promoting glucose metabolism via the pentose phosphate pathway (112). The BH3-only protein, Beclin-1, has also been shown to regulate autophagy (107). In light of the many functions of Bcl-2 family members, it is clear that these proteins have diverse roles in regulating cellular homeostasis, survival, and physiology.

Table 1-3. Non-canonical functions for Bcl-2 family members

Protein	Functions	Reference
Bax	Mitochondrial dynamics, calcium signaling	(101, 102, 107)
Bcl-xL	Oxidative phosphorylation, autophagy, calcium signaling	(103-105, 107)
Mcl-1	Mitochondrial structure, dynamics, and respiration, and autophagy	(106, 107)
Bcl-2	Autophagy, calcium signaling	(107)
Bcl-w	Autophagy	(107)
Beclin	Autophagy	(107)
Bid	DNA damage response, Innate Immunity	(1-5, 108)
Bad	Neuronal cell survival, glucose metabolism	(109-111)
Noxa	Glucose metabolism	(112)

BH3-only Bid

Bid was first identified by interactive cloning in 1996 as a BH3 only protein that interacts with Bcl-2 and Bax and promotes apoptosis in a BH3 domain-dependent manner (34). Bid was later identified as a substrate for Caspase-8 downstream of death receptor activation (32, 33, 113). These studies revealed that Bid is cleaved by Caspase-8 at aspartic acid 59 resulting in a 15 kDa truncated Bid (tBID) (32, 33, 113). Following cleavage, tBid rapidly translocates to mitochondria and is a potent inducer of Cytochrome *c* release and apoptosis (32, 33, 113).

In 1999, the solution structures of human and mouse Bid were determined (Fig. 1-7) (114, 115). Interestingly, Bid's structure is in contrast to most BH3-only proteins which are typically intrinsically disorderd (i.e. they lack a stable, ordered three dimensional structure) (116). In fact, Bid's structure is more similar to Bax, Bak, and the anti-apoptotic Bcl-2 family members, composed primarily of a compact arrangement of hydrophobic and amphipathic α-helices (117). Indeed, the NMR structure showed that Bid is composed of eight α-helices and an unstructured loop between helix 2 and 3. Interestingly, the unstructured loop contains many of the sites that regulate Bid function including the caspase cleavage site, providing valuable insight into the mechanism of caspase-mediated activation of Bid. By cleaving Bid in the unstructured

loop, the first two N-terminal α-helices of Bid could dissociate as the p7 fragment, revealing the BH3 domain located in helix 3 to allow interaction of the p15 fragment (tBid) with other proteins (114, 115, 117). This displacement of the p7 fragment has since been shown to be facilitated by Bid's association with membranes, thus promoting its activation (118).

Membrane targeting of tBid is dependent upon its cleavage by caspases. However, Bid cleavage is not solely mediated by Caspase-8. Indeed, Caspase-3 activated downstream of MOMP can also cleave Bid, which amplifies apoptotic signaling through the mitochondria (119). Bid can also be cleaved by other proteases including granzyme B (120), calpains (121, 122), and cathepsins (123-125). Cleavage by these enzymes occurs within the unstructured loop of Bid and facilitates targeting of Bid to mitochondria, promoting tBid mediated MOMP. Following cleavage, tBid is further modified by myristoylation, which may facilitate mitochondrial targeting of tBid (Fig. 1-7) (126). Of Bid's 8 α-helices, α-helix 6 & 7 form a highly hydrophobic core, while the remaining helices are amphipathic. Once cleaved, the presence of a membrane disrupts the hydrophobic interaction of α1 and α2 with α3, resulting in dissociation of the p7 fragment from tBid. This is followed by a conformational change and unfolding of tBid in the presence of the membrane, leading to a peripheral association of α-helices 4, 5, and 8 with the membrane surface and then an insertion of the hydrophobic α6 and α7 into the membrane (127). Mitochondrial carrier homolog 2 (Mtch2), a protein in the OMM, facilitates the targeting of tBid to the OMM and catalyzes the conformational changes required for tBid membrane insertion (127, 128). Also, as is discussed in later sections, the phospholipid composition of the OMM, especially of cardiolipin, is critically important for the targeting and activity of tBid at the mitochondria (129, 130).

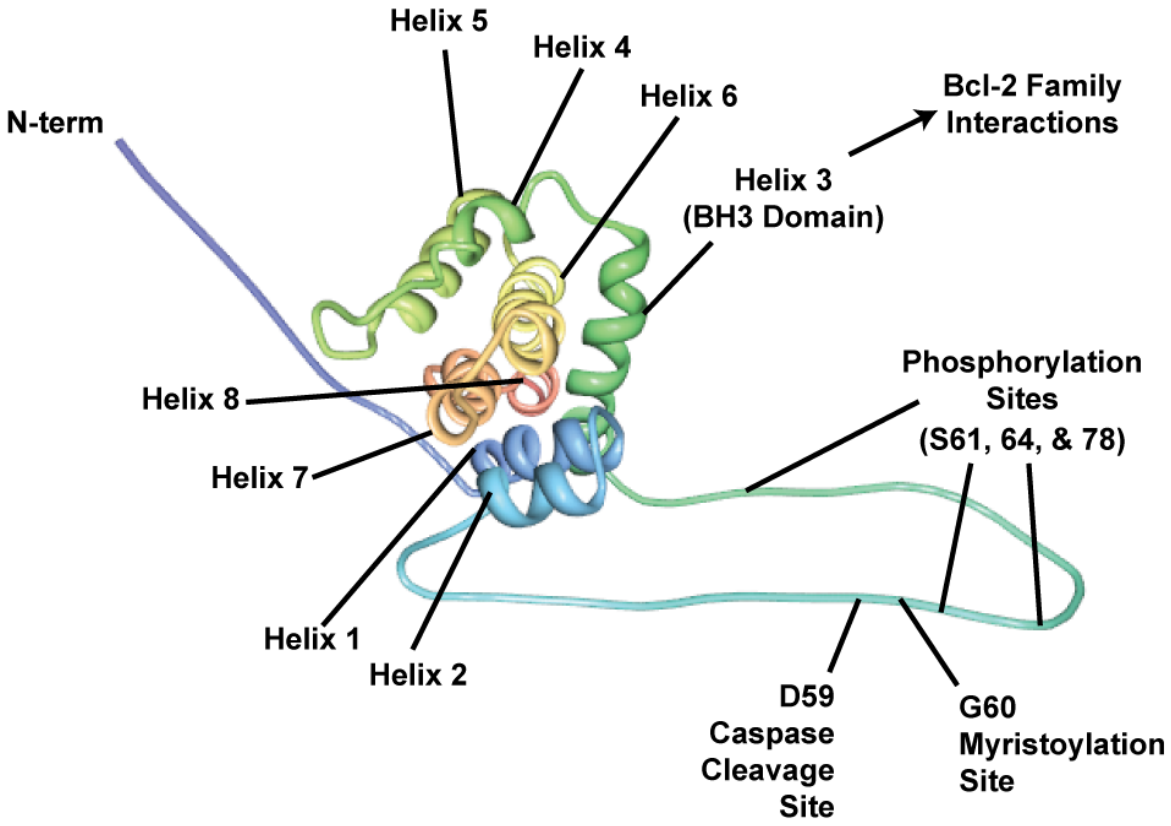

Figure 1-7. NMR structure of mouse Bid. Bid is composed of 8 alpha helices and a long unstructured loop region between helix 2 and 3. The Caspase cleavage site at Asp 59 and the myristoylation site at Gly 60 are located in the unstructured loop. Bid can also be cleaved by granzyme B, calpains, and cathepsins in its unstructured loop. Helix 3 of Bid contains the BH3 domain required for Bid's pro-apoptotic function. Following caspase cleavage, Bid associates with the mitochondrial membrane which facilitates removal of the N terminal p7 fragment containing helices 1 & 2 and as well as the insertion of helix 6 and 7 into the OMM. Bid is also phosphorylated by CK1 and CK2 (S61, S64) and by ATM/ATR (S61, S64, and S78) in its unstructured loop, inhibiting Bid cleavage and also regulating its function in the DNA damage response.

As an activator BH3-only protein, Bid elicits its apoptotic function by directly binding and activating Bax and Bak (93, 95, 97). Bak is activated by binding to membrane localized tBid (131). In contrast, Bax requires membrane insertion before it can induce MOMP. Bax undergoes conformational changes during peripheral association with the OMM that are required for tBid-mediated Bax activation and MOMP (132). This interaction induces further conformational changes in Bax that facilitate its activation, insertion into the membrane, and oligomerization to induce MOMP (90, 133).

Bid function is also regulated through phosphorylation. For example, casein kinase 1 and 2 (CK1 & 2) phosphorylate mouse Bid at Ser 61 and Ser 64 near the caspase cleavage site in the flexible loop region between helix 2 and 3 (Fig. 1-7) (86). This phosphorylation inhibits the caspase mediated cleavage and activation of Bid. Phosphorylation of S61 and S64 as well as S78 is also mediated by the DNA damage sensing kinases Ataxia telangiectasia mutated (ATM) and ATM and rad-3 related (ATR) in response to genotoxic stress (1, 2). In these studies, described in detail in the following sections, Bid phosphorylation by ATM and ATR was demonstrated to be important in inducing an efficient response to DNA damage, thus demonstrating a pro-survival function of Bid in regulating cell cycle arrest and DNA damage repair. Additionally, phosphorylation of human Bid at S64, S65, and S78 is required to regulate the innate immune response to NOD signaling activity (108). Thus, Bid phosphorylation plays a variety of roles in regulating Bid both in apoptotic and non-apoptotic settings.

In addition to *in vitro* studies of Bid regulation and activation, *Bid -/-* mouse models have revealed several physiological functions of Bid *in vivo*. For example, in Bid deficient mice, hepatocytes are resistant to Fas-induced apoptosis (85). Similarly, neural cells isolated from *Bid -/-* mice are resistant to oxygen/glucose deprivation and *Bid -/-* mice are protected from focal

cerebral ischemia (134). Furthermore, Bid deficient mice develop a myeloproliferative disorder that progresses to a chronic myelomonocytic leukemia-like disease which results in early mortality, indicating that Bid functions as a tumor suppressor *in vivo* (135). Moreover, bone marrow progenitors and stem cells in *Bid -/-* mice display increased sensitivity to replication stress with diminished bone marrow function after long term exposure to genotoxic stress (3). A recent study using Bid S61A/S78A knock-in mice implicated the ATM mediated phosphorylation of Bid in regulating ROS production and hematopoietic stem cell function *in vivo* (136). Overall, these studies highlight a critical role for Bid in regulating tissue homeostasis and tumorigenesis *in vivo*.

Bid, cardiolipin, and mitochondrial physiology

Cardiolipin: Structure and function

The primary role of mitochondria is to regulate cellular bioenergetics through both anabolic and catabolic pathways (137). Mitochondria are also central to the initiation and execution of programmed cell death. Disruption of normal mitochondrial function is involved in numerous pathologic conditions including aging, cancer, neurodegenerative disorders, Barth syndrome, and multiple types of cardiovascular disease, highlighting the physiological importance of mitochondrial homeostasis (138, 139).

Mitochondrial function is highly dependent upon the lipid composition of the IMM. Cardiolipin (CL), a phospholipid that is nearly exclusively localized to the IMM in eukaryotes, is particularly important for mitochondrial function (139). CL is composed of a double glycerophosphate backbone allowing for attachment of up to four fatty acyl chains (Fig. 1-8A).

In most animal tissues, the predominant form of CL is tetralinoleoyl cardiolipin (L_4CL), containing four linoleic acid groups composed of an 18 carbon fatty acyl chain with two unsaturated bonds (18:2) (Fig. 1-8B). The CL content and composition in the IMM affects mitochondrial function by modulating IMM structure, respiratory function, and apoptotic signaling. Thus, CL is an essential factor in regulating mitochondrial physiology and cellular homeostasis.

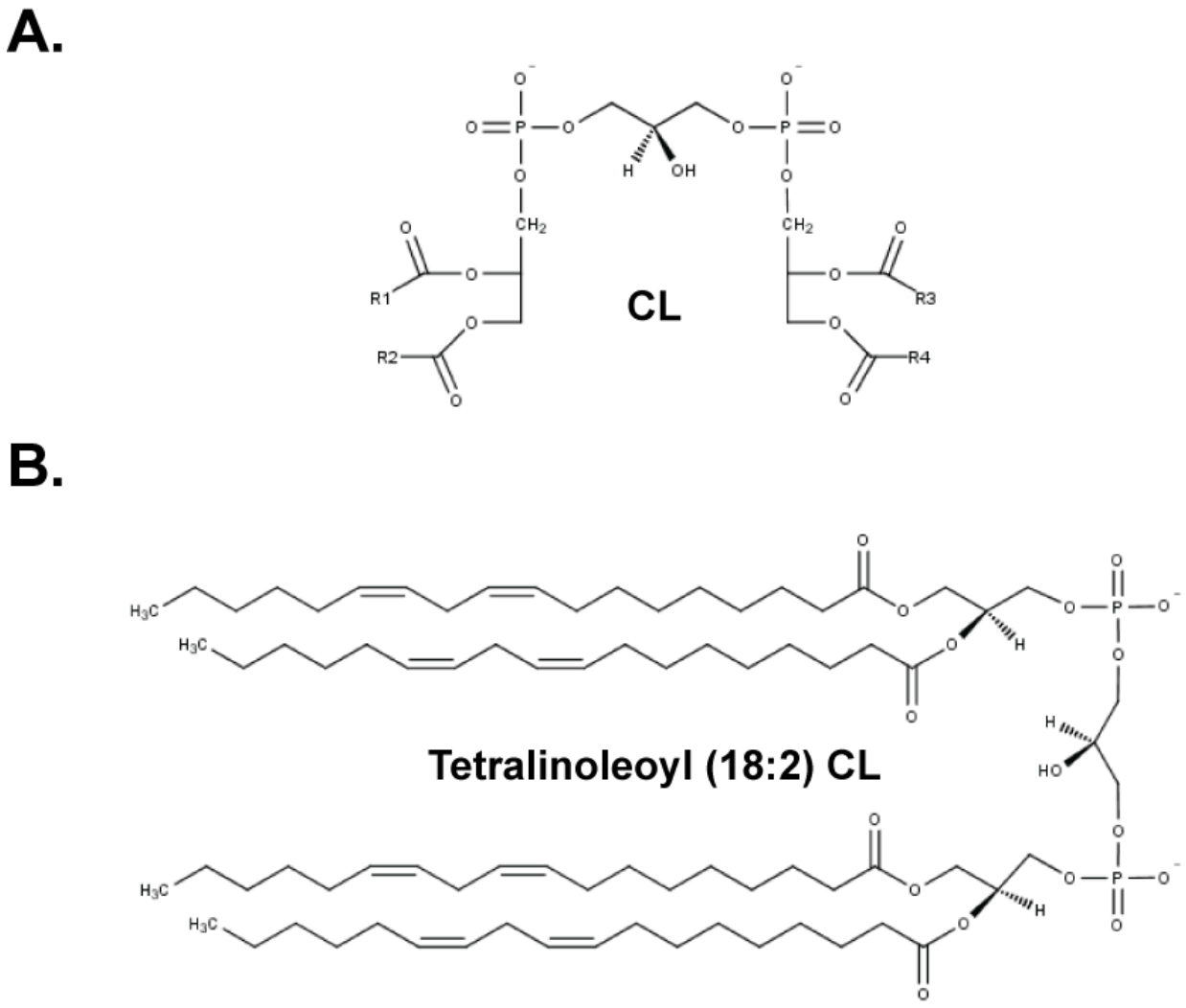

Figure 1-8. Cardiolipin structure. A) CL is a mitochondrial specific phospholipid made up of a double glycerophosphate backbone and, at physiologically relevant pH, harbors a -1 negative charge. CL can have up to four fatty acyl chains of varying compositions, depicted here as R groups 1-4. B) The most abundant form of CL is tetralinoleoyl CL (L_4CL) with four linoleic acid (18:2) fatty acyl chains. L_4CL is critical for maintaining normal mitochondrial structure and function.

Maintenance of a defined mitochondrial CL composition requires the *de novo* synthesis of CL from precursor phospholipids. In eukaryotes, CL synthesis occurs in a stepwise manner on the matrix side of the IMM, starting with the conversion of phosphatidic acid (PA) to cytidinediphosphate-diacylglycerol (CDP-DAG) by CDP-DAG synthase (CDS) (139, 140). CDP-DAG is then de-phosphorylated by phosphatidylglycerol phosphate synthase (PGPS) to phosphatidylglycerol phosphate (PG-P), which is further de-phosphorylated to PG by PG-P phosphatase (PGPP). Finally, CL is then synthesized by cardiolipin synthase (CS) from PG (Fig. 1-9). Although all of these steps can occur at the IMM, lipid transport from the endoplasmic reticulum to the mitochondria is an important source of PA and CDP-DAG, though some *de novo* synthesis of these lipids may take place at the mitochondria as well.

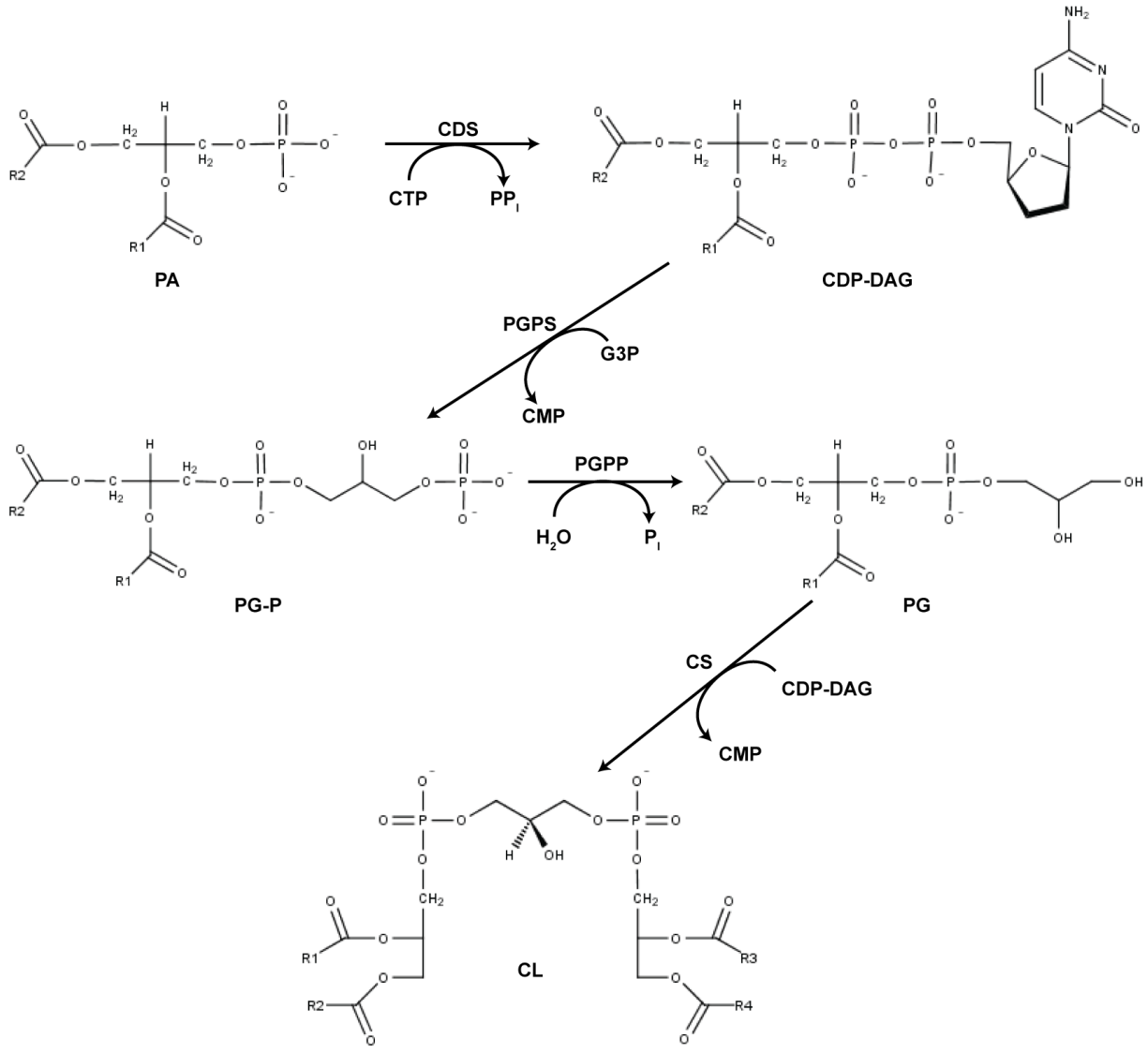

Figure 1-9. The cardiolipin biosynthetic pathway. Cardiolipin synthesis proceeds by condensation of cytidine triphosphate (CTP) and the precursor phospholipid, phosphatidic acid (PA), which is catalyzed by CDP-DAG synthase (CDS). CDP-DAG synthase is then converted to phosphatidylglycerol phosphate (PG-P) through the action of PG-P synthase (PGPS) using glycerol-3-phosphate (G3P) as a substrate and releasing cytidine monophosphate (CMP) as a product. PG-P is dephosphorylated through PG-P phosphatase (PGPP) mediated hydrolysis of the terminal phosphate, producing phosphatidylglycerol (PG). PG then reacts with CDP-DAG, catalyzed by cardiolipin synthase (CS), producing nascent CL and CMP.

Nascent CL is post-synthetically modified, or remodeled, by fatty acyl hydrolysis and re-acylation reactions (141). Though CL remodeling is still incompletely understood, several enzymes have been implicated in the remodeling process. For example, in *S. cerevisiae*, phospholipases hydrolyze CL (142), resulting in the production of monolyso-cardiolipin (MLCL). Similarly, calcium-independent phospholipase $A_2\gamma$ ($iPLA_2\gamma$) has been implicated to hydrolyze CL in mammals (143). Several enzymes have also been implicated in re-acylation of MLCL including MLCL acyltransferase (MLCLAT), acyl-CoA:lysocardiolipin acyltransferase (ALCAT), and tafazzin (141). Tafazzin, in particular, is well known to be critical for cardiolipin remodeling and mutation of tafazzin in victims of Barth syndrome results in decreased CL content and accumulation of MLCL (139). Altogether, through cycles of fatty acyl hydrolysis and re-acylation, the composition of CL in mitochondria can be controlled in order to regulate the structure of the IMM and overall mitochondrial function.

CL is essential for optimal and efficient mitochondrial respiration through several different mechanisms. For example, CL is required for optimal enzymatic function of the electron transport chain (ETC) complexes I, II, III and IV (144-146). In addition, CL binds Cytochrome *c* through electrostatic forces, anchoring Cytochrome *c* to the IMM and facilitating electron transfer between complex III and IV (144). CL also binds to (144) and regulates the supramolecular organization of ATP synthase (147). This has dual roles in regulating respiration by improving the enzymatic efficiency of ATP synthase (148) as well as by maintaining cristae morphology (149), which is required for optimal respiration (150). CL is also important for the organization of individual complexes into respiratory supercomplexes which significantly enhances the transport of electrons between complexes (144, 151-155).

In addition to its effects on proteins involved in electron transport, CL is also required for optimal function of other mitochondrial proteins. For example, CL is required for the function of ANT, a transporter responsible for the transfer of ADP and ATP between the mitochondrial matrix and the IMS (146, 156). Furthermore, CL anchors mitochondrial creatine kinase (mtCK) and nucleoside diphosphate kinase (NDPK) to the IMM which, in combination with ANT, promotes respiration by influencing exchange of ADP, ATP, and other metabolites across the IMM (157, 158).

With two phosphates in the double glycerophosphate backbone of CL, the head group of CL carries a -1 negative charge at neutral pH. This characteristic of CL's head group allows it to act as a proton trap, thus limiting pH changes in the IMS, providing protons for ATP synthase (159). In addition, the ability of CL to function as a proton trap increases the localized membrane potential that is required for ADP/ATP transport through the ANT (146).

Mitochondria are highly dynamic organelles, undergoing fission and fusion in response to cell cycle, stress, and cellular morphology. CL and other phospholipids are integral to the regulation of mitochondrial dynamics (160). CL is critical for mitochondrial fusion in yeast through interacting with Mgm1, the yeast ortholog of mammalian Opa1 (161, 162). Mgm1 exists in both a short (s-Mgm1) and long (l-Mgm1) isoform and forms an active GTPase upon dimerization that mediates mitochondrial membrane fusion. While dimerization and optimal activation of s-Mgm1 requires CL, l-Mgm1 does not require CL for optimal GTPase activity but does require CL for binding to membranes (161). Consistent with a role for CL in mitochondrial fusion, CL deficiency is associated with increased fragmentation of mitochondria (162). CL has also been shown to interact with dynamin-related protein 1 (Drp1) (163), which is required for mitochondrial fission (164). The Drp1-CL interaction is required for optimal Drp1 GTPase

activity and oligomerization, suggesting that CL is required for Drp1 mediated mitochondrial fission (165). CL has also been implicated in fission of membranes by the Parkinson's disease associated protein, α-Synuclein, *in vitro* (166). Interestingly, overexpression of α-Synuclein induces significant disruption of normal mitochondrial inner membrane morphology and respiration *in vivo* (166). Furthermore, mice lacking α-Synuclein display a 22% reduction in brain CL levels, alterations in CL fatty acid composition, and reduced ETC efficiency (167). Thus, CL has a considerable impact on mitochondrial dynamics and mitochondrial physiology.

Apoptotic function of cardiolipin

In addition to the role of CL in maintaining normal mitochondrial physiology under steady-state conditions, it also has an essential function in regulating apoptosis signaling through the mitochondria. Cytochrome *c* is localized to the IMM through interacting with CL (146) and is released from the mitochondria during MOMP to induce apoptotic cell death (6). In order for Cytochrome *c* to be released from the mitochondria, it must first dissociate from CL and the inner membrane before it can be released from permeabilized mitochondria into the cytosol and activate downstream caspases (168). This mobilization of Cytochrome *c* is promoted by the peroxidation of CL as a result of ROS production during apoptosis (169, 170) as well as by the intrinsic peroxidase activity of Cytochrome *c*, catalyzing H_2O_2-dependent CL peroxidation (171). Furthermore, peroxidation of CL is associated with depletion of total CL levels, presumably due to iPLA$_2$γ mediated degradation of CL (139, 146). A reduction in total mitochondrial CL content, whether as a result of peroxidation or by other processes, can also increase Cytochrome *c* mobilization, priming mitochondria for Cytochrome *c* release during an apoptotic stimulus (Fig. 1-10A) (172).

CL also regulates apoptosis through functioning as an activating platform for Caspase-8 on the OMM (173). During apoptosis, CL is transported from the IMM to the OMM (174). This movement of CL is thought to occur at mitochondrial contact sites, submitochondrial domains where the IMM and OMM interface (175). Mitochondrial contact sites are thought to be stabilized, in part, by mtCK and NDPK (175). Interestingly, both mtCK and NDPK facilitate the transfer of lipids, including CL, between membranes. Thus, mtCK and NDPK may facilitate the exposure of CL on the OMM at mitochondrial contact sites during apoptosis (175). Phospholipid scramblase 3 (PLS3) has also been implicated in translocation of CL to the OMM (176) and PLS3 overexpression can promote increased Caspase-8 processing *in vivo* (Fig. 1-10B) (177). As discussed in the next section, CL translocation to the OMM is also thought to target tBid to mitochondrial contact sites, facilitating activation of Bax/Bak and MOMP (Fig. 1-10C) (129, 130, 175). Thus, CL plays an important role in regulating the upstream events in apoptosis initiation.

CL has also been implicated in regulating the activity of the MPTP. CL is thought to play a key role in Ca^{2+} mediated MPTP opening through regulating ANT (59). Under normal conditions, CL is bound to ANT and the MPTP remains in a closed conformation. However, high Ca^{2+} levels promotes the binding of Ca^{2+} to the negatively charged head group of CL, which promotes a conformational change in the MPTP to an open conformation. CL peroxidation is also thought to promote opening of the MPTP through altering the activity of ANT (178, 179). Consistent with this, peroxidized CL synergizes with Ca^{2+} to mediate opening of the MPTP (180, 181) (Fig. 1-10D). Overall, these data indicate that CL is an important component of the MPTP and plays a key role in the regulation of MPTP mediated cell death.

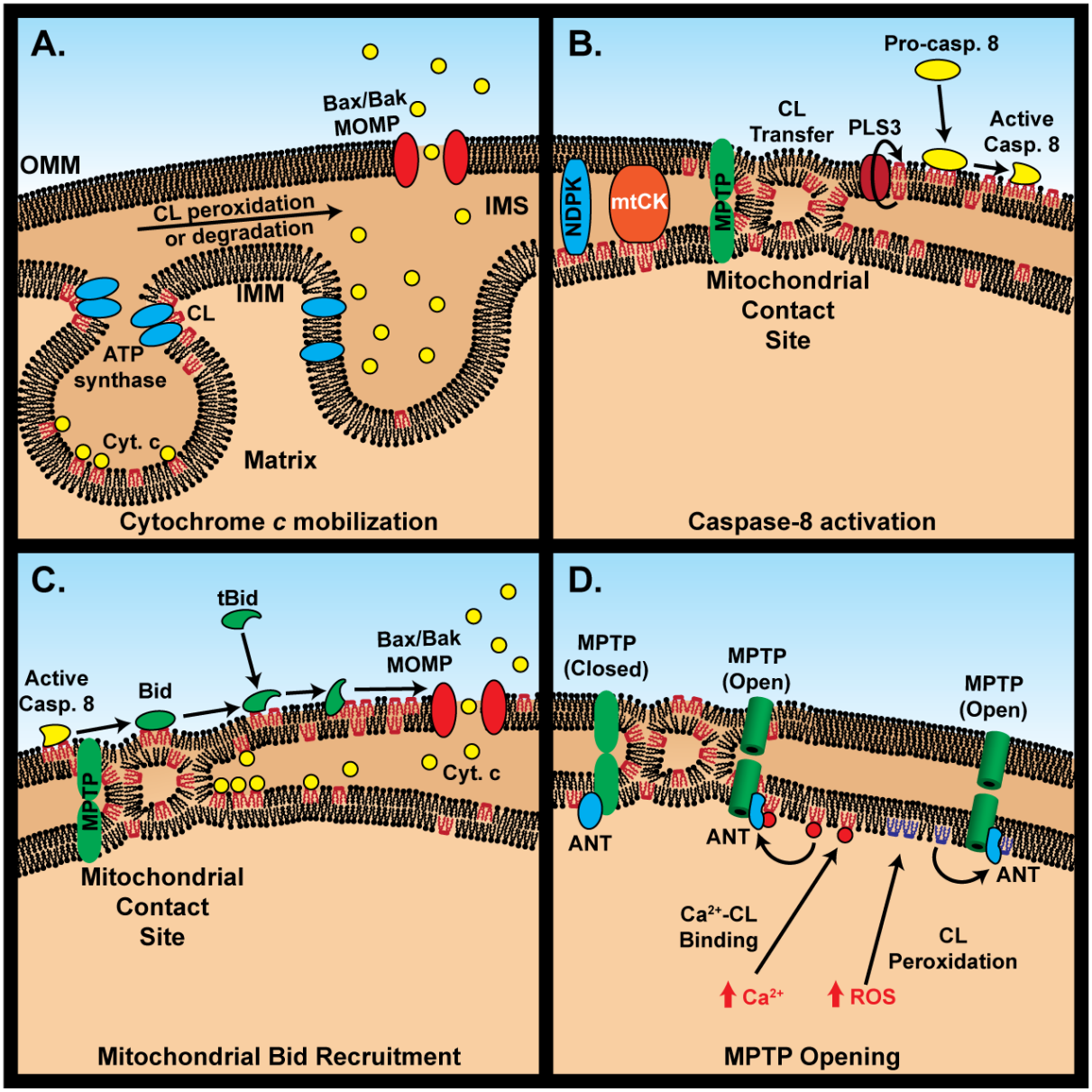
A.
Bax/Bak
MOMP
OMM
IMS
CL peroxidation
or degradation
IMM
CL
ATP
synthase
Cyt. c
Matrix
Cytochrome c mobilization
B.
Pro-casp. 8
CL
Transfer
PLS3
Active
Casp. 8
NDPK
mtCK
MPTP
Mitochondrial
Contact
Site
Caspase-8 activation
C.
tBid
Bax/Bak
MOMP
Active
Casp. 8
Bid
Cyt. c
MPTP
Mitochondrial
Contact
Site
Mitochondrial Bid Recruitment
D.
MPTP
(Closed)
MPTP
(Open)
MPTP
(Open)
ANT
ANT
ANT
Ca2+-CL
Binding
CL
Peroxidation
Ca2+
ROS
MPTP Opening

Figure 1-10. The role of cardiolipin in cell death. A) CL (shown as red phospholipids) interacts with Cytochrome *c*, anchoring it to the IMM, primarily within cristae. CL promotes the formation of ATP synthase oligomers through interacting with ATP synthase which is required to maintain cristae structure and facilitates sequestration of many proteins, including Cytochrome *c,* within the cristae. During apoptosis, high levels of ROS cause the peroxidation of CL which, in turn, increases CL degradation by phospholipases such as iPLA$_2\gamma$. Peroxidation and/or degradation of CL disrupts the interaction between Cytochrome *c* and CL and may facilitate cristae structure disruption, thus promoting the mobilization of Cytochrome *c* from the IMM to the IMS. Mobilized Cytochrome *c* is primed for diffusion to the cytoplasm upon MOMP via the activation of Bax/Bak at the OMM. B) During apoptosis, CL is rapidly transported to the OMM which is likely mediated by CL transfer at mitochondrial contact sites. Mitochondrial contact sites are stabilized, in part, by NDPK and mtCK. Upon transfer to the OMM, exposed CL functions as an activation platform for caspase-8, thus facilitating mitochondrial apoptotic signaling. PLS3 is implicated in facilitating CL transfer and caspase-8 activation at the mitochondria. One potential mechanism for PLS3 function in CL exposure is through mediating the transfer of CL to the outer leaflet of the OMM, as shown here. C) In addition to activating caspase-8, CL exposure facilitates the recruitment of tBid to the mitochondria. The OMM associated Caspase-8 can also promote the cleavage and activation of Bid at the OMM, facilitating tBid mediated Bax/Bak activation. Since CL is enriched at mitochondrial contact sites, this may also increase the local concentration of Cytochrome *c*, increasing the efficiency of Cytochrome *c* release during MOMP. D) CL regulates the opening of the MPTP, in part, through binding to ANT. In the presence of high Ca^{2+} concentration, Ca^{2+} can bind to the negatively charged CL head group. This interaction is proposed to regulate a conformational change in ANT which results in MPTP opening. Similarly, the presence of high ROS can also result in ANT mediated MPTP opening by peroxidation of CL (shown as blue phospholipids). Opening of the MPTP causes an influx of water into the mitochondria, resulting in mitochondrial damage and promoting cell death.

Cardiolipin, Bid, and the Bcl-2 family

Proteins of the Bcl-2 family are critical regulators of apoptosis that function through altering mitochondrial structure and physiology. In addition to permeabilization of the OMM, apoptosis elicits dramatic changes in mitochondrial dynamics (90), IMM structure (90, 182), membrane potential (183), and respiratory function (183). Although the mechanisms regulating the interaction of the Bcl-2 family members are well studied, it is less clear how these proteins elicit such dramatic changes in mitochondrial morphology and physiology. Interestingly, there is significant overlap in mitochondrial processes that are regulated by the Bcl-2 family and CL, suggesting the possibility that CL and the Bcl-2 family are functionally linked. The following section will discuss the current knowledge in the field regarding the relationship between CL and proteins of the Bcl-2 family both in apoptotic and non-apoptotic contexts.

The BH3-only protein Bid exhibits the most direct relationship between CL and a Bcl-2 family member. The first evidence of a role for CL in Bid function came from the observation that CL increased the affinity of Bid and tBid for binding liposomes in a concentration dependent manner (129). Full length Bid and, to a greater degree, tBid show a higher affinity for liposomes with a lipid composition similar to mitochondrial contact sites than to liposomes with other lipid compositions (129). Consistent with this finding, tBid preferentially binds to mitochondria at mitochondrial contact sites, where CL is enriched on the OMM (184). Truncation mutants of Bid revealed a putative membrane binding domain (MBD) spanning amino acids 103 to 162, containing α-helices 4-6, which was sufficient for binding to mitochondria *in vitro* (129), suggesting that the MBD may associate with CL or with CL rich membranes. Expression of the MBD in Chinese hamster ovary cells with a temperature sensitive mutation in PGS, an upstream enzyme required for CL synthesis, demonstrated that the MBD was dependent on PGS activity

for co-localization with mitochondria *in vivo* (129). Similarly, tBid was also dependent on PGS activity for mitochondrial binding and Cytochrome *c* release (129). A later report by Kuwana et al further supported a role for CL in Bid-membrane interaction, Bax activation, and membrane permeabilization by demonstrating that the release of dextran from liposomes by tBid and Bax was dependent on CL content in a dose dependent manner (130). Overall, these data indicated that CL was important for the association of tBid with membranes and for the pro-apoptotic function of Bid.

The discovery that CL facilitated tBid recruitment to membranes suggested that Bid may be able to interact with CL. Multiple studies provide support for an interaction between Bid and CL. For example, Esposti et al. demonstrated that full length Bid and, to a greater degree, tBid can compete with a free fatty acid and lysolipid indicator, acrylodated intestinal fatty acid binding protein (ADIFAB), for binding to MLCL (185). In the same study, the authors further demonstrated that CL, MLCL, and dilysocardiolipin (DLCL) induced the formation of Bid aggregates *in vitro* (185). Furthermore, addition of MLCL to mitochondria enhances Bid binding to mitochondria and Cytochrome *c* release (185). A later report by Liu et al. indicated an interaction between Bid and CL/MLCL by Biacore analysis, a label free analysis of interaction using surface plasmon resonance (186). Additionally, Kim et al. showed that incubation of tBid with mitochondria followed by electrospray ionization mass spectrometry resulted in a reduced signal for CL, potentially suggesting a Bid-CL interaction (187). The same study demonstrated that the dye nonyl acridine orange (NAO), known to bind to CL, inhibited the targeting of tBid to mitochondrial contact sites, Cytochrome *c* release, and cristae remodeling (187). Overall, these data provide multiple lines of evidence that support a direct interaction between Bid/tBid and CL. Nevertheless, it is important to note that the assays used above to investigate Bid-CL

interactions are either indirect observations or were performed using purified proteins and/or lipids *in vitro*. Therefore, though the data are consistent with a direct interaction, it remains undetermined whether these findings are in a membrane environment *in vivo*. Indeed, the effects of CL on Bid's mitochondrial targeting and function could all be explained by CL altering the membrane architecture or environment in a manner that is favorable for Bid/tBid binding , rather than a direct interaction between CL and Bid.

Although the above studies indicated that CL is important for the recruitment of Bid to membranes, mitochondrial proteins also appear to be equally important. Indeed, liposomes containing proteins extracted from the OMM, but lacking CL, can still be permeabilized by tBid (188), suggesting that both CL and mitochondrial proteins are sufficient to target tBid to membranes *in vitro*. Recent evidence suggests that the OMM protein Mtch2 plays a key role in targeting of tBid to the mitochondria (128). Although tBid localization to membranes can be facilitated by either CL or by OMM proteins *in vitro*, it is likely that CL and OMM proteins function synergistically *in vivo.* It is possible that CL enrichment at mitochondrial contact sites could create a membrane platform that is ideal for the interaction of membrane proteins that facilitates the recruitment and activation of pro-apoptotic proteins such as Bid. Indeed, as mentioned above, the MPTP is located at mitochondrial contact sites where several of its components associate with CL to regulate cell death (58, 59). In addition, CL serves as a Caspase-8 activation platform on the OMM (173) which has been shown to bind Bid and facilitate its cleavage and activation at the mitochondrial surface (189). Thus, *in vivo*, it is likely that both the lipid and protein composition of the OMM are critical in regulating the pro-apoptotic function of Bid.

Bid may also play a role in regulating the distribution of CL, and other lipids, in membranes. Interestingly, Bid displays lipid transfer activity capable of transferring phospholipids between membranes (190). Although, the physiological relevance of lipid transfer by Bid/tBid remains unclear, it is possible that Bid's lipid transfer function may contribute to the redistribution of CL during apoptosis (191). Since redistribution of CL occurs prior to mitochondrial permeabilization (174), Bid's effect on CL distribution could precede activation of Bax/Bak. The lipid transfer function of Bid/tBid could thus serve to amplify early apoptotic signaling prior to MOMP by increasing OMM localized CL, recruiting additional pro-apoptotic factors to the mitochondrial membrane including additional tBid molecules and Caspase-8. In addition, it is possible that by altering mitochondrial CL distribution Bid could contribute to Cytochrome *c* mobilization, cristae remodeling, or disruption of respiration. However, the mechanism by which Bid may mediate lipid transfer is undetermined. Thus, further work will be required to determine how Bid's mediates lipid transfer and its impact on apoptosis signaling and execution.

CL has also been implicated in the tBid-mediated binding and activation of Bax (192). Analysis of the lipid binding properties of the first α-helix of Bax (Bax-α1), required for Bax translocation to mitochondria (193, 194), demonstrated that the presence of CL in membranes alters the mechanism of interaction as well as the structure of Bax-α1 at the membrane surface (195). However, the role of CL in Bax function remains controversial as multiple studies suggest that Bax function is CL independent (188, 196-198). Indeed, CL has only a slight effect on Bax mediated liposome permeabilization following activation by Bid or Bim BH3 peptides or by octylglucoside treatment (188). In addition, recent evidence suggests that Bax can translocate to and permeabilize liposomes lacking cardiolipin in the presence of Bim, but not tBid (199). These

data suggest that CL is not essential for Bax activation, but rather impacts Bax activation through its effects on other proteins such as Bid. Nevertheless, it is still possible that CL could affect functions of Bax in other contexts or pathways.

CL may also play an important role in tBid induced cristae remodeling. For example, mitochondria treated with tBid undergo dramatic remodeling of the mitochondrial cristae (182). Cristae remodeling by tBid is inhibited by NAO treatment (187), which indirectly suggests that CL may be required for tBid induced cristae remodeling. In addition, tBid directly destabilizes CL containing liposomes by inducing negative curvature strain of the membrane (200), which may facilitate remodeling of mitochondrial membranes. This membrane destabilization is further facilitated by increased calcium concentration, which also induces negative curvature of CL in membranes (201, 202). Furthermore, tBid and Bax have been implicated in regulating ROS production and the activity of $iPLA_{2\gamma}$ (203), which could facilitate CL peroxidation and degradation, ultimately inducing cristae remodeling and promoting cytochrome *c* mobilization.

Bax has also been demonstrated to regulate mitochondrial morphology through modulating mitochondrial dynamics. Indeed, the soluble form of Bax promotes mitochondrial fusion and is required for normal mitochondrial dynamics (101, 102). In contrast, apoptotic activation of Bax inhibited mitochondrial fusion, suggesting that the membrane insertion and/or oligomerization may inhibit its ability to promote mitochondrial fusion (102) or, alternatively, that an opposing pathway during apoptosis overrides Bax mediated fusion. As described above, CL is required for normal mitochondrial dynamics by interacting with and regulating Drp1 function (160, 163-165). Bax has also been shown to regulate mitochondrial dynamics by associating with Drp1 (204), raising the possibility that Bax and CL may coordinately regulate mitochondrial dynamics.

Several anti-apoptotic Bcl-2 family members display a potential link to CL. For example, an alternative splice variant of Mcl-1 localizes to the mitochondrial matrix where it associates with the IMM and regulates cristae structure, mitochondrial fusion, and respiration (106). The same study found that the matrix form of Mcl-1 is required for assembly of F_1F_0 ATP synthase oligomers (106). Since CL synthesis occurs primarily in the matrix facing leaflet of the IMM (139, 140), it is feasible that Mcl-1 could regulate the production or remodeling of CL, thus influencing mitochondrial structure, dynamics, and respiration. Similarly, Bcl-xL has also been shown to associate with and regulate ATP synthase function where it inhibits proton leakage across the IMM and increases efficiency of oxidative phosphorylation (103-105). Formation of ATP synthase oligomers is CL dependent (147) and is required for maintaining IMM structure and ATP synthase enzymatic activity (148, 149). Though it currently remains to be determined, these data suggest a possibility that Mcl-1 and/or Bcl-xL coordinate with CL to regulate mitochondrial morphology and bioenergetics.

The Bcl-2 family and cardiolipin in heart function

Normal cardiac function is dependent on the constant production and turnover of ATP in order to provide the energy necessary for contractile work (205). Mitochondria serve as the primary source of ATP in the heart, which is predominantly generated through the oxidation of fatty acids and oxidative phosphorylation. Given the dependence of the heart on oxidative metabolism, it is also highly reliant on the availability of oxygen in the myocardium and the efficiency of oxygen utilization by mitochondria. A disruption in the balance of oxygen supply and demand can have severe consequences for cardiac function. Indeed, a reduction in oxygen supply to the myocardium leads to a rapid and progressive loss of mitochondrial function which

can ultimately lead to a loss of physiologic function and death of cardiomyocytes (206). Reduced oxygen utilization efficiency can also result in cardiac dysfunction by sensitizing the myocardium to stress. For example, aging leads to a decline in oxidative phosphorylation in cardiomyocytes, resulting from decreased activity of complexes III (207) and IV (206, 208). These defects likely contribute to the increased sensitivity of the aging heart to ischemia/reperfusion injury (206). Defects in mitochondrial oxygen utilization also contribute to the development of dilated cardiomyopathy and heart failure. In fact, genetic diseases of mitochondrial respiration and metabolism are often characterized by cardiomyopathy and heart failure (209). Thus, cardiac function is inextricably linked to mitochondrial function and mitochondrial defects that impair oxygen utilization efficiency contribute to myocardial dysfunction and injury in multiple contexts.

Prolonged or severe myocardial injury can ultimately lead to loss of cardiomyocytes by apoptotic cell death. Cardiomyocyte cell death is a major determinant in the development of cardiac dysfunction and heart failure (210). Given their important role in cell death regulation, it is predictable that the Bcl-2 family of proteins contribute to cardiomyocyte apoptosis and heart failure. Indeed, Bid (121, 211, 212), Bad, Bnip3, Nix, Puma, Bax, Bcl-2, and Mcl-1 (213) have all been shown to regulate cardiomyocyte cell death and heart function in multiple models of heart failure *in vivo* (Table 1-4) (210, 214). During myocardial infarction (215), dilated cardiomyopathy (216), and ischemic heart disease (217), both pro- and anti- apoptotic Bcl-2 family members are observed to be dynamically regulated. In addition, Bcl-2 overexpression protects against cardiac injury in both ischemia-reperfusion and cardiomyopathy in the mouse heart (218-220). Furthermore, Bcl-2 overexpression reduces ATP consumption in the heart during ischemia, indicating that Bcl-2 protects from cardiac injury, in part, by modulating

mitochondrial metabolism (220). Bcl-X_L has also been implicated in protecting from ischemia-reperfusion injury in rats (221). Thus, the proteins of the Bcl-2 family are critical players in determining cardiac injury in multiple types of cardiac stress and heart failure.

Table 1-4. Bcl-2 family members in cardiac function.

Bcl-2 Family Member	Cardiac Function	Reference
Bid	• Ischemia-reperfusion induced Bid cleavage by Caspases/Calpains • Induces mitochondrial damage/cytochrome c release	(121, 211, 212)
Bad	• Ischemia-reperfusion induced increase in Bad levels and Bad dephosphorylation	(222)
Bnip3	• Ischemia-reperfusion induces increase in Bnip3 levels, mitochondrial translocation, and activation of mitochondrial permeability transition pore • Bnip3 inhibition is cardioprotective	(223-225)
Nix	• Nix overexpression induces apoptotic cardiomyopathy	(226)
Puma	• Puma expression is induced by hypoxia-re-oxygenation *in vitro* • Puma knockout protects from ischemia-reperfusion injury *in vivo*	(227)
Bax	• Increased Bax expression and apoptosis in rat model of chronic pressure overload and in hypoxic rat hearts.	(228, 229)
Bcl-2	• Inhibits cardiomyocyte cell death *in vitro* • Overexpression protects from cardiac injury in mouse models of ischemia-reperfusion injury and cardiomyopathy • Overexpression inhibits ATP consumption *in vivo* following ischemia-reperfusion	(218-220, 230-232)
Mcl-1	• Cardiac tissue specific deletion of Mcl-1 results in a fatal dilated cardiomyopathy in mice characterized by structural deformation of cardiomyocyte mitochondria, reduced mitochondrial respiration, and decreased cardiac contractility.	(213)

In addition to the Bcl-2 family, CL is also an important factor in determining cardiac function. Through regulating mitochondrial structure and oxidative metabolism, CL is necessary to maintain normal mitochondrial function in the heart, and thus is critical for normal cardiac function. Dysregulation of mitochondrial CL content and/or composition has been implicated in multiple types of cardiac dysfunction. Perhaps the most compelling evidence for the role of CL homeostasis in heart function is demonstrated in the pathology of Barth syndrome. Barth syndrome is an X-linked cardioskeletal myopathy and neutropenia resulting from a mutation in the CL remodeling enzyme Tafazzin (233). Barth syndrome is characterized primarily by dilated cardiomyopathy accompanied by neutropenia and skeletal myopathy (233). Mitochondria from patients with Barth syndrome display multiple abnormalities including morphological defects, altered CL content and composition, and reduced mitochondrial respiration due to deficiency in multiple complexes of the ETC (233). Given the key role of Tafazzin in regulating CL composition, the pathology of Barth syndrome is thought to be driven by reduced mitochondrial function as a result of altered CL homeostasis.

In addition to Barth syndrome, alteration in CL homeostasis accompanies cardiac dysfunction in several other contexts. A decrease in L_4CL is observed both prior to and during heart failure in a model of spontaneously hypertensive heart failure in rats, which is accompanied by decreased Cytochrome oxidase activity, consistent with reduced mitochondrial respiration in cardiomyocytes (234). Similarly, alterations to CL composition are observed in rats during aortic constriction (235, 236), in a hamster model of cardiomyopathy (237), and has also been detected in human patients suffering from ischemic and dilated cardiomyopathies (238). During ischemia-reperfusion injury, decreased CL mass is thought to occur through ROS mediated peroxidation and degradation of CL (139, 206). This decrease in CL content correlates strongly with a

decrease in both cytochrome oxidase activity and complex IV activity and is also accompanied by a decrease in respiratory function of cardiac mitochondria (206). While these examples implicate CL modification in heart failure, further studies are required to fully understand the interplay between CL homeostasis and cardiac function.

Although they share many overlapping functions, little is known regarding the relationship between the Bcl-2 family and CL in cardiac dysfunction. This is particularly relevant in the case of Bid, which has been shown to require CL for its apoptotic function. Thus, it is important to consider whether Bid and the Bcl-2 family can influence heart function not just by regulating cardiomyocyte apoptosis but also through regulating mitochondrial homeostasis. If so, what role, if any, does CL play in this process? Finally, how can the disruption of the homeostatic function of Bcl-2 family members such as Bid contribute to the development of cardiac dysfunction? Chapter IV of this dissertation is focused on investigating these questions.

Bid and the DNA damage response

The DNA damage response

During their lifetimes, cells experience nearly constant genotoxic stresses that threaten their genomic integrity (239). To protect the integrity of the genome in the face of such insults, cells are equipped with a wide array of proteins that detect, signal, and repair DNA damage. The signaling pathways that monitor and maintain genome integrity are collectively referred to as the DNA damage response (DDR). Activation of the DDR induces multiple cellular responses including cell cycle arrest, DNA damage repair, and in cases of severe or persistent DNA damage, activation of apoptosis. Thus, the DDR functions to maintain homeostasis through

inhibiting or repairing damage to DNA or through removal of cells with potentially harmful mutations. The failure to maintain genomic integrity is linked to a broad spectrum of diseases including multiple neurodegenerative disorders, infertility, immunodeficiency, premature aging, and cancer (239).

DNA damage can result from both extrinsic and intrinsic sources. Extrinsic DNA damage results from exposure to environmental agents such as chemical genotoxic agents (e.g. cisplatin or etoposide) (239), infectious agents (e.g. Hepatitis C virus) (240), or radiation (e.g. ultraviolet or ionizing radiation) (239). Intrinsic sources of DNA damage include errors in DNA replication and reactive oxygen species produced by metabolism. These genotoxic stresses can lead to many different types of DNA lesions such as individual base alterations (e.g. base mispairing, chemical modification bases), interstrand or intrastrand crosslinks, single or double strand breaks (SSBs or DSBs), or replication stress. These different types of damage elicit different types of repair pathways. For example, mismatched bases are resolved through the mismatch repair pathway, base modifications by base excision repair, and crosslinks are resolved through nucleotide excision repair or interstrand crosslink repair. In cases of physical breaks in the DNA backbone, SSBs are resolved by the single strand break repair pathway while DSBs are resolved through one of two pathways, homologous recombination or the more error prone non-homologous end joining pathways (239).

Regardless of the type of DNA damage, the DDR functions by first recognizing DNA lesions and then activating signaling pathways that regulate downstream effectors which direct the cellular response to DNA damage. The sensing of DNA damage and initiation of the DDR is primarily mediated by ataxia telangiectasia mutated (ATM) and ATM and rad-3 related (ATR), members of the phosphatidylinositol 3-kinase-like protein kinase (Pikk) family (239). As master

regulators of the DDR, ATM and ATR are responsible for the phosphorylation of hundreds of downstream targets including the checkpoint kinases, Chk1 and Chk2, resulting in the transduction of DNA damage signaling to effectors that regulate cell cycle progression, transcription, DNA damage repair, and apoptosis. ATM and ATR display some specificity to the type of DNA damage present. ATM primarily responds to DSBs while ATR is more promiscuous, responding to multiple types of DNA damage including DSBs, but especially those that interfere with replication (241).

In the absence of DNA damage, ATM is present as an inactive dimer (242). During the DSB response (Fig. 1-11A), ATM is rapidly activated through recruitment to DSBs by the Mre11-Rad50-Nbs1 (MRN) complex (243), intermolecular autophosphorylation, and dimer dissociation (244). Upon activation, ATM phosphorylates numerous substrates including the histone variant H2AX (244). H2AX phosphorylation facilitates the recruitment of additional ATM monomers, DNA repair factors, and other DDR signaling proteins to the chromatin to propagate a feed-forward loop of DDR signaling at DSBs. Another key substrate of ATM is the checkpoint kinase Chk2, which phosphorylates and inactivates Cdc25 family members (245). The Cdc25 phosphatases are critical for the activation of Cdk/Cyclin by removing inhibitory phosphorylation. Through inhibition of Cdc25, ATM/Chk2 signaling initiates cell cycle checkpoints, to prevent cell cycle progression prior to resolution of DNA damage. In conditions of severe or unresolvable DNA damage, ATM can also promote activation of DNA damage induced apoptosis.

Although ATR can respond to multiple types of DNA lesions, it is most well-known for its response to replication stress (246). During replication stress (Fig. 1-11B), large stretches of ssDNA are formed at stalled replication forks, often due to uncoupling of DNA polymerase and

DNA helicase (247). In addition, ssDNA is formed during other types of DNA lesions due to nuclease activity and can activate ATR (246). Replication protein A (RPA) rapidly binds ssDNA, and recruits ATR to ssDNA through interacting with ATR-interacting protein (ATRIP), an obligate binding partner of ATR. RPA coated ssDNA also recruits the Rad9-Rad1-Hus1 (9-1-1) complex and topoisomerase-binding protein 1 (TOPBP1), which in turn activates the kinase activity of ATR.

ATR phosphorylates many substrates to induce inhibition of origin firing during S-phase, inhibition of cell cycle progression, stabilization of stalled replication forks, DNA repair/fork restart, and induction of apoptosis (248). Similar to ATM signaling, ATR phosphorylates a checkpoint kinase, Chk1, which functions as a transducer of ATR signaling and phosphorylates CDC25 to inhibit cell cycle progression. The ATR and ATM pathways also display significant crosstalk. For example, ATR phosphorylates several ATM substrates including H2AX (249), which may also lead to the ATR mediated recruitment and activation of ATM during replication stress. Similarly, ATM phosphorylates TOPBP1 to facilitate ATR activation (250, 251). Thus, while the ATM and ATR pathways have non-redundant functions, they also work cooperatively to engage the DDR to multiple DNA lesions.

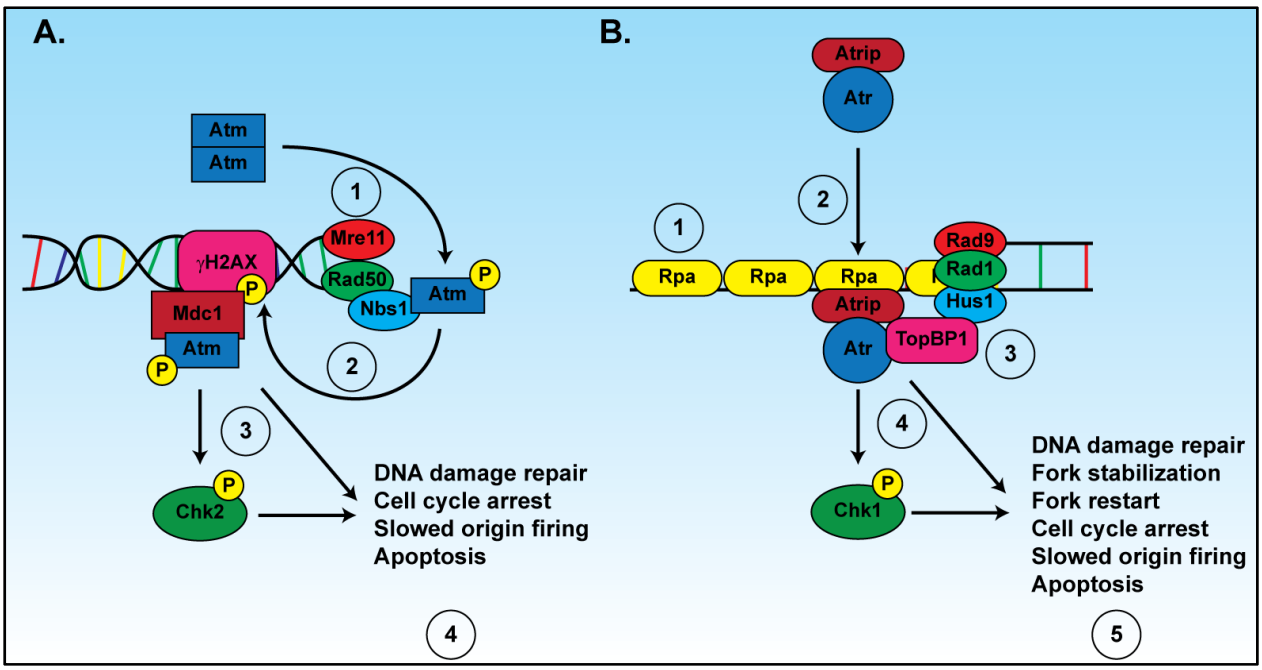

Figure 1-11. ATM and ATR in the DNA damage response. A) Following formation of a DSB, inactive ATM dimers undergo dissociation and cross phosphorylation. In addition, the MRN complex (composed of Mre11, Rad50, and Nbs1) is recruited to the broken ends and facilitates the recruitment of ATM to the DSB (1). During the double strand break response, ATM phosphorylates the histone H2AX (γH2AX), which recruits Mdc1 and additional molecules of ATM (2). ATM phosphorylates many downstream targets including Chk2 kinase, activating the kinase activity of Chk2. Through the kinase activity of ATM and Chk2, many DDR effectors are phosphorylated and activated (3). These effectors regulate DNA damage repair, cell cycle arrest, and origin firing. In cases of prolonged or severe DNA damage, they may also activate apoptotic effectors to induce cell death (4). B) Multiple types of genotoxic stress, such as replicative stress, can result in the production of large regions of ssDNA. The ssDNA is first coated in RPA (1) which recruits the ATRIP/ATR complex through a direct interaction with ATRIP (2). RPA coated ssDNA also recruits the 9-1-1 complex (composed of Rad9, Rad-1, and Nbs1) which, in turn recruits TOPBP1 to the DNA lesion. TOPBP1 then activates the kinase activity of ATR (3). Similar to ATM, ATR phosphorylates many substrates including a checkpoint kinase Chk1 (4). The substrates of ATR and Chk1 include effectors that activate DNA damage repair, fork stabilization/restart, cell cycle arrest, origin firing, and, in cases of unresolvable DNA damage, apoptosis (5) (Figure adapted from (248)).

In conditions where DNA damage is unresolvable, ATM and ATR may activate DNA damage-induced cell death as a protective mechanism to eliminate irreversibly damaged and potentially transformed cells (Fig. 1-12). DNA damage stimulates cell death through several mechanisms, the most common being through the phosphorylation and activation of the transcription factor p53. Phosphorylation of p53 is mediated in part through Chk1/Chk2 (252) and promotes the stabilization and activation of p53 as a transcriptional activator of multiple genes including the pro-apoptotic proteins such as Puma, Bax, and Noxa (253). In addition, p53 can stimulate MOMP and apoptosis by binding members of the Bcl-2 family at the mitochondria (254). Histone H1.2 has also been shown to be released into the cytoplasm to induce Cytochrome *c* release and apoptosis in a p53 dependent manner following X-ray and etoposide induced DNA damage (255). Caspase-2, a nuclear localized caspase, has also been demonstrated to be necessary for DNA damage induced apoptosis (253), possibly through cleavage and mitochondrial targeting of Bid (256).

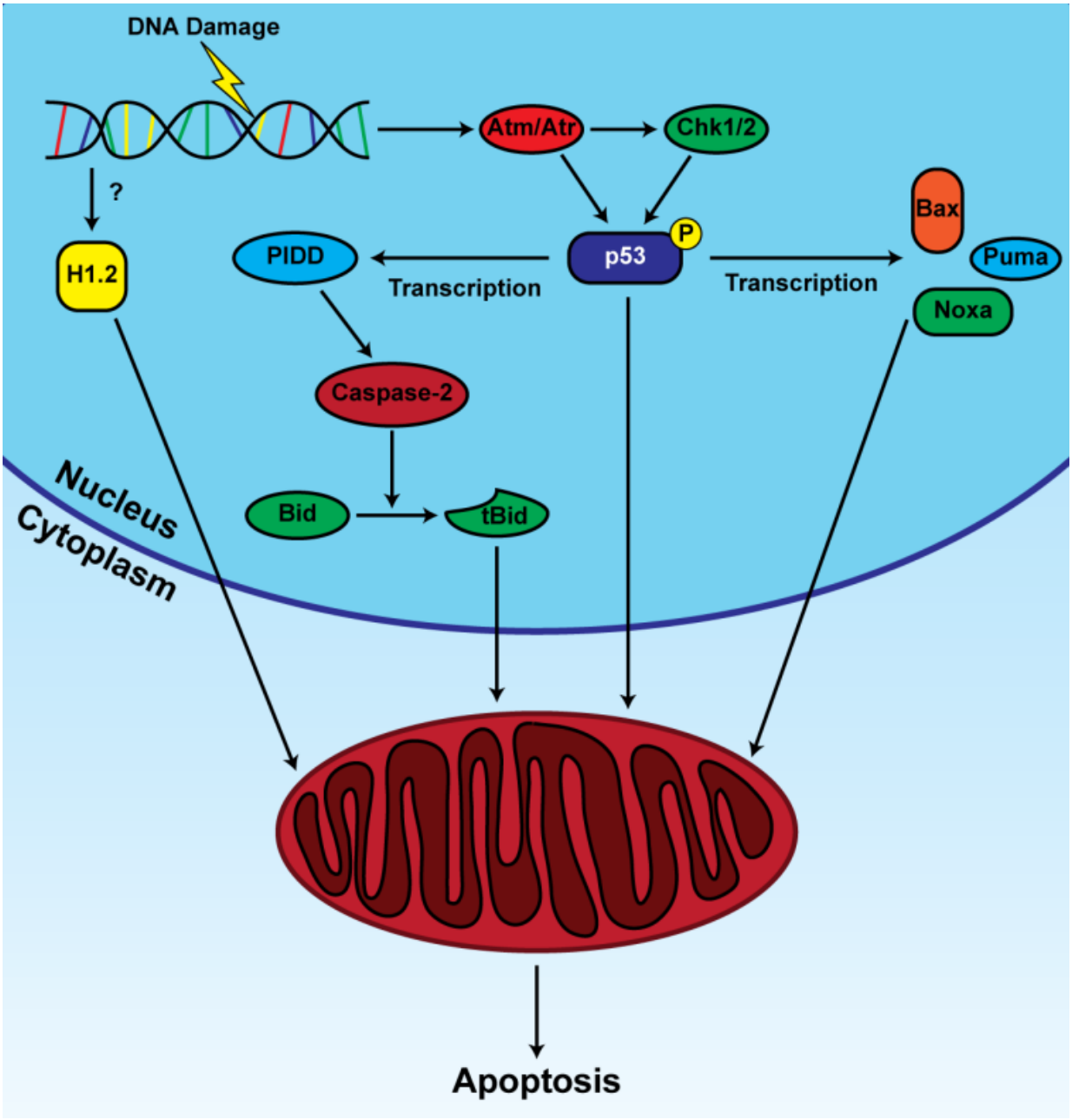

Figure 1-12. DNA damage induced apoptosis. In conditions of unresolvable DNA damage, cells may undergo DNA damage-induced apoptosis. DNA damage-induced apoptosis is mediated largely through activation of the transcription factor p53, which is stabilized upon phosphorylation by ATM/ATR or Chk1/2. p53 regulates transcription of numerous target genes, both directly and indirectly, including the pro-apoptotic Bcl-2 family proteins Bax, Puma, and Noxa which translocate to the mitochondria to promote MOMP and apoptosis. p53 induced death domain protein (PIDD) is also upregulated by p53 and promotes activation of the nuclear caspase, Caspase-2. Caspase-2 can cleave Bid to tBid, which then translocates to the mitochondria to activate apoptosis. Although the mechanism of activation is unclear, histone H1.2 has also been shown to be released from chromatin following DNA damage, allowing it to translocate to the mitochondria where it promotes Cytochrome *c* release and apoptosis.

Bid function in the DNA damage response

In addition to its pro-apoptotic function, Bid is now recognized to have a critical role in promoting the DNA damage response to multiple types of DNA damage. Early studies of Bid deficient mice demonstrated that Bid is required for maintaining normal myeloid cell homeostasis *in vivo*. As *Bid -/-* mice age, they developed a chronic myelomonocytic leukemia-like (CMML) pathology characterized by hepatosplenomegaly and multiple clonal chromosomal abnormalities (e.g. trisomy and translocations) (135). These findings indicate that Bid functions as a tumor suppressor *in vivo*. Later studies revealed that Bid deficient myeloid and lymphoid cells were sensitized to multiple DNA damaging agents including mitomycin c, hydroxyurea, and etoposide (1, 2). Indeed, *Bid -/-* cells displayed increased chromosomal damage, a defective S-phase checkpoint, and increased sensitivity to DNA damage-induced apoptosis (1, 2), suggesting that Bid regulates the DDR. In addition, DNA damage induced the localization of Bid to the nucleus as well as the ATM/ATR mediated phosphorylation of Bid at serines 61, 64, and 78 (1, 2). Phosphorylation of Bid is also required for induction of the DNA damage induced S-phase checkpoint and to protect from DNA damage induced apoptosis (1, 2). In contrast to Bid's pro-apoptotic function, a functional BH3 domain is not required to elicit Bid's function in the DDR (1). These findings revealed a novel and functionally distinct role for Bid in facilitating activation of the DDR.

The nuclear localization of Bid and its phosphorylation by ATM/ATR suggested that Bid may regulate the function of components of the DDR at sites of DNA damage. Indeed, results from our laboratory demonstrated that Bid was required for the accumulation of ATR/ATRIP on the chromatin following treatment with hydroxyurea (HU) (4). Bid deficient cells also displayed reduced activation of ATR activity following HU treatment characterized by decreases in Chk1

phosphorylation, Cdc25A phosphorylation/degradation, p53 phosphorylation/stabilization, and RPA32 phosphorylation (4). Our laboratory further demonstrated that Bid was present in a complex containing ATR/ATRIP and RPA, suggesting that Bid may regulate ATR activity and DDR signaling through interacting with components of the DNA damage-sensing complex (4). Indeed, structure-function studies demonstrated that Bid was able to directly interact with ATRIP through an interaction interface consisting of helix 4 of Bid and the coiled-coil domain of ATRIP (4). Consistent with these findings, Bid mutated in the helix 4 interaction face was unable to restore the normal chromatin accumulation of ATRIP/ATR, ATR activity, or the S-phase checkpoint following HU treatment, in contrast to wild type Bid (4). In contrast, the helix 4 mutation had no effect on Bid-mediated cell death function, establishing a separable and functionally distinct role for Bid in the DNA damage response (4).

The interaction of Bid with ATRIP/ATR indicates that Bid is present in the DNA damage sensing complex. Since ATRIP binds to RPA on ssDNA, these results suggested the possibility that Bid could potentially interact with RPA and ATRIP to facilitate ATR recruitment, stability, or activation at stalled replication forks. Indeed, *in vitro* interaction studies and NMR analysis demonstrated that Bid directly interacts with RPA70 through the N terminal basic cleft of RPA70 and an acidic region of Bid's helix 5 (5). Expression of Bid harboring a mutation of the RPA interaction domain (RPA-ID) in Bid deficient U2OS cells has no effect on Bid's pro-apoptotic activity (5). However, Bid deficient cells expressing the RPA-ID mutant remain sensitive to HU treatment, with impaired recovery of S-phase replication, reduced ATR activity, and increased DNA damage (5). Additionally, Bid deficient cells expressing either the RPA-ID mutation or the helix 4 mutation displayed deficient association with chromatin and abnormally low levels of chromatin associated RPA and proliferating cell nuclear antigen (Pcna), a cofactor of DNA

polymerase at the replication fork (5). These findings indicated that Bid is required for stabilization of the replication fork following replication stress (5). Altogether, these data demonstrate a functional interaction of Bid with RPA and ATRIP/ATR that is essential for efficient activation of the DNA damage response to replication stress.

Further studies demonstrated the physiological role of Bid's DNA damage function *in vivo*, particularly in regulating homeostasis of the hematopoietic system. For example, *Bid -/-* mice are more sensitive to HU treatment, displaying increased apoptosis *in vivo* in the Lin^- $Sca1^+Kit^+$ (LSK) hematopoietic stem cells and myeloid progenitor cell (MPC) populations from primary bone marrow (3). Bid deficient LSK cells also displayed increased proliferation, consistent with mobilization of hematopoietic stem cells (HSCs) to replace lost cells that underwent HU induced apoptosis (3). Long-term exposure to HU over a 6 month period caused increased DNA damage in *Bid -/-* primary MPCs as well as exhaustion of the self-renewal function of Bid deficient bone marrow, characterized by depletion of LSK and MPC populations and diminished repopulation ability in competitive transplants into lethally irradiated recipient mice (3). Bid has also been proposed to protect bone marrow *in vivo* during total body irradiation (136). This effect is proposed to be regulated by the ATM mediated phosphorylation of Bid, which then inhibits oxidative stress in HSCs and ultimately controls HSC quiescence and long-term regenerative capacity in the bone marrow (136). In addition to Bid's effect on normal hematopoietic homeostasis, our laboratory has also demonstrated that Bid deficiency can delay the progression of T-cell leukemogenesis in *ATM -/-* mice by sensitizing transformed ATM deficient T-lymphocytes to DNA damage induced apoptosis (257). Taken together, these findings highlight an important function for Bid in maintaining hematopoietic homeostasis through regulating the DNA damage response. Furthermore, these results suggest that Bid may

also be a valuable therapeutic target in sensitizing tumor cells to cell death in certain contexts, especially when combined with chemotherapies that induce DNA damage.

Although Bid is well characterized in the context of apoptosis, emerging evidence indicates that Bid also has important roles in maintaining homeostasis in the absence of an apoptotic stimulus. Indeed, by regulating the DDR, Bid promotes cell survival and recovery from genotoxic stress. Bid's function in the DDR is regulated by its phosphorylation and its association with the DNA damage sensing complexes. However, it is unclear how Bid's phosphorylation regulates its function in the DDR signaling pathway. It also remains undetermined how Bid's localization to sites of DNA damage is regulated. In addition, the role of Bid in regulating cell survival or fitness in the absence of a cellular stress has not been rigorously evaluated. In particular, although Bid regulates mitochondrial physiology in apoptotic conditions, its effect on mitochondrial biology under non-apoptotic conditions is not well studied. In the following chapters, I discuss my studies to determine the contribution of Bid localization and phosphorylation on the DDR. I also discuss the role of Bid in maintaining mitochondrial structure and homeostasis through a mechanism distinct from its pro-apoptotic function.

CHAPTER II

MATERIALS AND METHODS

Cell lines

Hox11-immortalized *Bid* +/+ and *Bid* -/- MPCs were cultured in IMDM medium supplemented with 20% FBS, 100 U/ml penicillin-streptomycin, 2 mM glutamine, 0.1 mM β-mercaptoethanol, and 10% conditioned medium from WEHI cells as a source of IL-3.

To generate MPCs and MEFs expressing exogenous wild type or BH3 mutated Bid, wild type or BH3 mutant mouse Bid was cloned into pOZ-FH-C-hCD25 (258). BH3 mutant Bid, described in (34), harbors mutations in amino acids 93-96 of mouse Bid mutating IGDE to AAAA. BH3-M148T mutants were designed according to the Quickchange II Site-directed mutagenesis Kit (Agilent Technologies) using the pOZ-FH-C-Bid-BH3-mut-hCD25 (described above) as template and the following primers:
5’GGAGAACGACAAGGCCATGCTGATAATGACAATGC3' and
5'GCATTGTCATTATCAGCATGGCCTTGTCGTTCTCC3'. Constructs were co-transfected with retroviral packaging vector into HEK 293T cells to produce retrovirus particles. *Bid* -/- MPCs or MEFs were infected with retrovirus and magnetically sorted for human CD25 expression using mouse anti-human CD25 antibody (eBioscience) and sheep anti-mouse dynabeads (Life Technologies).

To generate MPCs expressing exogenous Bcl-xL, *Bid* +/+ and *Bid* -/- MPCs were transduced with retrovirus carrying pMSCV-IRES-YFP plasmid with cloned hBcl-xL as described above. Bcl-xL expressing cells were enriched by FACS for YFP fluorescence.

Immunoblot Analysis

MPCs were treated as indicated and clarified cell extracts were prepared by lysis in RIPA buffer (10 mM Tris-HCl pH 8.0, 1 mM EDTA, 0.5 mM EGTA, 1% Triton X-100, 0.1% sodium deoxycholate, 0.1% SDS, 140 mM NaCL) supplemented with 1 mM sodium pyrophosphate, 1 μM microcystin, 10 mM sodium fluoride and 1X protease inhibitor cocktail (Roche)followed by centrifugation at 14,000 rcf. Proteins were separated by SDS-PAGE and transferred to PVDF membrane. Immunoblots were probed with the indicated antibodies and developed using chemiluminescent HRP substrate and autoradiography film. Antibodies used for immunoblot included anti-Bid (34), anti-Bid (Santa Cruz), anti-β-Actin (Sigma), anti-Bcl-xL (Santa Cruz), anti-cleaved Caspase-3 (Asp175) (Cell Signaling), anti-Erk2 (Santa Cruz), anti-phospho Erk1/2 (Thr202/Tyr204) (Cell Signaling), Anti-Stat5 (Santa Cruz), anti-phospho Stat5 (Tyr694) (BD Transduction Laboratories), anti-Akt1/2 (Santa Cruz), anti-phospho Akt1 (Ser473) (Millipore),anti-phospho Chk1 (Ser 345) (Cell Signaling), anti-MnSOD (Enzo Life Sciences), Anti-IkB-α (Santa Cruz), anti-histone H3 (Millipore), anti-HRP conjugated anti-rabbit (GE Healthcare), and HRP conjugated anti-mouse (Pierce).

IL-3 withdrawal and cell death assays

Cells were washed 2 times in calcium and magnesium free 1X PBS (sigma) and suspended in IMDM growth medium lacking WEHI conditioned medium (IL-3). Cells were incubated at 37^{o}C in 5% CO_2 for the indicated times prior to analysis. To assess cell viability, treated cells were incubated with Annexin V-FITC (Biovision) for 30 minutes in 1X Annexin V staining buffer (10 mM HEPES, pH 7.4, 140 mM NaCl, 2.5 mM $CaCl_2$). Immediately prior to analysis, propidium iodide (Sigma) was added to a final concentration of 1 μg/ml. Samples were analyzed on a Becton-Dickinson flow cytometer and FlowJo analysis software.

TNF-α/Actinomycin D death assays were performed by treating cells with 25 ng/ml TNF-α and 50 ng/ml Actinomycin D in complete IMDM growth medium. Cells were incubated during treatment and analyzed as described above.

To assess cell viability of *Bid* +/+ and *Bid* -/- MPCs expressing pMSCV-hBcl-xL-IRES-YFP, samples were gated on YFP positive cells before determining Annexin V/PI positivity.

To assess viability of Bid/BH3-mut MPCs, samples were stained first with PE conjugated anti-human CD25 antibody (Life Technologies) for 30 minutes then with Annexin V-FITC as described above. Samples were gated on CD25 positive cells and analyzed for Annexin V positivity.

Caspase activity assays

To measure DEVDase activity (Caspase-3-like activity) in MPCs, 1 million cells were treated as indicated and lysed in 50 μl of lysis/assay buffer (50 mM Tris-HCl pH7.5, 0.3% NP-40, and 1 mM DTT) for 30 minutes on ice. Lysates were sonicated briefly and clarified by centrifuging at 10,000 rcf. Protein concentration of clarified lysates was determined by Bradford assay then 200 μg of lysates were diluted into a final volume of 100 μl of lysis/assay buffer in a 96 well flat bottom plate. DEVD-pNA (BioVision) was added to a 200 μM final concentration for each sample then the plate was sealed and incubated for 90 minutes in a 37^{o}C incubator. The relative DEVDase activity was determined by measuring absorbance at 405 nm in a microtiter plate reader.

Cell growth analysis and BrdU incorporation

The growth rate of *Bid* +/+ and *Bid* -/- MPCs was determined by plating 1 X 10^6 cells at a density of 1 X 10^5 cells/ml in culture medium. Cells were incubated in 5% CO_2 at 37^{o}C for 3 days and viable cell numbers were determined at 24 hour intervals via trypan blue exclusion.

BrdU incorporation of *Bid* +/+ and *Bid* -/- MPCs was performed according to the BrdU flow kit (BD). Briefly, 2 X 10^6 MPCs were pulse labeled with 10 μM BrdU for 45 minutes. Cells were fixed and permeabilized using BD cytofix/cytoperm buffer, then incubated with BD cytoperm permeabilization buffer plus. Cells were re-fixed with BD cytofix/cytoperm buffer and treated with 30 μg of DNase for 1 hour at 37^{o}C to expose incorporated BrdU. Cells were then incubated with FITC-conjugated anti-BrdU antibody (eBioscience) for 20 minutes at room temperature. BrdU incorporation was determined using a Becton-Dickinson flow cytometer and analyzed using FlowJo analysis software.

Immunofluorescence and confocal microscopy

Bid -/- MEFs stably expressing FLAG-HA tagged wild type Bid were plated and grown on coverslips for 24 hours prior to staining. MEFs were stained with 300 nM MitoTracker Red CMXRos (Life Technologies) for 15 minutes at 37^{o}C prior to fixation with 3:1 MeOH:Acetone for 10 minutes at -20^{o}C. Cells were washed in PBS and blocked for 1 hour at room temperature in 5% NGS in PBS. Cells were stained with alexa-488 conjugated mouse anti-HA antibody (Life Technologies). Cells were then incubated in 300 nM TO-PRO-3 (Life Technologies) for 20 minutes at room temperature prior to imaging. Confocal imaging was performed using a Zeiss LSM 510 META Inverted Confocal Microscope. Image analysis and Z-stack 3D projections were performed using Image J and Zeiss LSM Image Browser software. For Bid localization studies during DNA damage, MEFs were plated and grown on coverslips for 24 hours, then treated for the indicated times with 1 mM hydroxyurea, 2.5 μM etoposide, or 10 Gy ionizing radiation. Cells were then stained and prepared for confocal imaging as described above.

Methylcellulose Culture

Methylcellulose culture was performed as previously described (135). Briefly, bone marrow was harvested from femurs and tibias of *Bid* +/+ and *Bid* -/- mice and erythrocytes were lysed in RBC lysis buffer (100 μM Tris pH 7.5, 155 mM NH_4CL). For each plate, 5 x 10^4 bone marrow cells were resuspended in methocult H4100 (StemCell Technologies) supplemented with 20% FBS, BSA, 0.1 mM β-mercaptoethanol, 1.5 mM L-glutamine, 100 U/ml penicillin, 100 μg/ml streptomycin, 10 μg/ml insulin (Sigma), and 1.5 mg/ml transferrin (Sigma) as well as the following cytokines: 0.4 μg/ml rhSCF (R&D), 80 ng/ml rmIL-3 (R&D), 80 ng/ml rmIL-6 (R&D), and 0.02 U/ml erythropoietin (R&D). For cultures grown in reduced IL-3, IL-3 concentration was added to a final concentration of 40 ng/ml. Cultures were incubated in 5% CO_2 at 37^{o}C for 1 week, and colonies were identified by morphology and quantified. For replating, methylcellulose cultures were collected and cells were washed free of methylcelluose in PBS. Following removal of methylcellulose, 5 x 10^4 cells were re-plated as before, maintaining the same treatment conditions between each set of plates.

Cell cycle and Bid-RPA co-localization analysis of synchronized MEFs

MEFs were synchronized by incubation in IMDM medium with 0.1% FBS for 24 hours. Medium was then replaced with fresh medium supplemented with 10% FBS and cells were incubated for 18 hours to allow entry into S-phase. During the final hour of incubation, cells were treated with either 1 mM hydroxyurea or vehicle (PBS). Cells were collected, washed in PBS, and resuspended in cold 70% ethanol. Cells were washed again, then resuspended in staining solution (0.1% Sodium citrate, 0.03% NP-40, 0.05 mg/ml propidium iodide, and 0.02 mg/ml RNAse A) and incubated in the dark for 30 minutes. DNA content was determined by flow cytometry analysis of PI staining intensity.

For Bid-RPA co-localization analysis, MEFs synchronized and treated as above were fixed with 3:1 MeOH:Acetone for 10 minutes at -20^{o}C and stained with alexa-488 conjugated mouse anti-HA antibody (Life Technologies), rat anti-Rpa32 antibody (Cell Signaling), and Alexa Fluor 546 conjugated goat anti-rat IgG antibody (Invitrogen). DNA was counterstained with 300 nM TO-PRO-3 (Life Technologies) for 20 minutes at room temperature prior to imaging.

Nuclear-cytoplasmic localization analysis

Bax-/- Bak-/- MEFs stably expressing FLAG-HA tagged wild type Bid were plated and grown on cover slips for 24 hours. MEFs were treated with 2 ng/ml Leptomycin B, 1 mM HU, or with Leptomycin B and HU in combination for 1 hour. During the final 15 minutes of treatment 300 nM MitoTracker Red CMXRos (Life Technologies) was added. Following treatment, MEFs were fixed with 3:1 MeOH:Acetone for 10 minutes at -20^{o}C and stained with alexa-488 conjugated mouse anti-HA antibody (Life Technologies) or with rabbit anti-IkB-α (Santa Cruz) and Alexa Fluor 488 conjugated goat anti-rabbit IgG antibody (Invitrogen). DNA was counterstained with 300 nM TO-PRO-3 (Life Technologies) for 20 minutes at room temperature prior to imaging.

For quantitative analysis of the nuclear:cytoplasmic ratio of IkB-α, four 20x magnification images were collected for each treatment condition for analysis. For analysis of the nuclear:cytoplasmic ratio of Bid, eleven 20x magnification images were collected for each treatment condition. Quantitative analysis of images was performed using auto isodata binary threshold image analysis (259) and image subtraction approach to isolate and quantify fluorescence intensity in the nuclear and cytoplasmic compartments. All images were processed using ImageJ by first applying a median filter on the blue (TO-PRO-3) and green (HA or IkB-α) fluorescence channels. The resulting images were processed with an isodata threshold, using the

same threshold for all images for each channel, to produce binary threshold masks for HA/IkB-α (green threshold mask) and TO-PRO-3 (nuclear threshold mask). Image subtraction was used as follows: (1) green threshold mask – nuclear threshold mask = cytoplasmic threshold mask, (2) unprocessed green fluorescence channel – nuclear threshold mask = cytoplasmic green fluorescence, and (3) unprocessed green fluorescence channel – cytoplasmic threshold mask = nuclear green fluorescence. To determine the nuclear and cytoplasmic fluorescence intensity, the integrated density of the cytoplasmic and nuclear green fluorescence was collected. The nuclear to cytoplasmic ratio (N:C ratio) was determined by dividing the nuclear integrated density by the cytoplasmic integrated density.

High Resolution Respirometry

To determine the basal respiration rate of *Bid +/+, Bid -/-*, and Bid/BH3-mut MPCs, oxygen consumption rates (OCR) were measured in an Oroboros O2K oxygraph (Oroboros Instruments). For each genotype, 2 X 10^6 viable cells, determined by trypan blue exclusion, were added to oxygraph chambers containing 2 ml of IMDM culture medium. The average OCR was measured over a 5 minute interval of stable oxygen flux following addition of cells to the chamber.

To determine the spare respiratory capacity, the basal respiration rate of MPCs was measured in MiRO5 buffer (0.5 mM EGTA, 3 mM $MgCl_2$, 60 mM K-lactobionate, 20 mM taurine, 10 mM KH_2PO_4, 20 mM HEPES, 110 mM Sucrose, and 1 g/L BSA, adjusted to pH 7.1 with KOH) supplemented with 10 mM glutamate, 4mM malate, and 2 mM ADP. Following measurement of basal respiration, the cells were treated sequentially with 0.5 μM oligomycin, 0.5 μM FCCP, and combined addition of 1 μM antimycin A/1 μM Rotenone. Prior to, and between treatments, the oxygen flux was permitted to stabilize to allow measurement of the average OCR for each interval. To determine the spare respiratory capacity, the basal respiration rate (untreated) was

subtracted from the difference of uncoupled respiration (FCCP) and non-mitochondrial respiration (antimycin/rotenone) [(uncoupled – non-mitochondrial) – basal = Spare respiratory capacity].

To measure basal respiration of cardiac myocytes, 2-3 mg of heart fibers isolated as described below were added to Oroboros O2K oxygraph chambers containing MiRO5 buffer supplemented with 10 mM glutamate, 4 mM malate, and 2 mM ADP. Respiration rate was determined during stabilized oxygen flux before and after 45 minutes of CL-liposomes treatment as indicated.

A procedure adapted from (182) was used to measure OMM permeabilization of mouse liver mitochondria by digitonin. Mitochondria were isolated from *Bid* +/+ mouse liver as described above and immediately following isolation, 600 μg of mitochondria were added to the chambers of an Oroboros O2K oxygraph containing 2 ml of MiRO5 buffer. State 3 respiration was stimulated by supplementation with 10 mM glutamate, 4 mM malate, and 2 mM ADP. Following stable state 3 respiration, 50 μg/ml digitonin (Sigma) was added to oxygraph chambers and monitored until oxygen flux stabilized. To restore mobilized cytochrome c loss, chambers were supplemented with 10 μM exogenous cytochrome c.

Mitochondrial Isolation

Mouse liver mitochondria were isolated using a protocol adapted from Brookes *et al* (260). Briefly, livers were harvested from 6-12 week old adult female mice and placed in ice cold isolation buffer (200 mM sucrose, 5 mM HEPES-KOH, pH 7.4, and 1 mM EGTA). Livers were homogenized in a glass-glass dounce homogenizer with 12 passes of a high clearance (A) pestle and 2 passes of a low clearance (B) pestle. The homogenized tissue was centrifuged at 1,000 rcf for 10 minutes at 4^{o}C. The clarified supernatant was centrifuged at 10,000 rcf for 10 minutes at 4^{o}C and the light fraction of the pellet was removed. The heavy membrane fraction was

resuspended in ice cold isolation buffer and centrifuged at 10,000 rcf for 10 minutes at 4°C. The mitochondrial pellet was then resuspended and the protein concentration was determined by Bradford assay.

Mitochondria were isolated from MPCs as described in (261). Briefly, 6 X 10^6 MPCs were washed with PBS, centrifuged at 600 rcf for 10 minutes, and resuspended with isolation solution (250 mM sucrose, 20 mM HEPES-KOH, pH7.5, 10 mM KCl, 1.5 mM $MgCL_2$ 1 mM EDTA, 1 mM EGTA, 1 mM dithiothreitol, 0.1 mM PMSF). Suspended cells were homogenized with a glass-glass dounce homogenizer with 20 passes of the pestle. The homogenized cells were centrifuged at 750 rcf for 10 minutes at 4°C. The supernatant was collected, and the pellet resuspended in isolation solution and centrifuged at 750 rcf for 10 minutes at 4°C. The two supernatants were pooled and centrifuged at 10,000 rcf for 15 minutes at 4°C. The mitochondrial pellet was then resuspended in isolation solution.

Saponin-permeabilized cardiac fibers preparation

For CL-liposomes treated cardiac myocytes, respiratory parameters were studied *in situ* in saponin-permeabilized fibers isolated from left ventricle (262). Hearts were collected from *Bid* +/+ and *Bid* -/- mice and the left ventricles were excised in ice-cold growth medium (IMDM medium, 20% FBS, 100 U/ml penicillin-streptomycin, 2 mM glutamine, 0.1 mM β-mercaptoethanol, and 10% conditioned medium from WEHI cells). Heart fibers were isolated by mechanical dissection. Briefly, fibers (5–7 mm length, 0.3–0.5 mm width, and 100–250 μm diameter) were prepared in ice-cold relaxation and preservation solution (2.77 mM CaK_2EGTA, 7.23 mM K_2EGTA, 6.56 mM $MgCl_2$, 5.7 mM Na_2ATP, 14.3 mM phosphocreatine, 20 mM taurine, 0.5 mM dithiothreitol, 50 mM K-MES and 20 mM imidazole, pH 7.1). Fibers were permeabilized by incubation at 4 °C for 20 minutes in relaxation and preservation solution

containing 50 μg/ml saponin. Finally, fibers were transferred into MiRO5 buffer prior to use in downstream applications.

Stat5, Akt, and Erk1/2 expression and phosphorylation following IL-3 stimulation

To investigate Stat5, Erk1/2, and Akt levels and phosphorylation state in *Bid* +/+ and *Bid* -/- MPCs, cells were plated in medium lacking serum and WEHI conditioned medium for 6 hours in order to establish an unstimulated state. WEHI conditioned medium was then added to the cells to 10% of the total volume as a source of IL-3. At the indicated timepoints following IL-3 stimulation, whole cell extracts were prepared from 1 X 10^6 PBS washed cells. Lysates were analyzed by immunoblot using the indicated antibodies as described above.

Cardiolipin quantitation by liquid chromatography-electrospray ionization tandem mass spectrometry (LC/ESI/MS/MS).

Analysis of cardiolipin content was performed as previously described (263). Briefly, lipids were extracted from MPCs (6 X 10^6), tissue (20 mg of saponin-permeabilized cardiac fibers), or mitochondria (isolated from 6 X 10^6 MPCs) by addition of 0.75% NaCl and chloroform:methanol (2:1, v:v) containing 0.1 mM butyrated hydroxytoluene, 0.1 mM triphenylphosphine, and 2.5 μg tetra-myristeoylcardiolipin (M_4CL) as an internal standard. The organic phase was evaporated and resuspended in methanol:acetonitrile:H_2O (60:20:20, v:v:v) and stored at -80^{o}C until analysis. The extracted lipids were separated online by UPLC using a Waters Acquity UPLC system (Waters). Analysis was performed using a Thermo Quantum Ultra triple quadrupole mass spectrometer (Thermo Scientific) operated in negative ion mode using selective reaction monitoring (SRM). Nitrogen was used as the sheath gas at 38 p.s.i. and the capillary temperature was 350^{o}C. The spray voltage was 4.5 kV and the tube lens voltage was 100 V. Data analysis was performed using Xcalibur software, version 2.0. The following ions

were monitored in SRM: M_4CL, m/z 619.6-227.2; L_4CL, m/z 723.6-279.2; and LO_3CL, m/z 726.5-281.2.

To quantitate the relative amounts of CL species, the area under the curve (AUC) was determined for M_4CL, L_4CL, and LO_3CL and the AUC of L_4CL or LO_3CL were normalized to the AUC of M_4CL. The normalized values represent the relative abundance of L_4CL and LO_3CL and normalized values were also used to calculate the ratio of L_4CL: LO_3CL.

Cardiolipin liposome preparation and treatments

To prepare cardiolipin liposomes, purified bovine heart cardiolipin (Avanti Polar Lipids) and 1, 2-Dioleoyl-sn-glycero-3-phosphocholine (DOPC) (Avanti Polar Lipids) were combined in a 1:1 molar ratio and dried under argon. Lipids were then resuspended in either complete growth medium or in MiRO5 supplemented with glutamate (10 mM), Malate (4 mM), and ADP (2 mM). The suspension was then sonicated on ice using a misonix ultrasonic liquid processor on a setting of 3 with two 10 second pulses. Liposomes were added to a final CL concentration of 125 μM (125 μM CL:125 μM DOPC). CL composition was measured after 30 minutes treatment with CL-liposomes and basal oxygen consumption rate was evaluated after 45 minutes of treatment. The effect of DOPC-liposomes on oxygen consumption rate was determined by treatment with 125 μM DOPC liposomes alone.

In regards to removing excess liposomes for LC/ESI/MS/MS experiments, intact cells, isolated mitochondria, and permeabilized fibers were washed twice with PBS before lipid extraction.

Bid knock-down and transient Bid expression in MPCs

For Bid knock-down experiments, 1 X 10^7 *Bid* +/+ MPCs were nucleofected with 300 pmol of either negative control siRNA (Qiagen) or mouse Bid siRNA (SI00929103, Qiagen). Transient expression of human Bid in *Bid* +/+ MPCs was performed by nucleofection of 1 X 10^7 *Bid* +/+

MPCs with 20 μg of pCDNA3 vector expressing wild type human Bid (pcDNA3-hBid). Co-nucleofection was performed using both mouse Bid siRNA and pCDNA3-hBid. All nucleofections were performed using the Mouse ES Cell Nucleofector Kit (Lonza) and program A-030 of the nucleofector 2b system (Lonza). Extracts from nucleofected cells were analyzed for Bid expression by immunoblot 48 hours post-nucleofection. Basal respiration rate was measured for 2 X 10^6 cells 72 hours post-nucleofection in complete medium as described above.

Cytochrome c mobility assays

Mitochondria were isolated from *Bid* +/+ and *Bid* -/- mice as described above and diluted to a final concentration of 0.3 μg/μl in mitochondrial isolation buffer (200 mM sucrose, 5 mM HEPES-KOH, pH 7.4, and 1 mM EGTA). Cytochrome c mobilization was determined using a protocol adapted from (182). Diluted mitochondria were either left untreated or were treated with 50 μg/ml digitonin for 45 minutes at 37^{o}C or with 0.5% triton X-100 for 45 minutes on ice (as a measure of total cytochrome c content). Mitochondria were centrifuged at 12,000 rcf for 3 minutes and supernatants collected for analysis of cytochrome c content using the rat/mouse cytochrome c Quantikine ELISA kit (R&D systems) according to the manufacturer's protocol. Cytochrome c levels from untreated and digitonin treated mitochondrial supernatants were normalized to 0.5% triton X-100 treated supernatants to determine the percent of mobilized cytochrome c.

Electron Microscopy and Image Quantitation

A total of 4 x 10^6 cells per sample were prepped for TEM and imaged in the Vanderbilt Cell Imaging Shared Resource-Research Electron Microscope facility. Cells were washed with 0.1 M cacodylate buffer and fixed in 2.5% gluteraldehyde/0.1M cacodylate for 1 hour at room temperature and left at 4°C overnight. The samples were post-fixed in 1% osmium tetraoxide and

washed 3 times with 0.1 M cacodylate buffer. The samples were dehydrated through a graded ethanol series followed by incubation in 100% ethanol and propylene oxide (PO) as well as 2 exchanges of pure PO. Samples were embedded in epoxy resin and polymerized at 60°C for 48 hours.

For each sample, 70-80 nm ultra-thin sections were cut and mounted on 300-mesh copper grids. Two sections per sample were stained at room temperature with 2% uranyl acetate and lead citrate. Imaging was done on a Philips/FEI Tecnai T-12 high resolution transmission electron microscope with a side mounted 2k x 2k AMT CCD camera. A total of 40 images were captured per cell type, 20 images from one grid and 20 from another. All images were taken at a magnification of 30,000x. Five different grid squares per section were chosen at random, and the first 4 cells that came into view were imaged.

Quantification was performed with FIJI ((Fiji Is Just) ImageJ) software utilizing a stereology plugin (Version 0.1) to create a multipurpose stereological grid (264). Horizontal grid lines were overlaid on each image using the same tile density setting for all samples. The end of each line was considered to be one point and points on the grid were counted as nucleus, extracellular space, cytoplasm or mitochondria. Total reference points per image were considered to be everything except nucleus and extracellular space. Cristae were counted when intersecting the grid line or point, and each crista was counted twice to account for double membranes. Data is represented as either area density (equivalent to volume density), which is the number of mitochondria divided by the number of reference points. Length density was calculated as 2 times the number of cristae intersections divided by the total length of line for all possible intersections. Representative mitochondrial images shown were cropped and scale bars added utilizing Adobe Photoshop.

Nuclear fractionation and immunoprecipitation of Bid

Bid +/+ and *Bid* -/- MPCs were treated for 30 minutes with 10 mM hydroxyurea then washed twice in PBS and resuspended in isolation buffer composed of 10 mM HEPES, pH7.9, 10 mM KCl, 340 mM sucrose, 1.5 mM $MgCl_2$, 10% glycerol, phosphatase inhibitors (1 mM sodium pyrophosphate, 1 μM microcystin, and 10 mM sodium fluoride), and a protease inhibitor cocktail (Roche). Cells were treated with 0.05% NP-40 for 5 minutes and centrifuged at 1,300 rcf for 5 minutes and the supernatant cytosol and nuclear pellet were separated. Nuclei were washed and centrifuged twice in isolation buffer, centrifuged at 1,300 rcf for 5 minutes, and resuspended in IP buffer composed of 25 mM HEPES, pH7.5, 250 mM NaCL, 2 mM EDTA, 0.5% NP-40, 10% glycerol, phosphatase inhibitors (1 mM sodium pyrophosphate, 1 μM microcystin, and 10 mM sodium fluoride), and 1X protease inhibitor cocktail (Roche). Nuclei were lysed by sonication and then pre-cleared with streptavidin agarose beads (Novagen) for 30 minutes. Pre-cleared nuclear lysate was then incubated for 1 hour with biotinylated goat anti-Bid IgG (R&D) followed by 1.5 hours with streptavidin agarose beads (Novagen). For the indicated samples, beads were washed twice with IP buffer without phosphatase inhibitors and incubated for 30 minutes at 30^{o}C with 2.5 units of PP1 phosphatase (New England Biolabs) in 1X PP1 buffer (50 mM HEPES, pH 7.5, 10 mM NaCl, 2 mM DTT, 0.01% Brij 35, and 1 mM MnCl2). Immunoprecipitated protein was collected by direct addition of SDS-PAGE loading buffer to beads and boiling for 10 minutes prior to loading on SDS-PAGE. All steps were performed at 4^{o}C unless otherwise specified.

For immunoblot analysis of the effect of PP1 on Bid phosphorylation in whole cell lysates, *Bid* +/+ and *Bid* -/- MPCs were treated with 10 mM hydroxyurea or vehicle (PBS) for 30 minutes and lysed in RIPA buffer for 30 minutes on ice. PP1 buffer (10X) was added to lysates to 1X

concentration and lysates were incubated with 2.5 units PP1 phosphatase (New England Biolabs) for 30 minutes at 30^{o}C. Samples were then run on SDS-PAGE and immunoblots were probed with the indicated antibodies.

Heart failure and echocardiography

Echocardiograms were performed under 2-3% isoflurane anesthesia using a VisualSonics Vevo 770 instrument housed and maintained in the Vanderbilt University Institute of Imaging Science core lab. Measurements of the left ventricular internal diameter end diastole (LVIDd) and the left ventricular internal diameter end systole (LVIDs) were determined from M-mode tracings in triplicate for each mouse immediately before and after IP injection of 30 μg Epinephrine. Hearts were then excised from mice, weighed, and fixed overnight in 10% formalin and embedded in paraffin. Coronal sections of hearts were cut and stained using H&E and Masson trichrome blue stain. Images were taken at 2.6 X and 35 X magnifications using a Nikon AZ100 M and Nikon DS-Ri1 color camera. The LVIDd and LVIDs index was determined by normalizing LVIDd and LVIDs measurements to average heart mass for each genotype.

BID SNP analysis

The human clinical cohort was derived from BioVU, a Vanderbilt University resource that links human DNA samples and genetic data to de-identified electronic medical records (EMRs). The development of BioVU has been previously described (265). Briefly, the biobank houses DNA from unused blood specimens collected during clinical care at Vanderbilt University Medical Center. Currently, DNA samples are available for >190,000 unique subjects. Genotyping was performed with the Illumina HumanExome BeadChip v1 by the Vanderbilt DNA resources core (VANTAGE) using standard quality control procedures.

Pre-specified clinical syndromes of cardiac injury were heart failure and myocardial infarction. Phenotypes were defined by extraction of International Classification of Disease (ICD9) billing codes and application of a code translation table used for phenome-wide association scanning (PheWAS), a validated method of mapping ICD9 codes to clinical phenotypes within the EMR environment (266, 267).

The three-dimensional structure of human Bid was made using Protein Workshop version 4.2.0 (268) using the solution structure of human Bid published in (114).

Statistical Analysis

Analyses of genotype-phenotype associations were performed using the R statistical package. Due to the individual rarity of variants, SNPs were collapsed prior to association testing. Pre-specified SNP groupings were: 1) presence of one or more of any genotyped missense variants in the *BID* gene, and 2) presence of one or more genotyped SNPs in the MBD. Association testing between SNPs and clinical phenotypes was performed using multivariable logistic regression with age, gender, systolic blood pressure, cholesterol levels, body mass index (BMI), and hemoglobin A1C included as covariates (in the case of heart failure, prior myocardial infarction was also included as a covariate). A Bonferroni correction was applied to account for multiple testing, resulting in an adjusted p-value for significance of 0.0125.

Graphs and statistical analysis were completed using GraphPad Prism software. Data were analyzed by either an unpaired or paired, two-tailed student's T-test for statistical comparisons of two means for unpaired or paired data, respectively. For statistical analysis of more than two means with a single grouping parameter, data were analyzed by one-way ANOVA with Tukey's multiple comparisons post-test. For statistical analysis of multiple means with multiple grouping parameters, data were analyzed using a two-way ANOVA, a two-way

ANOVA with Tukey's multiple comparisons post-test, or a repeated measures two-way ANOVA with Bonferroni's multiple comparisons post-test as appropriate. Within each experiment, all pairwise comparisons were made and all relevant and significant comparisons are indicated on the figures or in figure legends. ns = not significant, * = $P < 0.05$, ** = $P < 0.01$, *** = $P < 0.005$, **** = $P < 0.001$, error bars indicate SEM.

Study Approval

This study was approved by the IACUC of Vanderbilt University Medical Center in compliance with NIH guidelines for the use of experimental animals. Human blood and tissue samples were obtained with written informed consent under protocols approved by the Vanderbilt University Medical Center IRB.

CHAPTER III

BID PRESERVES MITOCHONDRIAL HOMEOSTASIS, CARDIOLIPIN COMPOSITION, AND PROTECTS AGAINST STRESS INDUCED CARDIAC DYSFUNCTION

Introduction

The members of the Bcl-2 protein family exert their key regulatory function in the mitochondrial apoptosis pathway through interaction and structural reorganization of the mitochondrial outer membrane. During apoptosis, death stimuli induce the translocation of BH3-only proteins to the mitochondria where they activate Bax and Bak to induce mitochondrial outer membrane permeabilization (MOMP) (90, 183). MOMP then results in the cytosolic release of Cytochrome c, an irreversible step in the execution of apoptosis.

Bid, a BH3-only member of the Bcl-2 family, is a potent activator of MOMP and apoptosis in *in vitro* assays (92) that significantly alters mitochondrial structure and physiology. Apoptotic activation of Bid occurs by caspase-mediated proteolysis to generate truncated Bid (tBid). tBid associates with the outer mitochondrial membrane (OMM) (90) and this association minimally requires a membrane binding domain (MBD) spanning helices 4, 5, and 6 (184). At the OMM, tBid interacts with other Bcl-2 family members through its BH3 domain to elicit apoptosis. tBid also impacts mitochondrial structure by inducing significant structural remodeling of cristae, thereby opening cristae junctions and promoting mobilization of Cytochrome c from the cristae to the inter-membrane space (IMS) (182). Furthermore, tBid inhibits mitochondrial respiration (269) which is, at least in part, due to disruption of cristae shape (150, 270). While the above studies elucidate how Bid impacts mitochondria during

apoptosis, it remains undetermined whether Bid can influence mitochondrial structure and physiology under non-apoptotic conditions.

The OMM localization (129) and the apoptotic function (130, 132) of tBid is facilitated by the mitochondrial specific phospholipid, cardiolipin (CL). CL is well established in maintaining mitochondrial physiology by regulating inner mitochondrial membrane (IMM) structure, electron transport chain (ETC) activity, oxidative phosphorylation, and apoptosis signaling (146). In mammals, the most prevalent form of CL is tetra-linoleoyl CL (L_4CL), composed of four linoleic acid chains (271). Changes in CL mass or composition disrupt IMM structure and result in decreased respiration (139). CL also directly interacts with Cytochrome c, promoting its association with the IMM (144). Interruption of the CL-Cytochrome *c* interaction, through loss or peroxidation of CL, results in Cytochrome c mobilization which is required for its release into the cytosol during apoptosis (168). Therefore, respiratory efficiency, mitochondrial structure, and control of apoptosis are influenced by CL content and composition. Although it is clear that CL is important for Bid function, the nature of the relationship between Bid and CL is not well understood. Nevertheless, both Bid and CL have significant influence on mitochondrial function through regulating mitochondrial structure and physiology.

Mitochondrial and cardiac function are intimately linked due to the reliance of the heart on oxidative metabolism (272). Cardiac dysfunction can result from either decreased oxygen supply, such as in atherosclerotic heart disease, or from insufficient oxygen utilization (impaired mitochondrial function) at the cellular level. Decreased oxygen utilization efficiency often translates to reduced myocardial function and susceptibility to cardiac injury. This is due to an inability of mitochondria to meet oxygen demand, especially during increased workload (206). Indeed, decreased myocardial respiratory function is closely associated with cardiovascular

diseases, and cardiac pathologies are a prominent feature of genetic disorders of mitochondrial respiration (209). Although much is known about how impaired oxygen supply influences cardiac injury, the impact of impaired oxygen utilization at the cellular level is not well understood.

We report for the first time that Bid is essential to maintain L_4CL levels, normal mitochondrial physiology, and heart function during cardiac stress. Bid deficiency results in malformation of cristae structure, decreased respiration, decreased L_4CL, increased Cytochrome c mobilization, and increased sensitivity to cell death. Furthermore, Bid deficiency results in decreased oxygen utilization efficiency in cardiomyocytes. Consequently, *Bid* -/- mouse hearts are sensitized to left ventricular (LV) dysfunction during increased workload induced by epinephrine. Interestingly, we report that single nucleotide polymorphisms (SNPs) in human *BID*, particularly for those within the MBD, significantly associate with myocardial infarction (MI) in humans. We also show that Bid harboring an inactivating mutation in the BH3 domain, but not Bid mutated in both its BH3 domain and M148T (identified as one of the above MBD SNPs), is sufficient to rescue mitochondrial respiration in *Bid* -/- MPCs. This study reveals a previously unrecognized role for Bid in preserving heart function in conditions of acute cardiac stress by maintaining efficient mitochondrial oxygen utilization in cardiomyocytes. Furthermore, these findings demonstrate that the membrane binding domain of Bid, specifically M148, is crucial for Bid's role in mitochondrial respiration, suggesting that Bid and the M148T SNP may warrant further investigation as a marker for susceptibility to myocardial infarction.

Results

***Bid -/-* MPCs display increased sensitivity to cell death.**

Although Bid is one of the most potent activators of Cytochrome c release in *in vitro* assays and even though multiple lines of evidence support a role for caspase-cleaved Bid (tBID) to promote apoptotic signaling, when we genetically deleted Bid in the germline of mice, we found that myeloid progenitor cells (*Bid -/-* MPCs) from these mice, while protected from death receptor-induced cell death, were more sensitive to multiple other death stimuli (1, 4), consistent with a survival function for Bid in certain situations. Closer examination of the cell death and cell proliferation properties of *Bid -/-* MPCs compared to *Bid +/+* MPCs in culture, even in the absence of a death stimulus, reveals a significantly reduced expansion rate, approximately 50% of *Bid +/+* MPCs (Fig. 3-1A). A reduced expansion rate would is most likely explained by either an increased rate of cell death or a decreased rate of cell growth. *Bid -/-* MPCs display a significant increase in Annexin V/PI staining relative to *Bid +/+* MPCs, indicating an increased sensitivity to cell death due to Bid deficiency (Fig. 3-1B). In contrast, the proliferation rate of *Bid -/-* MPCs is comparable to *Bid +/+* MPCs, as assessed by BrdU incorporation (Fig. 3-1C). Thus, loss of Bid in MPCs results in increased cell death even in the absence of a death stimulus, suggesting that Bid plays a survival role in homeostatic conditions.

To further evaluate how Bid deficiency affects sensitivity to cell death, we assessed cell death kinetics during withdrawal of Interleukin-3 (IL-3), a key cytokine required to support the growth and viability of myeloid cells (273). During IL-3 withdrawal, Bid deficient MPCs display significantly decreased viability compared to *Bid +/+* MPCs (Fig. 3-1D). Overexpression of anti-apoptotic Bcl-xL completely abrogates cell death in both *Bid +/+* and *Bid -/-* MPCs, consistent with apoptosis occurring through the intrinsic pathway (Fig. 3-1D and E).

Furthermore, immunoblot analysis reveals increased Caspase-3 cleavage in *Bid -/-* MPC extracts (Fig. 3-1F). We also observe increased caspase-like activity (DEVDase activity), measured with the caspase substrate DEVD-pNA, in *Bid -/-* MPC extracts after IL-3 withdrawal (Fig. 3-1G). Additionally, *Bid -/-,* but not *Bid* +/+ MPCs, display considerable Caspase-3 cleavage and DEVDase activity in the absence of a death stimulus, further demonstrating a homeostatic role for Bid in maintaining cell viability.

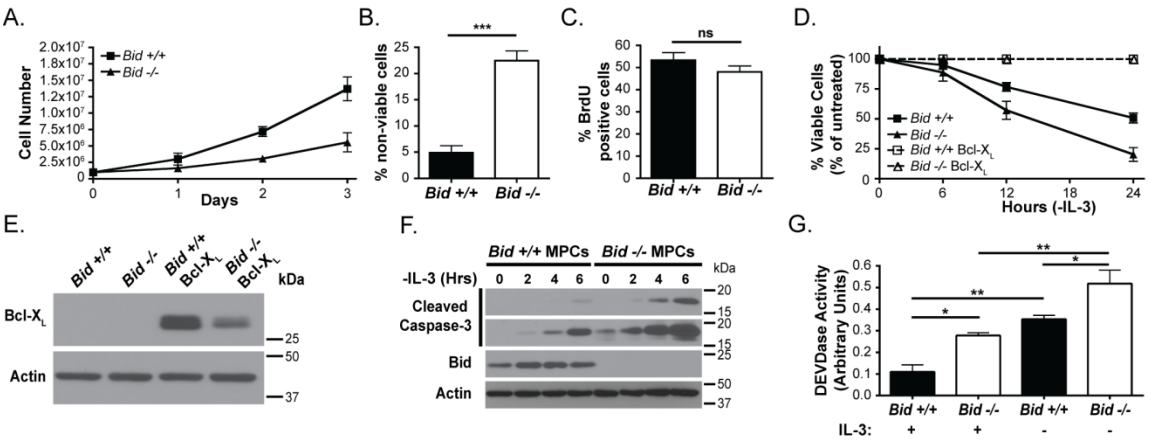

Figure 3-1. Bid protects MPCs from apoptotic cell death.
A) Growth rate of *Bid* +/+ and *Bid* -/- MPCs. B) Percent non-viable cells (Annexin V/PI) in *Bid* +/+ and *Bid* -/- MPCs grown in culture for 24 hours. C) BrdU incorporation of *Bid* +/+ and *Bid* -/- MPCs labeled with 10 μM BrdU for 45 minutes. D) Viability (Annexin V/PI staining) of *Bid* +/+ and *Bid* -/- MPCs, untransduced or transduced with Bcl-xL, in medium lacking IL-3. Data are normalized to cells grown with IL-3. E) Representative immunoblot analysis of Bcl-X_L expression in whole cell lysates of untransduced or Bcl-X_L transduced *Bid* +/+ and *Bid* -/- MPCs. F) Immunoblot of cleaved Caspase-3 in whole cell lysates of *Bid* +/+ and *Bid* -/- MPCs following IL-3 withdrawal. Lower cleaved Caspase-3 immunoblot shows longer exposure. Arrows indicate p19 and p17 Caspase-3 fragments. G) Relative DEVDase (Caspase-3-like) activity for *Bid* +/+ and *Bid* -/- MPCs grown with or without IL-3 for 20 hours. (A-G) N=3, error bars indicate SEM. P values were determined by two-way ANOVA with Tukey's test (A, D, & G), and unpaired student's t-test (B & C).

***Bid-/-* bone marrow displays diminished colony forming ability in methylcellulose.**

To further establish the impact of Bid on the survival, growth rate, and renewal of primary bone marrow myeloid progenitors, we isolated and cultured bone marrow from *Bid* +/+ and *Bid -/-* mice in methylcellulose supplemented with varying amounts of IL-3. At one-week intervals, we quantified CFU-GM (colony forming unit-granulocyte, monocyte) myeloid colonies. *Bid -/-* but not *Bid* +/+ bone marrow display significantly increased GM colony formation in methylcellulose with reduced IL-3 at two and three weeks of culture (Fig. 3-2A-C). These data indicate that Bid supports the colony forming ability of primary bone marrow derived myeloid progenitors in conditions of limiting IL-3 availability.

To further interrogate the role of Bid in IL-3 induced survival, we starved MPCs of IL-3 and serum for 6 hours to establish an unstimulated state and then added back IL-3. We then assessed the expression levels and phosphorylation state of the three key modulators of IL-3 signaling: Stat5, Erk1/2, and Akt (274). Interestingly, *Bid -/-* MPCs display increased expression of both Stat5 and Akt and increased phosphorylation of Stat5, Erk1/2, and Akt following 30 minutes of IL-3 stimulation relative to *Bid* +/+ MPCs (Fig. 3-2D). These data suggest an increase in responsiveness of *Bid -/-* MPCs to IL-3 signaling and a compensatory up regulation of pro-survival signaling pathways.

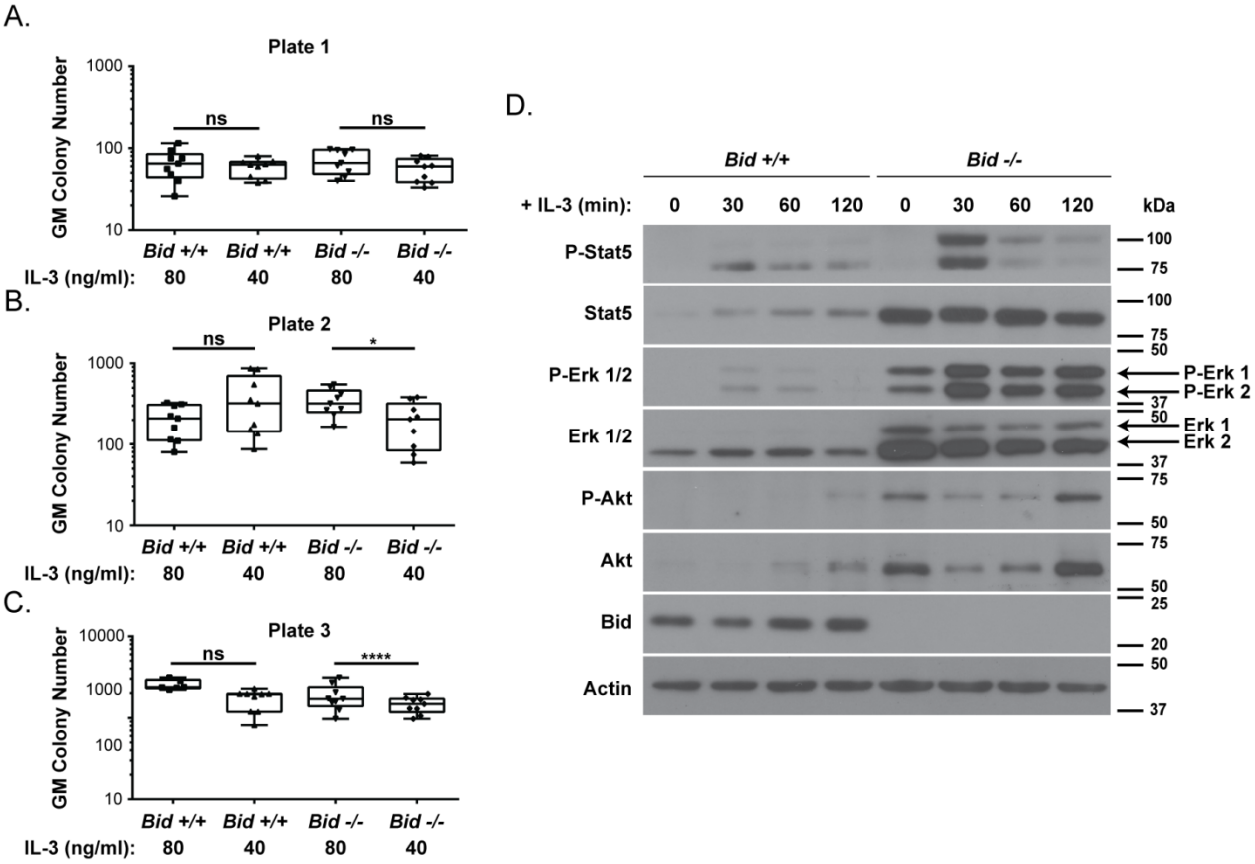

Figure 3-2. Bid deficiency sensitizes bone marrow derived GM progenitors to IL-3 withdrawal and increases Stat5, Akt, and Erk1/2 signaling in MPCs following IL-3 stimulation. First (7 Days, A), second (14 Days, B), and third plate (21 days, C) GM colony counts from *Bid* +/+ and *Bid* -/- bone marrow methylcellulose cultures supplemented with either 40 or 80 ng/ml recombinant IL-3. D) Representative immunoblot analysis of expression and phosphorylation of Stat5, Akt, and Erk1/2 in whole cell lysates of *Bid* +/+ and *Bid* -/- MPCs following stimulation with IL-3. Arrows indicate bands for Erk1, Erk2, phospho-Erk1, and phospho-Erk2. (A-C) N=3. P values were determined by two-way ANOVA with Tukey's test.

Bid localizes to the mitochondria in non-apoptotic conditions.

Considering that Bid primarily functions in apoptosis by regulating mitochondrial integrity, structure, and function, we asked whether Bid is associated with mitochondria in non-apoptotic conditions. We used confocal immunofluorescence microscopy to assess the localization of Bid in *Bid -/-* mouse embryonic fibroblasts (MEFs) retrovirally transduced with FLAG-HA tagged Bid (Fig. 3-3A). Immunofluorescence using anti-HA antibody and the mitochondrial specific dye Mitotracker Red CMXRos, reveals distinct co-localization of Bid and mitochondria in unstressed MEFs (Fig. 3-3B, white arrowheads). Untransduced *Bid -/-* MEFs are negative for HA expression, demonstrating specificity of the staining (Fig. 3-3B, yellow arrowheads). Optical sectioning shows that, while most Bid staining is diffuse and cytosolic, discrete foci of Bid co-localize with mitochondria (Fig. 3-3C) in the absence of a death stimulus. Thus, it is feasible that Bid could localize at or near mitochondria to regulate mitochondrial physiology and consequently regulate cell death sensitivity.

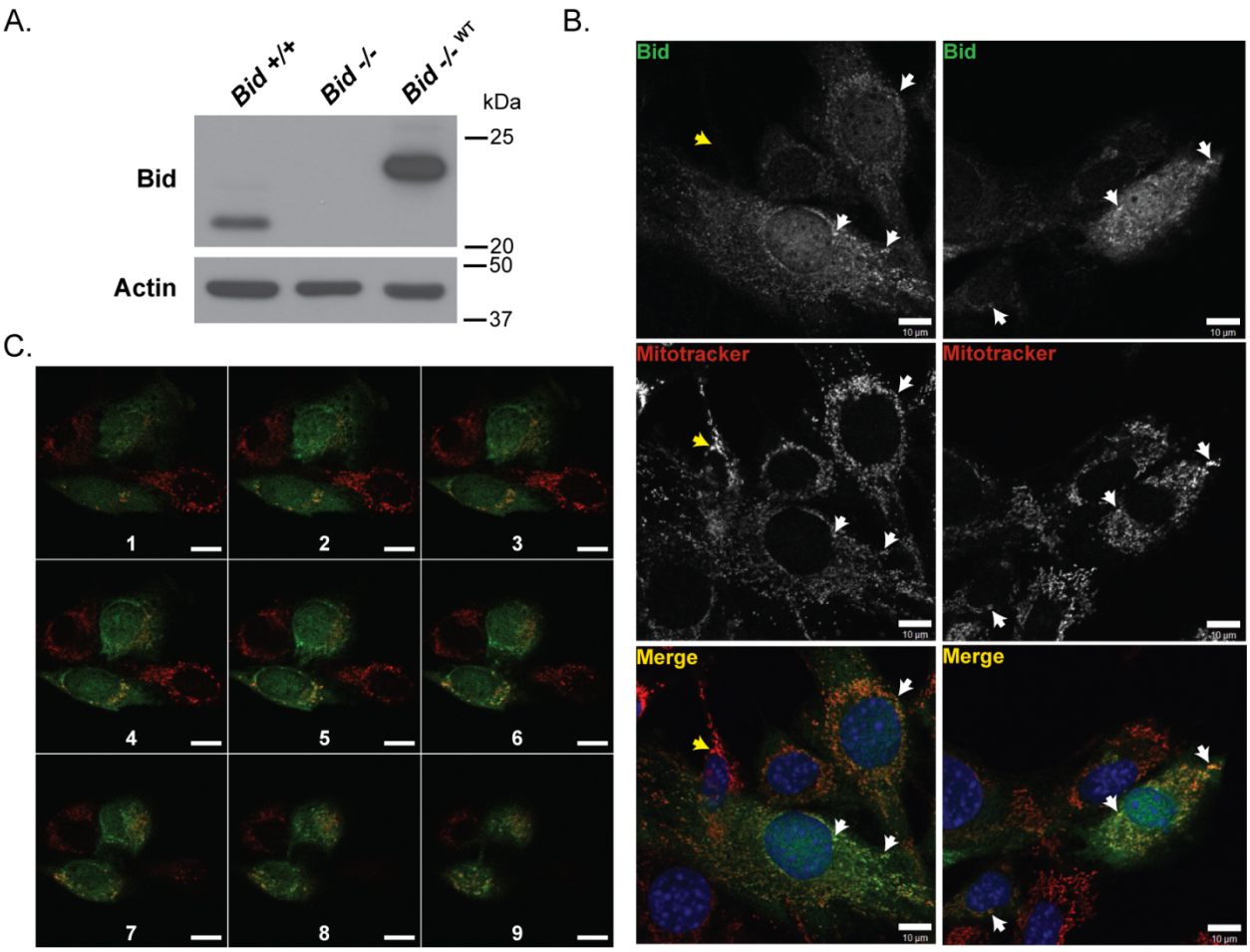

Figure 3-3. Bid co-localizes with mitochondria under non-apoptotic conditions.
A) Representative immunoblot analysis of Bid expression in *Bid* +/+, *Bid* -/-, and *Bid* -/- MEFs transduced with FLAG-HA tagged WT Bid. B)Confocal immunofluorescence micrographs of Bid (green) localization to mitochondria (red) in *Bid* -/- MEFs transduced with FLAG-HA tagged Bid. White arrowheads indicate co-localization of Bid and mitochondria. Yellow arrowheads indicate untransduced cells lacking Bid. Nuclei are stained with TO-PRO-3 (Blue). Scale bars represent 10 μm. C) Layers from a confocal z-stack series of MEFs described in (B). Z-slices are numbered from the basal to apical plane of the cells. Scale bars represent 10 μm.

Bid regulates mitochondrial respiration rate and tetra-linoleoyl cardiolipin levels in MPCs.

Interleukin 3 withdrawal in hematopoietic cells has been shown to induce stress in mitochondrial metabolism that precedes activation of the apoptotic pathways to death (275, 276). Given the apparent survival function of Bid in this setting, we sought to determine if Bid regulates mitochondrial physiology in non-apoptotic conditions. We measured the oxygen consumption rate (OCR) of equal numbers of *Bid* +/+ and *Bid* -/- MPCs, as determined by trypan blue exclusion. Bid -/- MPCs display a significant reduction in OCR in comparison to *Bid* +/+ MPCs, indicating reduced mitochondrial respiration rate (Fig. 3-4A) and demonstrating that Bid positively regulates mitochondrial respiration in MPCs.

CL has been proposed to associate with, and regulate, Bid (129, 130, 132, 184). In addition, CL composition is critical in regulating mitochondrial respiration (146). Therefore, we sought to determine whether Bid deficiency alters normal mitochondrial CL composition. We monitored the levels of the most abundant CL species, tetra-linoleoyl CL (L_4CL), as well as the less abundant linoleoyl-tri-oleoyl CL (LO_3CL) (271), in *Bid* +/+ and *Bid* -/- MPCs using quantitative liquid chromatography-electrospray ionization tandem mass spectrometry (LC/ESI/MS/MS). To quantify the relative levels of each CL species, tetra-myristoyl CL (M_4CL) was used as an internal standard. Bid deficient MPCs display reduced levels of L_4CL (Fig. 3-4B) but not LO_3CL (Fig. 3-4C) relative to *Bid* +/+ MPCs, indicating that Bid is required to maintain normal L_4CL levels in MPCs.

To determine if the decreased L_4CL levels in *Bid* -/- MPCs contributes to their reduced mitochondrial respiration rate, we measured the OCR of *Bid* +/+ and *Bid* -/- MPCs following the addition of exogenous liposomes composed of a 1:1 molar ratio of CL from bovine heart

mitochondria, of which 47% of the total CL mass is the predominant L_4CL species (271), and the synthetic lipid dioleoylphosphatidylcholine (DOPC). Addition of CL-containing liposomes (CL-liposomes) results in increased respiration of *Bid* -/- MPCs but not *Bid* +/+ MPCs (Fig. 3-4D). Addition of liposomes containing DOPC alone has no effect on respiration, demonstrating that restoration of respiration rate in CL-liposomes treated *Bid* -/- MPCs is CL-dependent (Fig. 3-4E). CL-liposomes treatment of *Bid* -/- MPCs restores L_4CL to levels similar to *Bid* +/+ MPCs (Fig 3-4F), but has no effect on L_4CL levels in *Bid* +/+ MPCs. Furthermore, mitochondria isolated from CL-liposomes treated *Bid* -/- MPCs display a significant increase in L_4CL to levels comparable to mitochondria from CL-liposomes treated *Bid* +/+ MPCs (Fig. 3-4G). These results indicate that altered L_4CL content in *Bid* -/- MPCs contributes to their reduced respiratory rate.

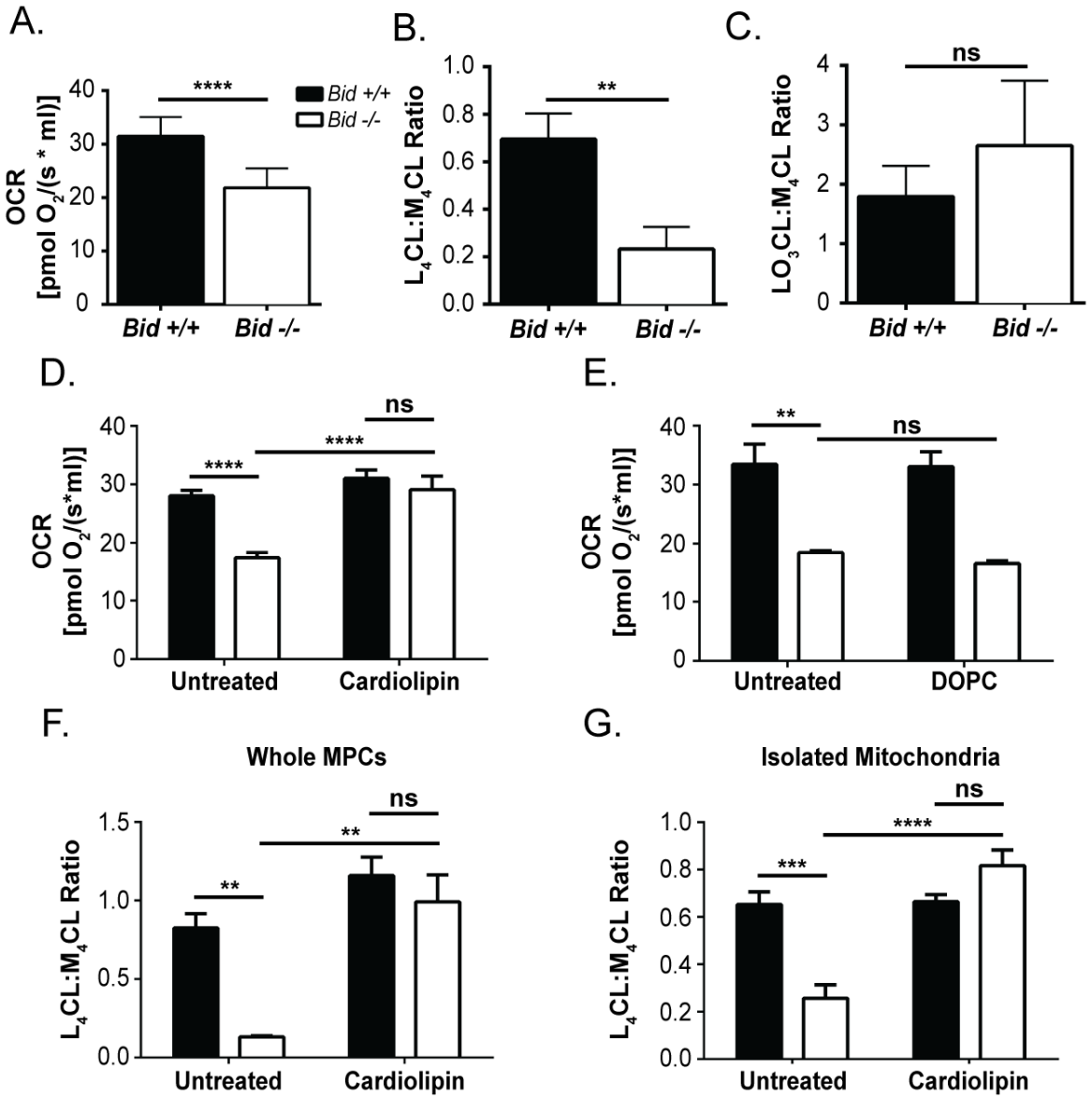

Figure 3-4. Bid maintains tetralinoleoyl cardiolipin levels to facilitate efficient mitochondrial respiration.

(A, N=3) Oxygen consumption rate (OCR) of *Bid* +/+ (black bars) and *Bid* -/- (white bars) MPCs. B-G) *Bid* +/+ and *Bid* -/- MPCs were used to study the effects of Bid on CL composition (B, C, F, and G) and respiration (D, and E). L_4CL (B, N=5) and LO_3CL (C, N=5) levels in *Bid* +/+ and *Bid* -/- MPCs expressed as the ratio to the internal standard, M_4CL. OCR of *Bid* +/+ and *Bid* -/- MPCs before and after 45 minutes treatment with 125 μM (1:1) CL:DOPC liposomes (D, N=4), or with DOPC (250 μM) liposomes (E, N=3). L_4CL levels in whole cells (F, N=4) or in mitochondria (G, N=4) isolated from *Bid* +/+ and *Bid* -/- MPCs either untreated or treated for 30 minutes with CL:DOPC liposomes. (A-H) Error bars indicate SEM. P values were determined by unpaired student's T-test (A-C) or repeated measures two-way ANOVA with Bonferroni's test (D-G).

***Bid -/-* mice are sensitized to acute, epinephrine-induced cardiac dysfunction.**

Mitochondrial function is especially critical to cell types such as cardiac myocytes that have high energy requirements for normal function. To determine if this phenomenon is unique to MPCs and to assess whether Bid's role in mitochondrial respiration could potentially impact the physiological function of energy demanding tissues, we investigated the effect of Bid deficiency on respiration and L_4CL levels in primary cardiomyocytes. State 3 respiration and L_4CL levels were measured in saponin-permeabilized cardiac fibers isolated from the left ventricle of *Bid* +/+ and *Bid* -/- mouse hearts, both before and after treatment with CL-liposomes. Bid deficient cardiac fibers display a significant reduction in respiration rate and L_4CL levels compared to *Bid* +/+ (Fig. 3-5A & B). CL-liposomes addition restores respiration and L_4CL levels of *Bid* -/- cardiac fibers to levels similar to *Bid* +/+ cardiac fibers (Fig. 3-5A & B). Thus, as in MPCs, Bid is required to maintain normal L_4CL levels and efficient oxygen utilization in cardiomyocyte mitochondria.

Mitochondrial dysfunction is a well-established contributing factor to heart failure (272, 277-279) as well as cardiac injury in the face of a variety of myocardial insults (206, 280-282). Therefore, we sought to determine whether *Bid* -/- mice have a decreased capacity for high myocardial demand. Accordingly, we subjected *Bid* +/+ and *Bid* -/- mice to acute cardiac stress by injection with 30 μg of epinephrine and measured heart function by echocardiography (Fig. 3-5C). *Bid* -/- mice display a significantly higher left ventricular internal diameter at end diastole (LVIDd) index (LVIDd index = LVIDd/g heart tissue) and left ventricular internal diameter at end systole (LVIDs) index (LVIDs index = LVIDs/g heart tissue) both before and after epinephrine treatment (Fig. 3-5D & E). Moreover, epinephrine treatment results in a significant increase in the LVIDd and LVIDs index in *Bid* -/- hearts, but has no significant effect on *Bid* +/+

hearts (Fig. 3-5D and E), indicating that Bid deficiency sensitizes mouse hearts to acute cardiac stress. Histological sections of *Bid* +/+ and *Bid* -/- hearts display no gross morphological abnormalities by H&E stain, nor do they display substantial fibrosis, as determined by Masson's trichrome stain (Fig. 3-5F). However, heart weight is significantly reduced in *Bid* -/- mice as compared to *Bid* +/+ suggesting that, while structurally normal, Bid deficient hearts have reduced mass (Fig. 3-5G). These results indicate that Bid protects against LV dysfunction following acute stress mediated by epinephrine.

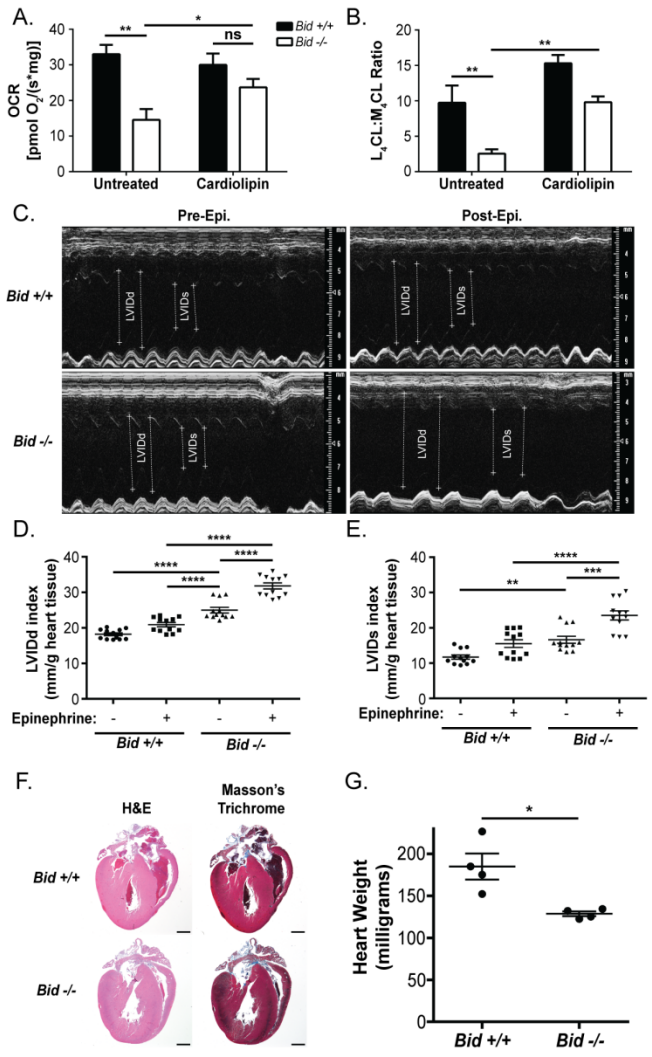

Figure 3-5. Bid maintains efficient cardiomyocyte respiration and protects against epinephrine-induced LV dysfunction.
A) OCR (N=3) and B) L_4CL levels (N=4) in permeabilized cardiac fibers dissected from the left ventricle of *Bid* +/+ (Black bars) and *Bid* -/- (White bars) mouse hearts in MiRO5 supplemented with glutamate (10 mM), malate (4 mM), and ADP (2 mM) before and after 45 minutes treatment with CL:DOPC liposomes. C) Representative M-mode traces of *Bid* +/+ and *Bid* -/- echocardiograms before (Pre-Epi.) and after (Post-Epi.) IP injection with 30 µg epinephrine. Examples of the LVIDd and LVIDs are indicated for each image. D) LVIDd index and E) LVIDs index of *Bid* +/+ and *Bid* -/- mice before and after IP injection with 30 µg epinephrine. LVIDd and LVIDs measurements were collected in triplicate from 4 mice. F) H&E (left) and Masson's trichrome (right) staining of coronal heart sections from *Bid* +/+ and *Bid* -/- mice following epinephrine treatment. Images were taken at 2.6X magnification. Scale bars represent 1000µm (2.6X). G) Heart mass (N=4) in milligrams following collection from *Bid* +/+ and *Bid* -/- mice treated with 30 µg epinephrine. Error bars indicate SEM. P values were determined by repeated measures two-way ANOVA with Bonferroni's test (A, B, D, & E) or unpaired Student's t-test (G).

BID SNPs associate with myocardial injury in human patients

Since *Bid* -/- mice display increased sensitivity to cardiac stress, we sought to determine if the status of Bid was associated with clinically relevant cardiac phenotypes in human patients. Using BioVU (described in methods), we developed a cohort of 23,195 self-reported Caucasian subjects (median age 63 years [IQR 43 to 57 years] and 52% female) who had previously undergone genotyping with the Illumina HumanExome BeadChip v1. Genotype data were available for 6 missense single nucleotide polymorphisms (SNPs) within the *BID* gene (NM_001244567.1), including 2 variants in the N-terminal region (S10G and R35G), 1 variant at the extreme C-terminus of Bid (M194T), 2 SNPs within α-helix 5 (E120D and R123Q), and 1 SNP in α-helix 6 (M148T) (Fig. 3-6A & B). The SNPs in α-helix 5 and 6 are within the minimal membrane binding domain (MBD) of Bid that spans helix 4, 5, and 6 (129). Individually, SNPs are uncommon, with minor allele frequencies (MAF) ranging from 0.0004% to 2.1%; however, at least one missense variant is present in 4.5% of the population (N=1,033). Variants in the MBD are present in 62 subjects (0.2%).

In multivariable logistic regression, no association is seen between *BID* SNPs and heart failure. However, a significant association is observed between carrier status (i.e. presence of any missense variant) and myocardial infarction (MI) (Fig. 3-6 C & D, p=0.013; OR 1.7 [95% CI 1.1-2.6]). This association is primarily driven by variants in the MBD. Carrier status for MBD variants (i.e. presence of any missense variant in the MBD) is strongly associated with MI (Fig. 3C & D, p=0.002; OR 8.5 [95% CI 2.1-33.6]). These data are consistent with a cardioprotective role for Bid in situations of acute cardiac stress and reveal a previously unrecognized association between Bid and MI.

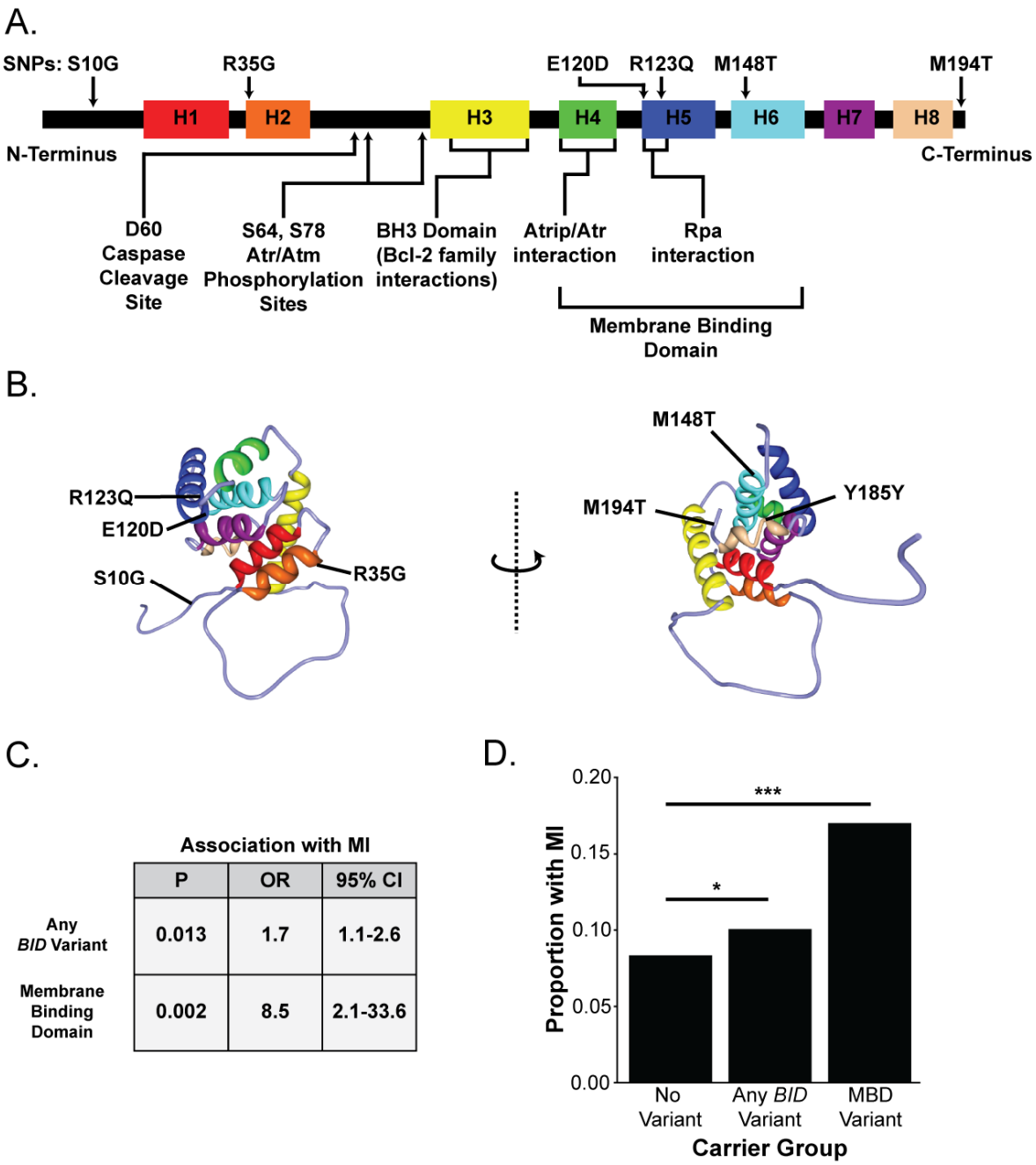

Figure 3-6. Bid SNPs associate with myocardial infarction in humans.
A) Linear representation of Bid protein structure and the locations of SNPs. Human *BID* SNPs and several key domains and regions of Bid are indicated. B) Three-dimensional structure of Bid annotated with *BID* SNPs. Helices are colored to match those shown in (A). C) Statistical values including p value, odds ratio (OR), and 95% confidence interval (95% CI) for Bid SNP association with MI in carrier groups with any Bid variant or with variants in the membrane binding domain. D) Graphical representation of the proportion of patients with MI in carrier groups with no SNPs in *BID* (no variant), any *BID* variant, or MBD variant as in (C). Analysis was performed as discussed in materials and methods. P values were determined by multivariable logistic regression with Bonferroni correction as described in methods (C & D).

Bid regulates mitochondrial respiration independent of its death domain.

In order to provide some insight into how Bid may regulate mitochondrial physiology we developed a stable expression system to assess the effects of re-introducing Bid, and Bid mutants, into *Bid* -/- MPCs. We first re-introduced wild type Bid to *Bid* -/- MPCs (*Bid* -/- ^{WT}) to determine if we could restore respiration of *Bid* -/- MPCs to *Bid* +/+ levels. Surprisingly, stable expression of wild type Bid has little effect on respiration rate (Fig. 3-7A & B). However, *Bid* -/- ^{WT} MPCs display cell death kinetics similar to *Bid* +/+ MPCs during IL-3 withdrawal (Fig. 3-7C). These results suggest that either Bid deficiency is not responsible for decreased respiration in *Bid* -/- MPCs, or that stable overexpression of pro-apoptotic Bid exerts an apoptotic selective pressure on MPCs that selects for a compensatory change in mitochondrial biology and apoptotic sensitivity.

To distinguish between these two outcomes and determine whether WT Bid can restore mitochondrial respiration, we transiently manipulated Bid expression levels in *Bid* +/+ MPCs to avoid compensatory changes induced by long term selection. Transient alteration of Bid expression was accomplished by nucleofection with a mouse Bid-specific siRNA or with plasmid expressing human Bid, which is insensitive to the siRNA. Both the knockdown of endogenous mouse Bid (siBID) as well as the transient overexpression of human Bid (+hBid) results in a significant reduction in the respiration rate of *Bid* +/+ MPCs compared to the negative control siRNA (siCtrl) (Figure 3-7D and E). However, co-nucleofection of human Bid and Bid siRNA (siBID + hBid) is sufficient to maintain respiration of *Bid* +/+ MPCs at levels similar to control cells. Thus, our results indicate that WT Bid can, in fact, modulate respiration, but that long term expression selects for compensatory changes in mitochondrial function. In addition, our findings suggest that Bid expression levels can impact respiration rates. Thus, if

Bid levels are abnormally high or low mitochondrial respiration is inhibited, possibly due to competition between Bid's pro-apoptotic function and its non-apoptotic role in regulating mitochondrial physiology.

In light of these results, we next asked whether the apoptotic function of Bid is required for its ability to regulate mitochondrial function. Mutation of Bid's BH3 domain abrogates the pro-apoptotic activity of Bid by inhibiting its association with other Bcl-2 family members (34). Since mutation of Bid's BH3 domain would prevent any pro-apoptotic selective pressure on MPCs by Bid, we again used stable re-introduction to determine the effects of BH3 mutated Bid on *Bid -/-* MPCs (Bid -/- ^{BH3m}) (Fig. 3-7 B). Interestingly, BH3 mutated Bid completely restores respiration to *Bid* +/+ levels, indicating that Bid positively regulates respiration independent of its BH3 domain (Fig. 3-7F). This result is consistent with the failure of stably re-introduced WT Bid to rescue respiration due to a selected compensation since BH3 mutant Bid is deficient for apoptotic function but still restores normal mitochondrial respiration.

Mutation of M148 inhibits Bid function in regulating mitochondrial respiration.

Since Bid SNPs, particularly those within the MBD, associate with MI in human patients, we sought to determine the functional consequences of the membrane binding domain on mitochondrial function. In particular, α-helix 6 regulates mitochondrial association and cristae remodeling during apoptosis (127, 150, 283). Among the SNPs identified in this study, M148T is the only one localized within α-helix 6. Therefore, we investigated whether introducing the M148T mutation prevents Bid from rescuing normal respiration in *Bid -/-* MPCs. Since Bid harboring a wild type BH3 domain is insufficient to restore respiration, we assessed respiration in *Bid -/-* MPCs stably transduced with Bid carrying mutations of both M148T and the BH3 domain (*Bid -/-* $^{BH3m/MT}$) (Fig. 3-7G). Expression of the Bid BH3/M148T double mutant is

insufficient to restore respiration to levels comparable to *Bid* +/+ or *Bid* -/- ^{BH3m} MPCs (Fig. 3-7F). To establish that the M148T mutation does not disrupt the overall structure of Bid, we assessed the ability of Bid $^{BH3m/MT}$ to induce cell death in response to TNF-α/Actinomycin D in comparison to *Bid* +/+, *Bid* -/-, and *Bid* -/- ^{BH3m} MPCs. As expected, *Bid* -/- MPCs and, to a lesser degree, *Bid* -/- ^{BH3m} MPCs, are resistant to TNF-α/Actinomycin D when compared to *Bid* +/+ MPCs (Fig. 4H and I). *Bid* -/- $^{BH3m/MT}$ MPCs display similar death kinetics to *Bid* -/- ^{BH3m} MPCs, indicating that the M148T mutation has little effect on Bid protein function in the apoptotic pathway in the presence of a mutated BH3 domain. Altogether, these results indicate that α-helix 6, or more specifically M148, is required to maintain normal mitochondrial respiration. In addition, these results demonstrate that the pro-apoptotic and metabolic roles of Bid are biologically and structurally separable.

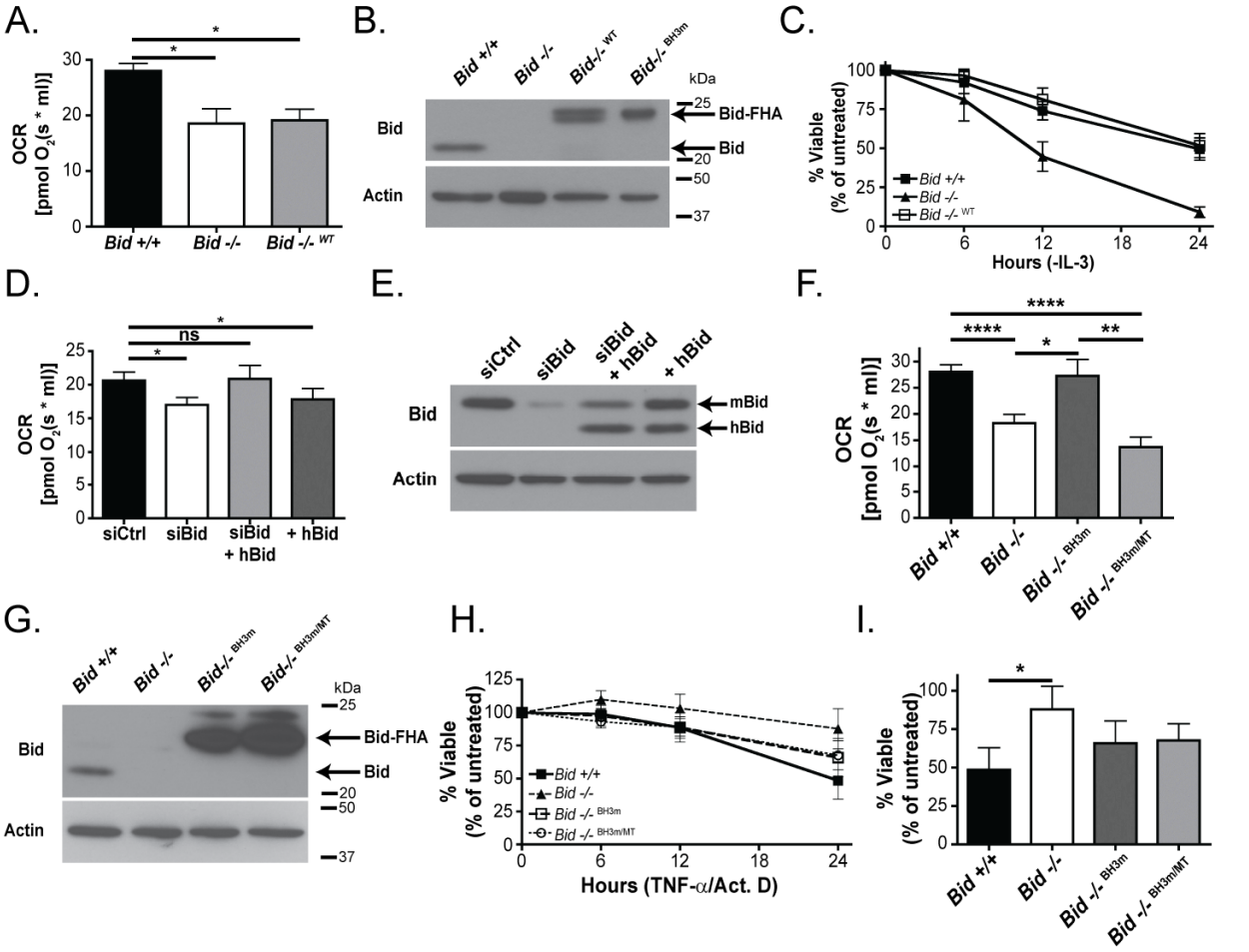

Figure 3-7. Bid requires M148 but not the BH3 domain to regulate respiration.
A) OCR of *Bid* +/+, *Bid* -/-, *Bid* -/- ^{WT} MPCs. B) Representative immunoblot of Bid expression in whole cell lysates of *Bid* +/+, *Bid* -/-, *Bid* -/- ^{WT}, and *Bid*-/- ^{BH3m} MPCs.
C) Viability (Annexin V/PI staining) of MPCs as in (A) for indicated times following IL-3 withdrawal. The percent of viable cells in IL-3 deprived samples was normalized to cells grown in the presence of IL-3. (A & B) N=3 D) OCR of *Bid* +/+ MPCs 72 hours post-nucleofection with non-targeting siRNA (siCtrl), mouse Bid specific siRNA (siBid), siBID co-transfected with pCDNA3 plasmid expressing human Bid (siBid + hBid), or hBid alone (+ hBID). N=7. E) Representative immunoblot of Bid expression in whole cell lysates of *Bid* +/+ MPCs 48 hours post nucleofection as in (D). Arrows indicate bands for full length, endogenous mouse Bid (mBid) and full length, exogenous human Bid (hBid). F) OCR of *Bid* +/+, *Bid* -/-, *Bid* -/- ^{BH3m}, and *Bid* -/- $^{BH3m/MT}$ MPCs. N=5. G) Representative immunoblot of Bid expression in whole cell lysates of *Bid* +/+, *Bid* -/-, *Bid*-/- ^{BH3m}, and *Bid* -/- $^{BH3m/MT}$ MPCs. Arrows indicate bands for full length, endogenous Bid (Bid) and exogenous Bid (Bid-FHA). H) Viability timecourse (Annexin V/PI staining) of MPCs as in (E) for indicated times following TNF-α/Actinomycin D treatment. The percent of viable cells was normalized to cells of same genotype immediately prior to treatment with TNF-α/Actinomycin D. I) 24 hour timepoint samples from (H) in column graph format. P values were determined by one-way ANOVA with Tukey's test (A, D, and F) or two-way ANOVA with Tukey's test (C, H, & I).

Bid is essential to maintain mitochondrial cristae structure.

During apoptosis, tBid induces significant remodeling of cristae structure (182). CL has also been shown to be necessary to maintain cristae structure of the IMM (146). Maintenance of cristae structure is critical for the organization of complexes in the ETC into respiratory chain supercomplexes, promoting efficient mitochondrial respiration (150). Thus, we reasoned that the reduced respiration rate in *Bid -/-* MPCs may be due to disruption of normal cristae structure. Therefore, we investigated the structure of mitochondria in *Bid +/+* and *Bid -/-* MPCs by transmission electron microscopy (TEM). TEM reveals clear cristae malformation in Bid deficient mitochondria (Fig. 3-8A). Furthermore, quantitative analysis of TEM images reveals a significant reduction in the average number of cristae per mitochondrion (determined by stereological measurement of average length density) in *Bid -/-* compared to *Bid +/+* mitochondria (Fig 3-8B). In addition, Bid deficient MPCs display a non-significant trend towards a decrease in the average number of mitochondria per cell (determined by stereological measurement of average area density) compared to *Bid +/+* MPCs (Fig. 3-8C). To determine if the BH3 domain was required for maintenance of cristae structure we also examined cristae morphology of *Bid -/-* ^{BH3m} MPCs. BH3 mutated Bid restores cristae structure (Fig. 3-8A) and the cristae per mitochondrion to levels observed in *Bid +/+* mitochondria (Fig. 3-8B), indicating that Bid regulates cristae structure independent of its BH3 domain.

Since restoration of L_4CL by CL-liposomes treatment improved respiration of *Bid -/-* MPCs, we investigated the effects of CL-liposomes on cristae structure. CL-liposomes improve cristae morphology and significantly increase the cristae per mitochondrion in *Bid -/-* mitochondria (Fig 3-8A and B). CL-liposomes also significantly increase the mitochondria per

cell of *Bid* -/- mitochondria (Fig 3-8C). These data indicate that reduced L_4CL levels contribute to cristae malformation in *Bid* -/- MPCs.

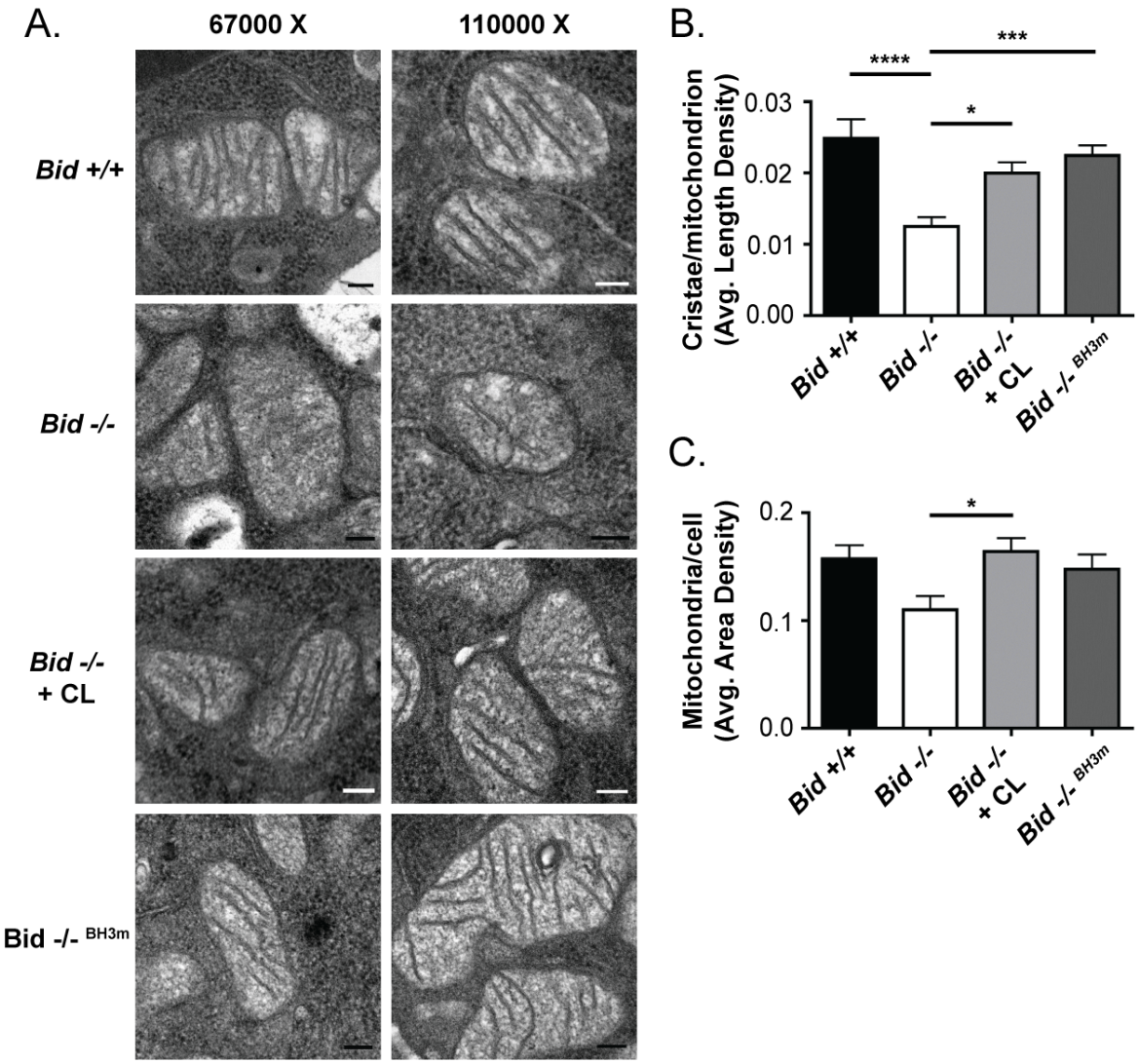

Figure 3-8. Bid regulates mitochondrial cristae morphology independent of its BH3 domain.

A) Representative transmission electron microscopy micrographs of mitochondria from *Bid* +/+, *Bid* -/-, *Bid* -/- ^{BH3m} MPCs or from *Bid* -/- MPCs treated with CL:DOPC liposomes for 30 minutes. Scale bars represent 100 nm. B) Quantitative analysis of the cristae per mitochondrion (average length density) and C) of the mitochondria per cell (average area density) of samples described in (A). Data were collected from 40 images at 30,000X magnification, error bars indicate SEM. P values were determined by one-way ANOVA with Tukey's test (B & C).

***Bid -/- MPCs* display increased Cytochrome *c* mobilization.**

The mobilization of Cytochrome c from the cristae to the IMS is required for the execution of apoptosis (168) and is increased during tBid induced cristae remodeling (182). In addition, CL regulates Cytochrome c mobility by binding and anchoring Cytochrome c to the IMM and by maintaining cristae structure (146). Furthermore, changes to CL composition sensitize cells to cells to death stimuli (172). Since *Bid -/-* MPCs display altered cristae structure and CL composition, we asked whether the increased sensitivity of *Bid -/-* MPCs to cell death could be due to increased mobilization of Cytochrome *c*. To evaluate Cytochrome *c* mobilization in the IMS, we used digitonin to permeabilize the OMM without disrupting the IMM using a procedure adapted from (182). A concentration of 50 μg/mL digitonin slightly decreases respiration in isolated mouse liver mitochondria during state 3 respiration, representing the permeabilization of the OMM and release of soluble Cytochrome c. Addition of excess exogenous Cytochrome c to digitonin-permeabilized mitochondria restores normal state 3 respiration rates, confirming that 50 μg/ml digitonin is sufficient to permeabilize the OMM without significant disruption of the IMM (Fig. 3-9A).

To assess the mobilized pool of Cytochrome *c* in *Bid* +/+ and *Bid -/-* mitochondria, 50 μg/ml digitonin was incubated with isolated mouse liver mitochondria for 45 minutes, and the Cytochrome c released (mobilized fraction) was quantified by ELISA. *Bid -/-* mitochondria release a significantly larger percentage of Cytochrome *c* than *Bid* +/+ mitochondria during exposure to digitonin (Fig. 3-9B) but both genotypes have similar levels of total Cytochrome *c* (Fig. 3-9C), indicating that Bid deficiency results in increased Cytochrome *c* mobilization. These results are consistent with an increased sensitivity to cell death stimuli in *Bid -/-* MPCs.

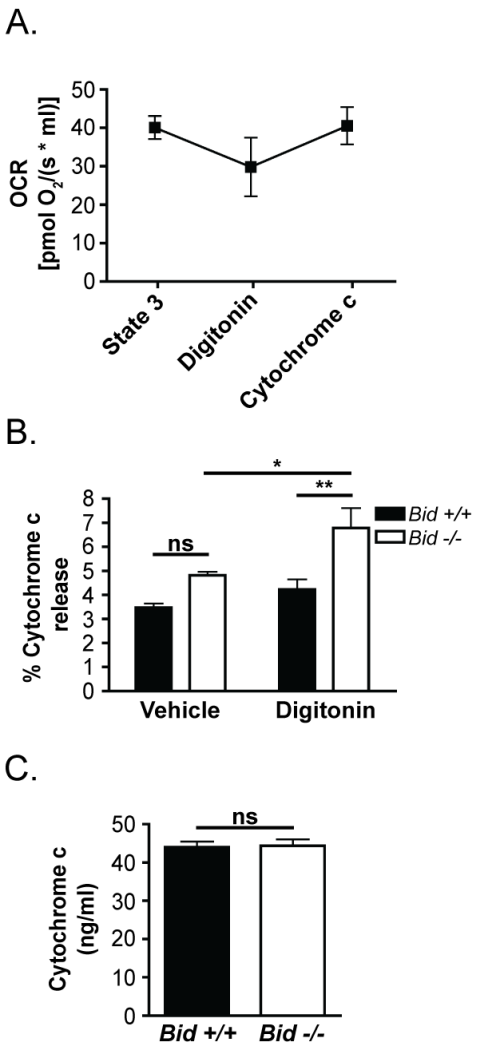

Figure 3-9. Bid deficiency increases mobilization of Cytochrome *c* to the IMS.
A) OCR of 600 μg of isolated liver mitochondria from *Bid* +/+ mice in mitochondrial respiration buffer (MiRO5) during state 3 respiration, following outer mitochondrial membrane permeabilization (50 μg/ml digitonin), and in the presence of excess Cytochrome c (10 μM Cytochrome c). N=3. B) Percent of total Cytochrome c released from untreated or digitonin (50 μg/ml) treated *Bid* +/+ and *Bid* -/- mouse liver mitochondria. N=7. C) Total Cytochrome c content in *Bid* +/+ and *Bid* -/- mouse liver mitochondria. N=7. (A, B and C) Error bars indicate SEM. P values were determined by one-way ANOVA with Tukey's test (A), two-way ANOVA with Tukey's test (B), and unpaired student's t-test (C).

Discussion

Mitochondria play a key role in maintaining cellular homeostasis through regulating metabolism and cell viability. By impairing efficient oxygen utilization, mitochondrial respiratory dysfunction has severe consequences and contributes to a wide variety of pathological conditions including multiple forms of cardiac disease (284). While the effects of decreased oxygen delivery have been extensively studied in cardiac disease, the impact of impaired oxygen utilization on cardiomyocytes during conditions of increased oxygen demand is not well understood. Our data reveal a previously unrecognized and BH3 domain-independent function for the Bcl-2 family member, Bid, in regulating mitochondrial respiratory efficiency in MPCs and primary cardiomyocytes. We also demonstrate the importance of Bid status in both the mouse and human heart in the context of acute cardiac stress and MI, respectively. In our human studies, we also identify a SNP that leads to a missense mutation of methionine 148 to threonine, a residue present in α-helix 6 of Bid. We demonstrate that the M148T mutation abrogates Bids ability to regulate respiration in MPCs. Our findings identify a novel, BH3-independent function for Bid in the maintenance of mitochondrial structure and physiology which is required for normal cardiac function and cellular viability.

Proteins of the Bcl-2 family are incontrovertibly linked to bioenergetics, functioning as effectors of apoptosis during metabolic stress as well as directly regulating metabolism and metabolic signaling (285). During apoptosis, tBid significantly alters mitochondrial metabolism by regulating cristae remodeling, respiratory complex organization, and membrane potential (150, 182). However, little is known about the effects of Bid on the mitochondria under non-apoptotic conditions. Our findings demonstrate that loss of Bid protein results in a significant reduction in mitochondrial respiration efficiency, disruption of cristae structure, and reduced

L_4CL content. Maintenance of cristae structure is essential for mitochondrial respiration through segregating respiratory complexes to the cristae to increase their local concentration (286, 287) and by promoting the stability of respiratory chain supercomplexes (150). Disruption of normal cristae structure results in a significant decline in mitochondrial respiration rate due to diminished ETC efficiency (150, 182). CL regulates cristae structure by influencing membrane curvature and facilitating the oligomeric assembly of F_0F_1 ATP synthase, which is required for cristae formation (146, 147, 149). CL also regulates respiration by modulating the activity of individual respiratory complexes (145, 288-291), anchoring cytochrome c to the IMM (292), functioning as a proton trap in the IMM (159), and stabilizing respiratory supercomplexes (146, 151, 153). Our findings are therefore consistent with a model in which Bid maintains cristae structure and CL composition to ultimately facilitate efficient mitochondrial respiration.

Considering the well-established role for Bid in activating apoptosis, it was surprising to find that Bid deficiency increases the sensitivity of MPCs to cell death. This result indicates that Bid can increase or decrease the threshold for cell death depending on the context. For example, tBid promotes apoptosis through facilitating the activation of Bax/Bak, MOMP, and release of Cytochrome c to the cytosol (32, 34). Cytochrome c release occurs through a two-step process in which it is first mobilized from the IMM to the IMS by dissociation from CL (168) and through cristae remodeling (182). Once mobilized, Cytochrome c is then free to diffuse into the cytosol upon permeabilization of the OMM by Bax/Bak (168). Our findings suggest that the absence of Bid increases Cytochrome c mobilization, likely through the combined effects of decreasing L_4CL levels and through disruption of cristae structure. Thus, our data are consistent with a model in which Bid promotes cell survival through maintaining cristae structure, CL composition, and Cytochrome c localization to the IMM. In the absence of Bid, Cytochrome c

mobilization increases, priming mitochondria by increasing the kinetics of Cytochrome *c* release to the cytosol and thus sensitizing Bid deficient cells to apoptosis.

As in MPCs, we observe reduced respiration and L_4CL levels in Bid deficient cardiac fibers. Additionally, our data indicate that Bid deficiency sensitizes mice to epinephrine-induced LV dysfunction. Consistent with a role for Bid in regulating cardiac function, we identify a significant association between missense Bid SNPs and MI in human patients. Mitochondrial function is essential to maintaining normal cardiac function by providing the energy necessary for contractile work (205). This energy is primarily generated through oxidative metabolism of fatty acids and, to a lesser degree, carbohydrates (293). Defects in oxygen utilization can contribute to a loss of physiologic function in cardiomyocytes, ultimately leading to a decline in heart function and the development of cardiac pathologies such as cardiomyopathies, myocardial infarction, and heart failure (206). Furthermore, alterations in CL mass or composition are commonly associated with cardiac dysfunction such as in Barth syndrome, which results from a mutation in the CL remodeling enzyme Tafazzin. Barth syndrome is characterized by a loss of L_4CL, mitochondrial respiratory chain dysfunction, and an early onset (and often fatal) dilated cardiomyopathy (233). L_4CL also decreases prior to, and during, the development of heart failure (HF) in spontaneously hypertensive HF rats, which closely correlates with decreased Cytochrome oxidase activity (234). CL dysregulation also occurs following aortic constriction in rats (235, 236), cardiomyopathy in hamsters (237), and ischemic and dilated cardiomyopathies in human patients (238). Our results are consistent with a model in which Bid maintains efficient oxygen utilization in cardiomyocytes through regulating cristae structure and CL composition, thus supporting improved tolerance to acute cardiac stress.

As regulators of mitochondrial homeostasis and physiology, the members of the Bcl-2 family have been linked to cardiac function, primarily through contributing to cardiomyocyte death (214). However, several studies indicate that the Bcl-2 family can also impact cardiac function through non-apoptotic mechanisms as well. For example, cardiac overexpression of Bcl-2 inhibits ATP decline during ischemia-reperfusion of the heart, preserving mitochondrial function and reducing ischemic injury (220). In addition, Mcl-1 has recently been reported to be required for normal heart function. This function is predominantly attributable to Mcl-1's impact on cell death, however part of Mcl-1's effect on cardiomyocyte mitochondrial respiration was independent of Bax/Bak inhibition (213). Interestingly, a matrix localized splice form of Mcl-1 has also been shown to regulate mitochondrial structure, respiration, and dynamics independent of its apoptotic function, which may contribute to its effect on cardiac function (106). We report a novel cardioprotective role for Bid that is biologically and structurally separable from its apoptotic role.

Among the SNPs in the MBD of Bid, M148T stands out as the one with the greatest potential for physiological significance given its position within α-helix 6 of Bid. The membrane association of Bid minimally requires a MBD spanning α-helices 4, 5, and 6 for association with mitochondrial membranes (129). Interestingly, α-helix 6 and 7 form the highly hydrophobic core helices of Bid which, upon association with membranes, undergo a conformational change and partially integrate into the OMM (114, 115, 127, 283). In addition to being necessary for mitochondrial association of tBid, Helix 6 is required for tBid-mediated cristae remodeling and respiratory inhibition (150). As we have shown here, the BH3 domain of Bid is not required for regulating mitochondrial respiration. However, methionine 148 is essential for normal mitochondrial respiration, suggesting that α-helix 6 is important for this function. Given the role

of α-helix 6 in membrane binding, we propose a model in which the M148T mutant inhibits Bid association with membranes, thus preventing Bid from maintaining cristae structure, CL composition, and efficient respiration. This finding also suggests that the M148T SNP may have functional cardiac consequences *in vivo* and may indicate susceptibility to acute cardiac stress such as during MI.

The findings presented here are an important contribution to the emerging paradigm of non-apoptotic functions for Bid and the Bcl-2 family members in regulating mitochondrial bioenergetics. Our findings suggest a model in which Bid associates with the mitochondrial membranes through α-helix 6. Upon membrane binding, Bid may either directly alter membrane structure, or may interact with other proteins independent of its BH3 domain to ultimately regulate mitochondrial physiology. In the absence of Bid, cristae structure is disrupted, resulting in diminished efficiency of the ETC, increased mobilization of Cytochrome c, and a decreased threshold for the induction of apoptosis (Fig. 3-10). Although the mechanism by which Bid maintains mitochondrial function is currently unclear, our findings suggest it may be mediated through regulation of cristae structure and/or CL composition. In tissues with high dependence upon mitochondrial function such as the heart, the functional status of Bid can influence cardiac function and sensitivity to myocardial stress and increased oxygen demand. The precise mechanism by which Bid exerts this novel function at the mitochondria and investigation of other Bcl-2 family members in the context of mitochondrial physiology warrants further study. Furthermore, these findings highlight the potential importance of the Bcl-2 family in regulation of mitochondrial physiology, particularly in the setting of heart function.

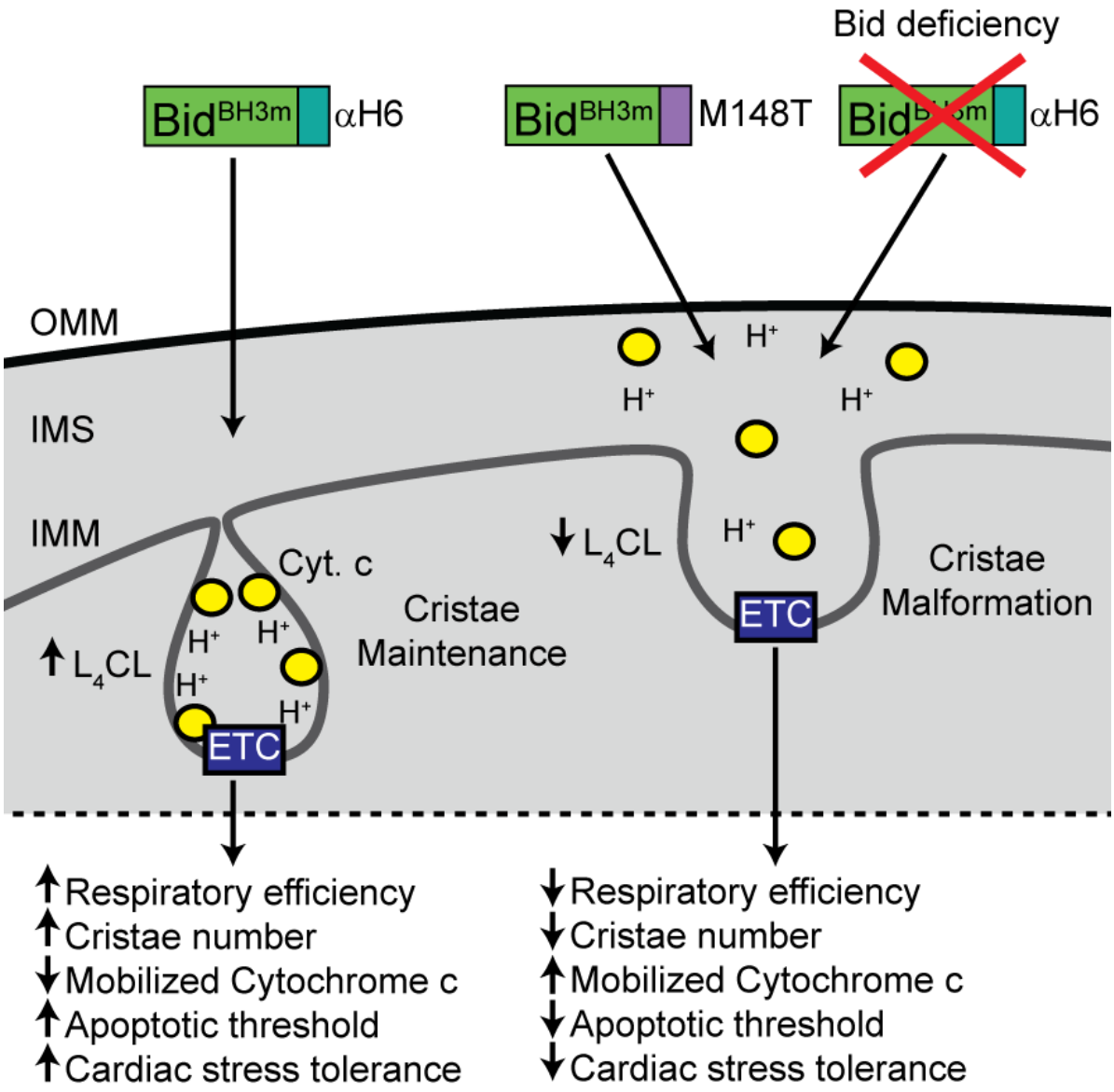

Figure 3-10. Bid protects from acute cardiac stress by regulating mitochondrial structure and physiology. A) Model of Bid's function in regulating mitochondrial structure, and physiology. In *Bid* +/+ mitochondria Bid maintains cristae structure in an α-helix 6 dependent, but BH3 independent manner to facilitate efficient respiration and to sequester Cytochrome c to the cristae. As a result, *Bid* +/+ mitochondria display high cristae numbers, high respiration rates, and resistance to aberrant apoptosis. In contrast, the absence of Bid, or mutation of M148 (M148T) in α-helix 6 of Bid results in cristae remodeling and malformation. Disruption of cristae structure leads to increased cytochrome c mobilization, and decreased stability in respiratory chain supercomplexes. As a result, Bid deficient mitochondria display low cristae number, reduced respiration rates, and are primed for Cytochrome c release and apoptosis. In addition, L_4CL levels are regulated in a BH3 domain independent manner, consistent with a role for Bid in regulating CL composition. Due to the reliance of the heart on oxidative metabolism, *Bid* -/- mitochondrial dysfunction can also lead to increased sensitivity to cardiac injury in conditions of acute cardiac stress. Thus, we have defined a novel function for Bid that is biologically and biochemically independent of its apoptotic function.

CHAPTER IV

DNA DAMAGE INDUCES THE NUCLEAR LOCALIZATION OF PRO-APOPTOTIC BID

Introduction

The members of the Bcl-2 family of proteins are critical regulators of apoptosis that function downstream of a wide variety of death stimuli. BH3 only proteins such as Bid act as sensors of cellular stress and promote apoptosis through activation of Bax and Bak (39). The activation of Bax/Bak leads to mitochondrial outer membrane permeabilization, resulting in the release of pro-apoptotic factors such as Cytochrome *c*, Smac/Diablo, and AIF to the cytosol (40, 43, 46). Ultimately, these proteins promote the activation of effector caspases which execute the apoptotic cell death program (6). In addition to their function in apoptosis, Bcl-2 family members have been shown to regulate multiple other cellular processes including mitochondrial dynamics (101, 102, 106), glucose metabolism (110-112), NOD signaling (108), and the DNA damage response (1-5, 294, 295). In some of these contexts, the non-apoptotic functions of Bcl-2 family members act in opposition to their canonical apoptotic roles.

DNA damage is induced by a variety of sources including radiation, exposure to genotoxic agents, reactive oxygen species, viral integration, and replication stress (239, 240). To survive genotoxic stresses, cells have evolved a complex signaling pathway collectively known as the DNA damage response (DDR) (239). The DDR is responsible for sensing DNA damage and activating effectors that regulate DNA repair, DNA replication, cell cycle, and, in cases of severe or irreparable DNA damage, apoptosis (241). Dysregulation of the DDR can promote mutation, transformation, and tumorigenesis in many different tissues (239).

Replication stress typically results from the formation of large stretches of single-stranded DNA (ssDNA), usually due to uncoupling of the DNA helicase and DNA polymerase (296). The resulting ssDNA is coated in replication protein A (RPA) which recruits multiple proteins including the DNA damage sensing kinase ataxia telangiectasia mutated (ATM)- and Rad3-related (ATR) and its constitutively bound partner ATR interacting protein (ATRIP) (246). ATR phosphorylates multiple substrates including the checkpoint kinases (Chk1/2), ultimately inhibiting cell cycle progression, halting origin firing, stabilizing stalled replication forks, and activating stalled fork repair processes (248). In cases of irreparable damage, p53 is stabilized through phosphorylation by Chk2 and other kinases, resulting in transcription of numerous downstream targets including the pro-apoptotic Bcl-2 family members Bax, Puma and Noxa (253).

We and others have previously demonstrated that Bid is a critical mediator of the DDR following multiple types of DNA damage including replication stress and that Bid is a substrate for the DNA damage sensing kinases ATR and ATM (1, 2). Bid regulates the DDR to replication stress by interacting with key regulators of the DDR including ATR/ATRIP and RPA (4, 5). The association of Bid with these nuclear regulators of the DDR suggests that Bid has a critical nuclear function in addition to its pro-apoptotic role at the mitochondria. Previous reports have indicated that Bid localizes to the nucleus following DNA damage and is exported during DNA damage induced apoptosis, suggesting nucleocytoplasmic shuttling of Bid regulated by the DDR (1, 297). Interestingly, the role of Bid in the DDR is structurally and functionally distinct from its role in regulating apoptotic cell death (4, 5). In addition, Bid's role in regulating the DDR is in contrast to its typical pro-apoptotic function. Through facilitating the activation of the DDR, Bid can promote cell survival through enabling recovery from replication stress.

Here, we investigate the nuclear relocalization of Bid during the DNA damage response. We find that DNA damage results in the recruitment of Bid to distinct nuclear foci and accumulates in regions associated with RPA foci following replicative stress, suggesting association of Bid with sites of DNA damage. We also quantitatively evaluate the localization change of Bid during replication stress, demonstrating an increase in the nuclear to cytoplasmic ratio of Bid during DNA damage. The nuclear targeting of Bid by replication stress is further enhanced by treatment with leptomycin B, an inhibitor of the nuclear export protein Crm1, supporting a regulated nucleocytoplasmic shuttling of Bid during DNA damage. We also provide evidence that Bid's association with chromatin is increased by replicative stress and that chromatin associated Bid is phosphorylated. This data suggests that phosphoregulation by the DDR pathway regulates Bid's nuclear localization, where it is able to associate with sites of DNA damage.

Results

DNA damage induces focal accumulation of Bid in the nucleus

Previous studies from our lab and others have demonstrated a role for Bid in the regulation of the DNA damage response through associating with components of the DDR machinery such as ATR/ATRIP and RPA (4, 5). In order for Bid to regulate the DNA damage response directly, it is likely that Bid must localize to the nucleus where it would be accessible for binding to DDR regulators. To assess the localization of Bid during DNA damage, we used confocal immunofluorescence microscopy of *Bid -/-* MEFs retrovirally transduced to express wild type Bid harboring a FLAG-HA epitope tag (*Bid -/-* + WT Bid MEFs). In the absence of a DNA damage stimulus, anti-HA immunofluorescence of *Bid -/-* + WT Bid MEFs reveals a

predominantly cytoplasmic localization of Bid with some mitochondrial localization and a diffuse nuclear localization (Fig. 4-1A). In contrast, treatment with multiple DNA damage stimuli such as hydroxyurea (HU), Etoposide, and ionizing radiation (IR) induces an accumulation of Bid into nuclear foci (Fig. 4-1A). We also observe a progressive change in Bid distribution during long term treatment with HU (Fig. 4-1B). During the first two hours of HU treatment, only a slight increase in focal accumulation of Bid occurs, but nuclear localization of Bid consistently increases through 6 hours of treatment with a slight increase in mitochondrial localization in some cells. Following 24 hours of HU, Bid predominantly localizes to the mitochondria and nuclear staining is diminished relative to 6 hour timepoints. These data are consistent with an initial localization of Bid to the nucleus following DNA damage followed by a later shift to mitochondrial localization. This result is consistent with an early response to DNA damage where Bid regulates the DDR, but a later shift to mitochondria to induce apoptosis in the presence of persistent or unresolvable DNA damage.

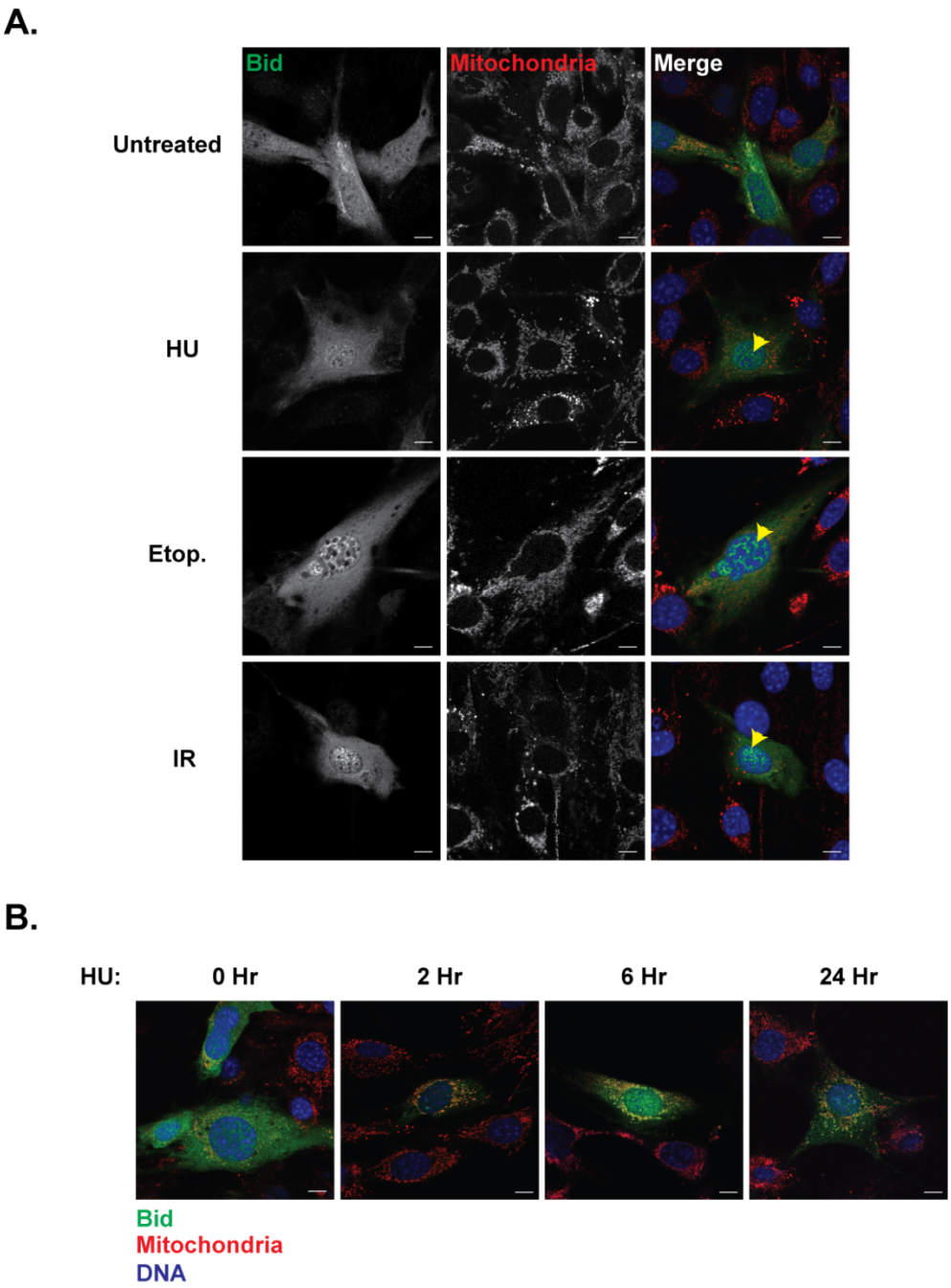

Figure 4-1. Bid localization is regulated by replicative stress. A) Representative confocal immunofluorescence micrographs of the sub-cellular localization of Bid (green) in *Bid* -/- + WT Bid MEFs. Imaging was performed 6 hours following exposure to 1 mM hydroxyurea (HU), 2.5 μM etoposide (Etop), or 10 Gy ionizing radiation (IR). Yellow arrowheads indicate regions of focal accumulation of Bid in the nuclear compartment following DNA damage. Mitochondria are shown in red and DNA in blue. Scale bars represent 10 μm. B) *Bid* -/- + WT Bid MEFs were stained and imaged as in (A) following treatment with 1 mM HU for the indicated times. Scale bars represent 10 μm.

Bid is enriched at nuclear RPA foci following HU-induced replication stress

Bid associates with RPA at sites of replication stress following treatment with HU (5) suggesting that the focal accumulation of nuclear Bid may reflect localization of Bid to sites of stalled replication forks. To determine if nuclear Bid foci were associated with stalled replication forks, we used confocal immunofluorescence microscopy to assess the relative distribution of nuclear Bid and RPA following HU treatment. To ensure efficacy of HU in inducing replication stress, we synchronized *Bid -/-* + WT Bid MEFs in G1 by incubation in reduced serum for 24 hours followed by release into complete medium. At 17 hours post release, cells are enriched in S-phase cells, at which point we either treated them with 1 mM HU or left them untreated for 1 hour (Fig 4-2A). Immunofluorescence analysis reveals clear HU-induced RPA foci formation, indicating induction of replication stress (Fig 4-2B). In addition, RPA foci are in close association with regions of enriched nuclear Bid, consistent with enrichment of Bid at sites of replication stress.

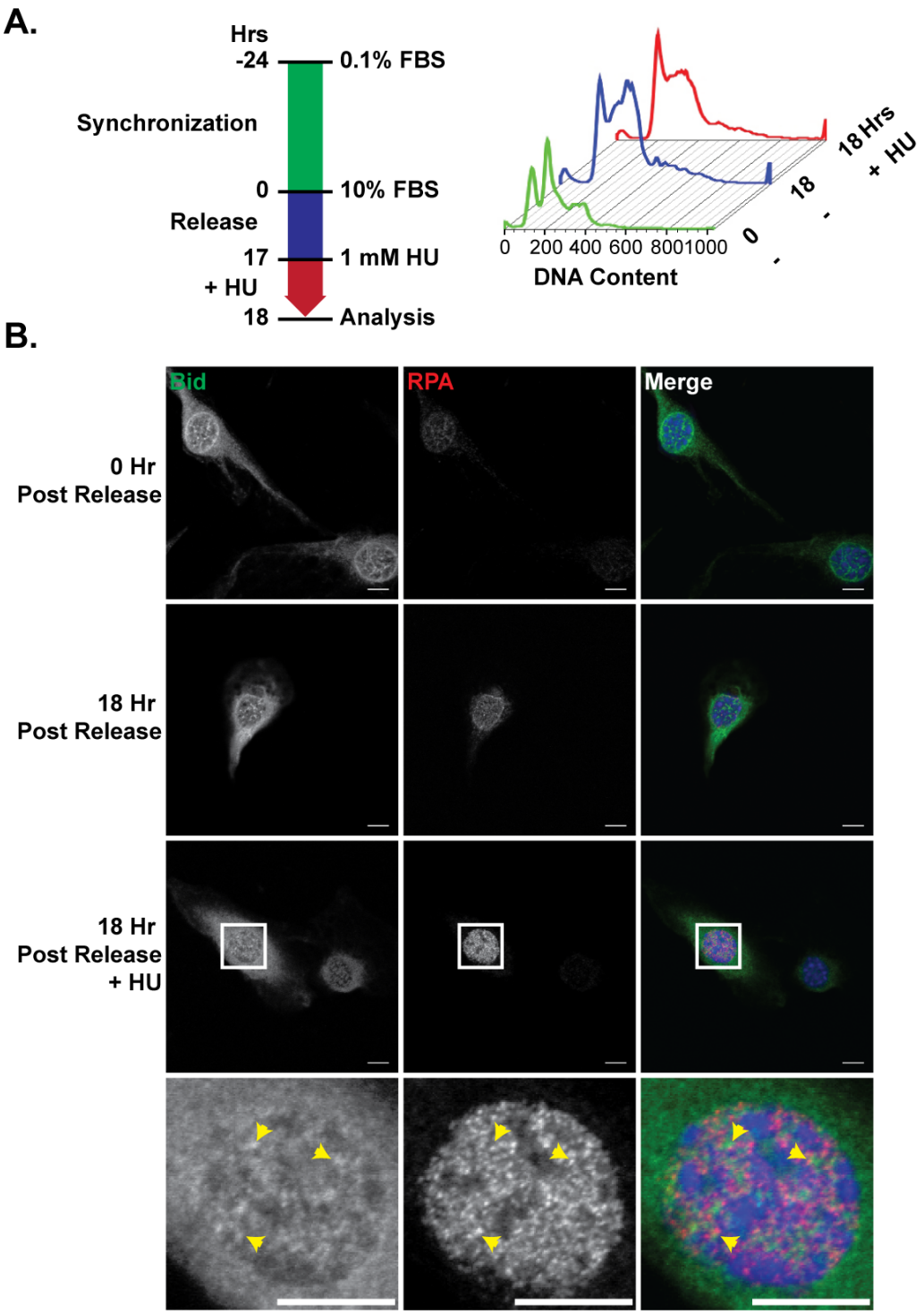

Figure 4-2. Nuclear Bid foci are associated with RPA foci following replication stress. A) *Bid* -/- + WT Bid MEFs were enriched in S-phase through synchronization and release as indicated and then treated with PBS or 1 mM HU. DNA content is shown for cells at time of release (0) and 18 hours post-release with and without a 1 hour treatment with 1 mM HU. B) Representative confocal immunofluorescence micrographs of *Bid* -/- + WT Bid MEFs treated as in (A), stained and imaged for HA (Bid shown in green), RPA (Red), and DNA (Blue). Yellow

arrowheads show examples of association between nuclear Bid foci and RPA foci. Scale bars represent 10 μm.

Replicative stress regulates the nuclear localization of Bid

The redistribution of Bid into nuclear foci suggests that Bid's sub-cellular distribution may be regulated by the DDR. To measure sub-cellular distribution changes in Bid, we used auto isodata binary threshold image analysis (259) and image subtraction to isolate and quantify the nuclear:cytoplasmic ratio (N:C ratio) of Bid fluorescence in *Bax -/- Bak -/-* MEFs transduced with wild type FLAG-HA tagged Bid (DKO + WT Bid). To validate this approach, we monitored the sub-cellular distribution of IκB-α in the presence and absence of the Crm1/exportin1 inhibitor, leptomycin B (298). IκB-α is normally excluded from the nucleus via Crm1 mediated export but rapidly localizes to the nucleus in the presence of leptomycin B (299). Treatment of DKO + WT Bid MEFs with leptomycin B results in clear redistribution of IκB-α from the cytoplasm to the nucleus (Fig. 4-3A). Quantitative analysis further demonstrates a significant increase in the N:C ratio (Fig. 4-3B). Similarly, HU treatment also induces a significant increase in the N:C ratio of Bid in DKO + WT Bid MEFs, indicating that DNA damage induces relocalization of Bid to the nucleus (Fig. 4-3C). Combined treatment of DKO + WT Bid MEFs with HU and leptomycin B results in a further increase in the N:C ratio, suggesting that Bid's nuclear localization may, at least in part, be regulated by a Crm1 dependent mechanism. Even in untreated DKO + WT Bid MEFs the density of Bid is, on average, slightly higher in the nucleus than the cytosol, suggesting that even in the absence of an exogenous DNA damage stimulus, Bid's localization is slightly biased towards the nucleus. This may be due to intrinsic DNA damage such as during replication or transcription.

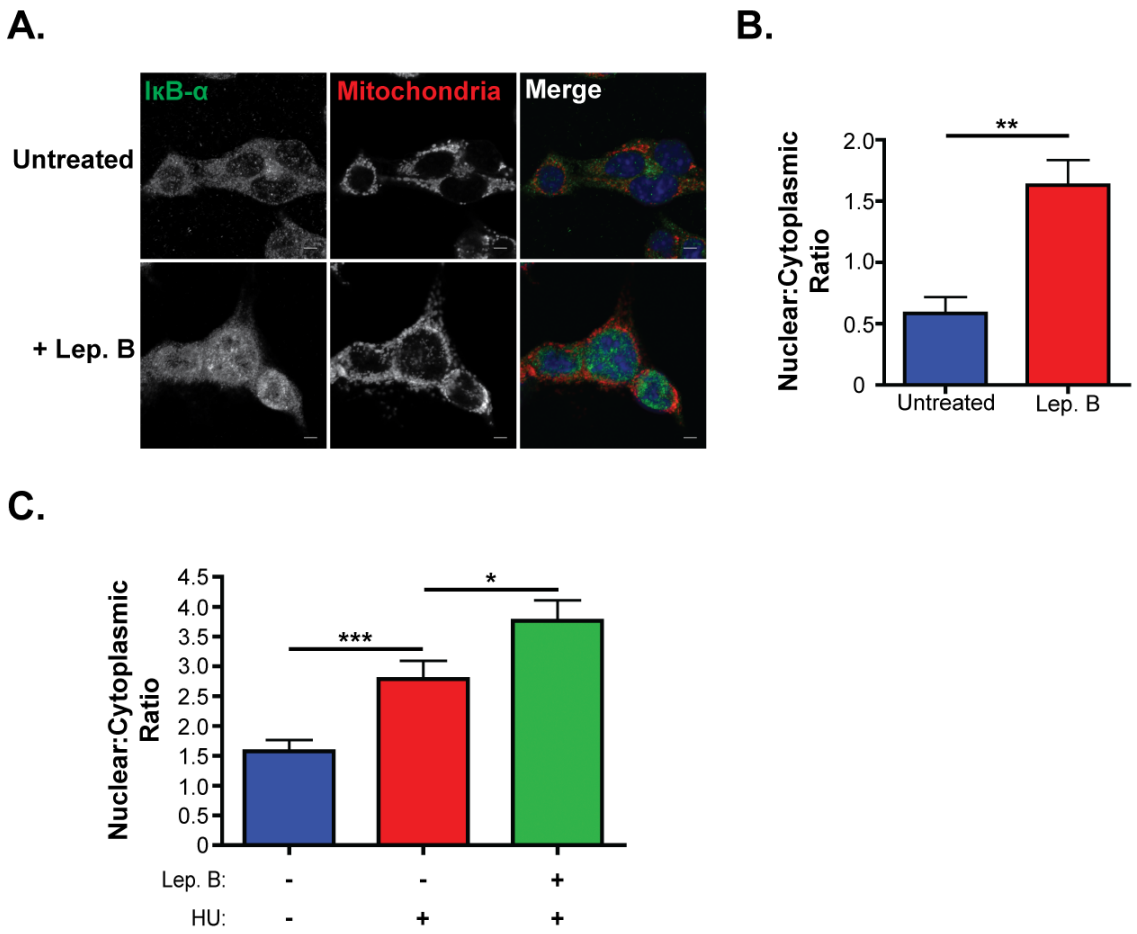

Figure 4-3. Bid undergoes Crm1 dependent nucleocytoplasmic shuttling in response to replicative stress. A) Representative confocal immunofluorescence micrographs of the sub cellular localization of IκB-α in DKO + WT Bid MEFs either untreated or following 1 hour treatment with 2 ng/ml Leptomycin B. DKO + WT Bid MEFs are stained for IκB-α (green), mitochondria (red), and DNA (Blue) as discussed in materials and methods. Scale bars represent 10 μm. B) Quantitation of the nuclear:cytoplasmic ratios of IκB-α in DKO + WT Bid MEFs treated as in (A). Results represent quantitation of the average nuclear:cytoplasmic ratio of IκB-α from all IκB-α positive cells in 4 fields taken at 20x magnification for each treatment condition. N=1, error bars indicate SEM. C) Quantitation of the nuclear:cytoplasmic ratios of HA (Bid) in DKO + WT Bid MEFs left untreated or treated for 1 hour with 1 mM HU, or with 1 mM HU and 2 ng/ml Leptomycin B together. Results represent quantitation of the average nuclear:cytoplasmic ratio of HA from all HA positive cells in 11 fields taken at 20x magnification for each treatment condition. N=1, error bars indicate SEM.

Replication stress induces chromatin association and phosphorylation of Bid

The focal buildup of nuclear Bid following HU treatment suggests that Bid may accumulate at sites of replicative stress or DNA damage. We and others have previously shown that Bid is phosphorylated at serines 61, 64, and 78 by the DNA damage sensing kinases ATM and ATR. We sought to determine if the phosphorylation of Bid can regulate its localization to sites of DNA damage. Therefore, we investigated the localization and phosphorylation state of chromatin associated Bid with and without HU treatment in myeloid progenitor cells (MPCs) by biochemical fractionation. Surprisingly, crude chromatin fractions display no detectible Bid following HU treatment (Fig 4-4A). To enrich for Bid and increase sensitivity, we performed immunoprecipitation of Bid from crude chromatin fractions. Immunoprecipitation reveals two distinct bands in WT MPCs (Fig 4-4A). Surprisingly, treatment of immunoprecipitated Bid with protein phosphatase 1(PP1) results in complete loss of signal for both bands suggesting that both bands are phosphorylated. However, it remains unclear why PP1 results in loss of signal, rather than a downward shift such as that seen in similarly treated whole cell lysates (Fig. 4-4B). Overall, these results suggest that replication stress induces phosphorylation and chromatin association of Bid.

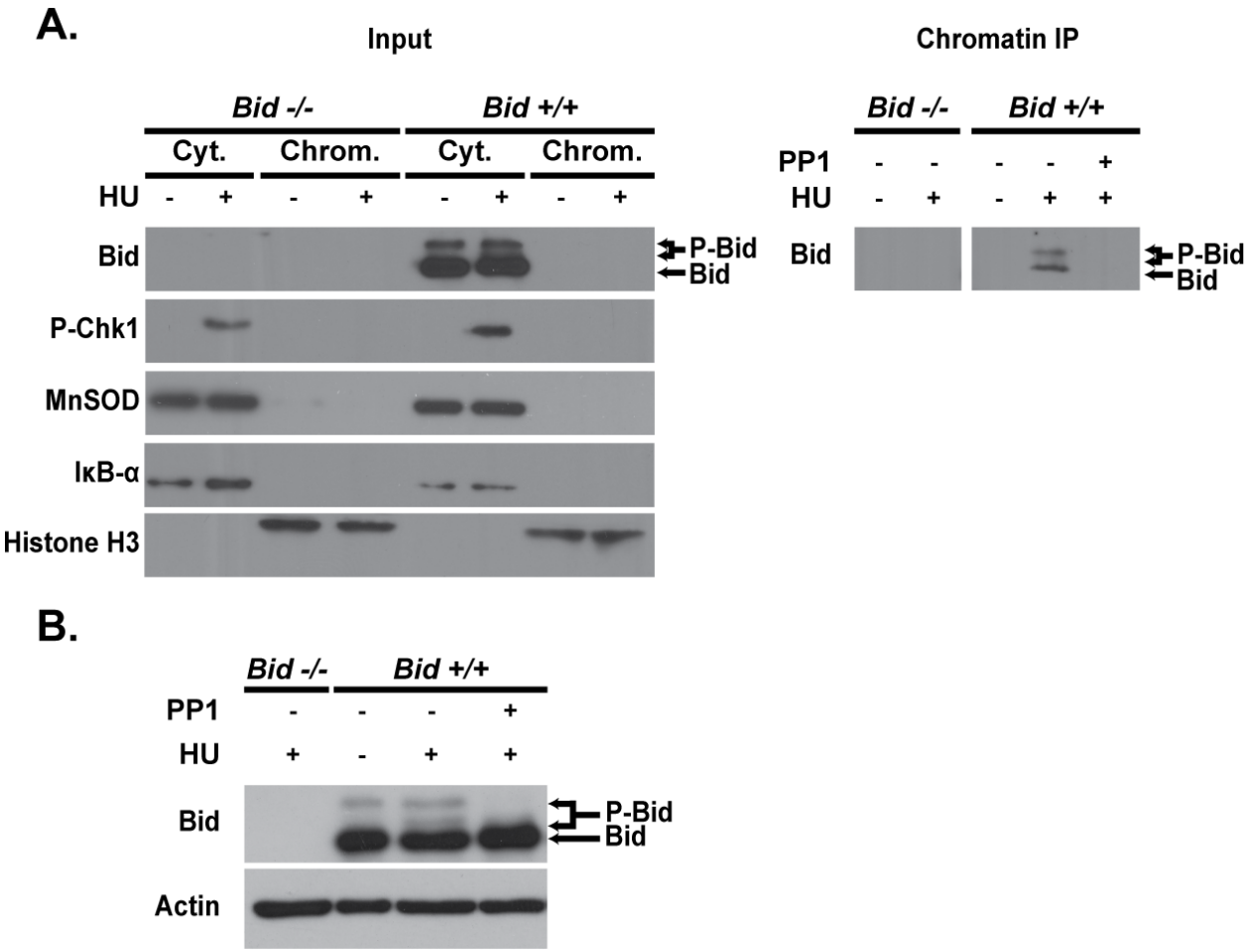

Figure 4-4. Bid undergoes phosphorylation and chromatin association following replication stress. A) Representative immunoblot analysis of Bid localization to chromatin fractions of *Bid* +/+ and *Bid* -/- MPCs following 30 minutes of treatment with vehicle (PBS) or 10 mM HU. Left immunoblots show input from cytosolic fractions and chromatin fractions. P-Chk1 demonstrates induction of replication stress while MnSOD, IκB-α, and Histone H3 indicate mitochondrial, cytosolic, and chromatin fraction separation respectively. Right immunoblot shows Bid immunoprecipitated from chromatin fractions with and without 30 minute incubation with 2.5 units PP1 phosphatase at 30^{o}C. B) Representative immunoblot analysis of whole cell lysates from *Bid* +/+ and *Bid* -/- MPCs treated for 30 minutes with vehicle (PBS) or with 10 mM HU. HU treated lysates were further treated with buffer alone or with PP1 phosphatase as in (A).

Discussion

During apoptosis, Bid is processed into tBid through proteolysis, leading to its translocation from the cytosol to the outer mitochondrial membrane (32, 33, 113) where it facilitates activation of apoptosis through binding to other Bcl-2 family members (34, 93, 95, 97). In contrast, Bid's role in DNA damage regulation is mediated by full length Bid and requires its association with components of the DNA damage sensing complex (4, 5). Unlike Bid's apoptotic function, which is dependent on the BH3 domain, the association of Bid with ATRIP and RPA is mediated through helix 4 and helix 5 of Bid. The phosphorylation of Bid is also critical for Bid's role in the DDR (1, 2), but is inhibitory of Bid's pro-apoptotic function (86), suggesting that phosphorylation may function as a switch between the pro-survival and apoptotic functions of Bid. Thus, the dual role of Bid in apoptosis and the DDR are structural and functionally separable. Our findings suggest that the regulation of Bid's sub-cellular localization may play a key role in regulating Bid function in different cellular processes.

Our data indicate that the sub-cellular distribution of Bid is altered following replication stress and is characterized by in an increase in total nuclear Bid levels as well as the redistribution of Bid from a diffuse to focal pattern in the nucleus. This finding suggests both an overall increase in targeting of Bid into the nucleus and an accumulation of Bid to specific focal sites within the nucleus. The focal accumulation of nuclear Bid is consistent with Bid's association with components of the DNA damage sensing complex at sites of stalled replication forks. In addition the increased localization of Bid to the nucleus suggests that the DNA damage response also promotes the shuttling of Bid to the nucleus. Furthermore, the relocalization of Bid from the nucleus to the mitochondria following long term HU treatment suggests that the initiation of DNA damage induced apoptosis is mediated, in part, through the cytoplasmic

targeting of Bid in cases of unresolvable DNA damage. The synergistic effect of HU treatment and leptomycin B on nuclear localization of Bid indicates a role for CRM1 in regulating the shuttling of Bid between cellular compartments. These data are consistent with previous reports that leptomycin B inhibits Bid export from the nucleus during DNA damage induced apoptosis (297).

It is currently unclear how Crm1 may regulate Bid's localization since mutation of a putative N-terminal nuclear export signal (NES) did not affect Bid's localization (297). In our studies, an *in silico* NES prediction method, NetNES 1.1 Server (300), revealed an alternative potential NES in helix 6 of human Bid spanning amino acids 149 to 156. However, mouse Bid, used in our experiments reported here, did not display a significant NES prediction score. Thus, while it remains possible that Bid localization may be directly regulated by Crm1, it seems more likely that Crm1 may indirectly regulate Bid's localization through trafficking of a protein complex that Bid associates with, possibly in a DNA damage-dependent manner.

Bid has been shown to be a substrate for ATM and ATR mediated phosphorylation at serines 61, 64, and 78 following DNA damage and this phosphorylation is critical for Bid's function in the DDR (1, 2). Interestingly, chromatin fractions from wild type MPCs display chromatin associated Bid with two distinct mobilities, consistent with modification of nuclear Bid. Surprisingly, upon treatment of chromatin fractions with phosphatase, both bands are lost in contrast to the expected downward shift to a non-phosphorylated band which is observed in whole cell lysates or other fractions. It is currently unclear why phosphatase treatment of chromatin fractions causes a loss of Bid signal. One possible explanation is that Bid phosphorylation stabilizes Bid when at sites of DNA damage by inhibiting its degradation. Nevertheless, these data support a role for phosphorylation regulating Bid's function at sites of

DNA damage, possibly through promoting the interaction of Bid with components of the DDR, enforcing nuclear localization of Bid, or inhibiting its turnover.

In summary, our findings indicate that the sub-cellular localization of Bid is regulated by the DDR. Thus, the DDR promotes the nuclear localization of Bid and its accumulation to the chromatin at sites of DNA damage. The accumulation of Bid on chromatin is consistent with Bid's ability to associate with the DNA damage sensing complex and promote downstream DDR signaling. Our data also suggest that the DNA damage dependent phosphorylation of Bid, as well as Crm1 activity, are important for the regulation of Bid function in the DDR, possibly by regulating the shuttling of Bid between the nuclear and cytoplasmic compartments. Interestingly, our data suggest a model in which Bid localization and phosphorylation facilitate a role for Bid as a sensor of DNA damage, where it first localizes to the nucleus and is phosphorylated to mediate pro-survival DDR signaling. However, in conditions of unresolvable DNA damage, Bid functions primarily to relay a pro-apoptotic signal to the mitochondria through nuclear export and localization to the mitochondria. Thus, Bid may function as a key factor in determining cell fate during genotoxic stress through alterations to its localization within the cell and its phosphorylation state. Gaining a better understanding of the functional consequences of Bid phosphorylation and the mechanisms controlling Bid localization will provide further insight into how the dual function of Bid in the DDR and apoptotic pathway are balanced and regulated.

CHAPTER V

SUMMARY AND FUTURE DIRECTIONS

Summary & Significance

Regulating Bid function in the DNA damage response

As a BH3 only protein, Bid is typically regarded as an activator of apoptosis , however it also regulates the activation of the DNA damage response. In contrast to Bid's canonical pro-apoptotic function, Bid's role in the DDR promotes cell survival by facilitating activation of DDR signaling, DNA damage checkpoints, and stabilization of stalled replication forks (1, 2, 4, 5), which ultimately promotes the repair of DNA damage and recovery from genotoxic stress (248). Bid facilitates activation of the DDR to replication stress by directly binding to ATRIP and RPA, components of the DNA damage sensing complex (4, 5). While progress has been made in understanding how Bid regulates the DDR, several key questions still remain unanswered. For example, how are the pro-apoptotic and DDR functions for Bid regulated to determine cell fate during genotoxic stress? How does the DNA damage-mediated phosphorylation of Bid regulate its function in the DDR? How is the localization of Bid controlled to regulate its cytosolic, pro-apoptotic function versus its nuclear, DDR function? In the following section, I summarize my investigations regarding Bid localization and phosphorylation changes that occur during genotoxic stress.

Using confocal microscopy, I investigated the localization of exogenous Bid in *Bid -/-* MEFs following treatment with DNA damage stimuli. Before treatment, Bid is present in the

cytoplasm and nucleus in a diffuse pattern. However, DNA damage induced a gradual increase in nuclear Bid foci followed by a late relocalization to mitochondria. These findings suggest that Bid initially localizes to the nucleus to promote DDR activation, but upon extended exposure to DNA damage, Bid relocalizes to the mitochondria to promote DNA damage induced apoptosis.

One possible mechanism of Bid's nucleocytoplasmic shuttling was through a DNA damage-induced and Crm1 dependent trafficking through nuclear pores. Quantitative analysis of Bid localization revealed an HU dependent increase in Bid's localization to the nucleus which was further increased with Leptomycin B treatment. Thus, my findings indicate that Bid localization is regulated by nuclear exportins. These findings are consistent with previous reports that Leptomycin B inhibits nuclear export of Bid during DNA damage induced-apoptosis (297). Interestingly, my data indicate that even prior to the induction of apoptosis, DNA damage regulates Bid's localization through Crm1.

DNA damage induces the phosphorylation of Bid at serines 61, 64, and 78 by DNA damage sensing kinases and is required for efficient activation of the DDR (1, 2). However, the role of this phosphorylation in the DDR is unclear. My findings indicate that chromatin associated Bid is phosphorylated, treatment with PP1 phosphatase results in loss of chromatin associated Bid. It is surprising that dephosphorylation causes a loss, rather than a downward mobility shift in Bid. This finding suggests that de-phosphorylation destabilizes Bid when localized to the chromatin. One possible mechanism for this outcome is that dephosphorylation of Bid makes it more susceptible to degradation, perhaps by ubiquitylation and proteasomal degradation. This is feasible since ubiquitin ligation regulates multiple components of the DDR at the chromatin (301).

My studies reveal new information regarding how Bid's dual functions in the DDR and apoptosis may be regulated. I have provided evidence that the localization of Bid is actively regulated by DNA damage and that phosphorylated Bid is present on the chromatin during DNA damage. The shuttling of Bid between cellular compartments over time suggests that the pro-survival and pro-apoptotic functions of Bid are compartmentalized. The distribution of Bid also appears to be mediated, at least in part, by Crm1-dependent nuclear export of Bid. It currently remains unclear how Crm1 regulates the trafficking of Bid as no functional nuclear export signal has been identified. I have identified a putative nuclear export signal in helix 6 of human Bid using *in silico* sequence analysis (300), however this region is not conserved in mouse Bid and is normally buried in the hydrophobic core of the protein. Thus, it seems unlikely that the Crm1 mediated transport of Bid occurs through a direct interaction, but rather through trafficking of other proteins with which Bid associates. Although my findings suggest Crm1 regulates Bid localization, it is also likely that nuclear Bid localization is increased through nuclear sequestration by RPA bound ssDNA. In other words, normally Bid is diffusely localized throughout the cell, but upon replication stress, ssDNA is coated by RPA at stalled replication forks which provides a binding site for Bid at the chromatin. This would result in an increase in chromatin bound Bid, causing a shift in the equilibrium of Bid localization to favor nuclear localization. Thus, both passive and active mechanisms could influence Bid's nuclear localization during DNA damage. Regardless of how Bids nuclear accumulation occurs, my findings suggest a unique role for Bid as a sensor of nuclear damage in which it first promotes DDR signaling but, if the damage is irreperable, Bid then relays an apoptotic signal from the nucleus to the mitochondria to induce cell death.

Bid phosphorylation may also play a significant role in how Bid function is regulated during DNA damage. My findings suggest the possibility that phosphorylation promotes or stabilizes the association of Bid with chromatin fractions and also that dephosphorylation destabilizes chromatin associated Bid. Bid phosphorylation is also known to inhibit its caspase-mediated processing into tBid (86). Thus, Bid phosphorylation may act as a molecular switch between the pro-survival and pro-apoptotic function of Bid in the DDR. Overall, my data highlight two potential mechanisms (phosphorylation and localization) by which Bid's cell death and DDR functions may be regulated to make cell fate decisions during genotoxic stress. Understanding how Bid's dual functions are regulated is critical to understanding how Bid influences cellular physiology and homeostasis. It is also critical to understand Bid function in these pathways for the purpose of manipulating Bid for therapeutic purposes. My data presented here provide further insight into mechanisms that may determine how Bid can exist at the threshold of life and death decisions in cells, playing seemingly contradictory roles by both preserving and antagonizing cell viability.

Bid-mediated regulation of mitochondrial physiology

Bid is critical for tissue homeostasis and normal physiology through both apoptotic and non-apoptotic mechanisms (1-5, 32-34, 85, 108, 113, 134, 135). While the apoptotic function of Bid has been extensively studied, we are only just beginning to understand the effects of Bid in other contexts. In my studies, I sought to identify novel non-apoptotic functions of Bid by investigating the consequences of Bid deficiency at the cellular level as well as in *Bid -/-* mice. My findings revealed an essential role for Bid in maintaining normal mitochondrial structure, respiratory function, lipid composition, and cell viability. In addition, I have established a role

for Bid in maintaining heart function during acute cardiac stress. In the following section, I discuss the conclusions of these findings and their broader significance.

Using Bid deficient MPCs, I demonstrated that Bid is required to maintain a normal threshold for the execution of cell death. Since Bid is well established to associate with the mitochondria during apoptosis (32, 33, 113), I hypothesized that Bid maintains cell viability by regulating mitochondrial physiology. Consistent with this hypothesis, exogenous Bid co-localized with mitochondria in *Bid -/-* MEFs. Although it is well established that tBid localizes to mitochondria in apoptotic conditions (32, 33, 113), my findings reveal that Bid can localize at or near the mitochondria even in the absence of an apoptotic stimulus. This finding is suggestive that Bid could have an impact on mitochondrial physiology in non-apoptotic conditions. Indeed, I determined that Bid is essential for normal mitochondrial respiration in both MPCs and primary cardiac fibers. This finding has significant implications since the mitochondria are central to cell viability and bioenergetics (137).

The above findings led to the question of how Bid might regulate mitochondrial respiration. Since CL is well established in regulating mitochondrial function (139) and has been shown to impact Bid function (129, 184-187), I hypothesized that CL dysregulation may contribute to the mitochondrial dysfunction of *Bid -/-* MPCs. Indeed, my studies indicated that Bid positively regulates CL levels, and that CL deficiency is at least partially responsible for the mitochondrial dysfunction in *Bid -/-* MPCs. This finding further establishes Bid as a key regulator of mitochondrial homeostasis since disruption of CL composition has many consequences on mitochondrial function and is associated with many diseases (139). Furthermore, these results open up a new avenue of study to investigate the mechanism of CL regulation by Bid and the Bcl-2 family.

Cardiac function is inexorably linked to the efficiency of mitochondrial respiration due to the dependence of cardiomyocytes on oxidative phosphorylation (205). Several lines of evidence suggest that CL composition is important for the proper function of the heart through regulating mitochondrial function (139). In light of our findings, I investigated the consequences of Bid deficiency on cardiac function in conditions of increased workload where oxygen demand, and thus the need for efficient oxygen utilization, would be increased. Bid deficient mice were sensitized to cardiac dysfunction when subjected to epinephrine-induced cardiac stress. This finding raised the possibility that the function of Bid may also be linked to cardiac pathologies in human patients. Using Vanderbilt's BioVU resource, we determined that Bid SNPs within the MBD (E120D, R124Q, and M148T) spanning α-helices 4, 5, and 6 displayed a significant association with MI. Thus, my results establish for the first time that, through regulating mitochondrial function, Bid is cardioprotective in conditions of stress. Furthermore, my results suggest that Bid function may be linked to susceptibility to MI.

Bid and CL have both been shown to impact cristae structure (139). Furthermore, mitochondrial function is dependent upon cristae structure (150). To begin addressing how Bid may influence mitochondrial structure and function it was first necessary to discern whether the homeostatic role of Bid is dependent upon, or distinct from, its canonical apoptotic function. Thus, I compared the effects of re-introducing either WT Bid, or the apoptotic deficient BH3 mutant Bid, on respiration in *Bid -/-* MPCs. BH3 mutant Bid restored normal respiration in *Bid -/-* MPCs but, surprisingly, WT Bid did not. These data demonstrate that Bid positively regulates respiration without its BH3 domain or its apoptotic function. In retrospect, the inability of WT Bid to restore respiration is logical since its overexpression would establish a significant apoptotic stress by upsetting the normal balance between pro- and anti-apoptotic Bcl-2 family

members. This stress, if present over a substantial time (such as in our stable lines), would confer a selective pressure, selecting for cells with altered apoptotic and mitochondrial function. Consistent with this, both transient knockdown and overexpression of Bid inhibited respiration. Thus, WT Bid can regulate respiration, but expression of too much or too little is detrimental to mitochondrial physiology. From these data, it is possible to envision a model in which Bid's homeostatic function and its apoptotic function are balanced, at least in part, by the amount of Bid present in the cell. Low levels of Bid are insufficient to maintain normal mitochondrial respiration, but too much Bid drives mitochondrial dysfuntion, possibly through its apoptotic activity. This finding is important as it suggests that, not only could alteration or loss of Bid's homeostatic function impact mitochondrial physiology, but the dysregulation of Bid's normal expression may also cause mitochondrial dysfunction.

In light of the finding that SNPs in the MBD of Bid associated with with MI, I performed structure-function studies into the M148T SNP. The M148T SNP was of particular interest as it is located in α-helix 6 of Bid which is critical for Bid's membrane association and function (114, 115, 127, 129, 150, 283). Since stable expression of Bid harboring an intact BH3 domain is insufficient to restore respiration, I made a stable line expressing Bid mutated in both its BH3 domain and the M148T site. While BH3 mutant Bid restores respiration, the double mutant (BH3-M148T) was insufficient to significantly affect respiration, indicating that M148 is essential for Bid's role in regulating mitochondrial physiology. This finding is intriguing as it is likely that, given its position in α-helix 6, M148T may impact membrane binding. Thus, this mutation may result in preventing Bid from mainting mitochondrial function by blocking its association with the mitochondria or mitochondrial proteins. Furthermore, it is possible that this site may be functionally linked to the susceptibility of patients harboring MBD SNPs to MI.

Both Bid (150, 182) and CL (139) regulate cristae structure and the distribution of Cytochrome *c* within the mitochondria; however Bid's role in regulating these processes has only been investigated in the context of apoptosis. *Bid -/-* MPCs displayed cristae malformation that was rescued by either exogenous CL or BH3-mutated Bid. Furthermore, mobilization of Cytochrome *c* to the IMS was increased in Bid deficient mitochondria. Together these data suggest that the combined effects of cristae disruption and decreased CL levels leads to increase Cytochrome *c* mobility, which would then sensitize cells to apoptosis (172), as was observed in *Bid -/-* MPCs.

Overall, my studies demonstrate a novel pro-survival function for Bid in regulating mitochondrial structure and physiology at the mitochondria. These findings have significant consequences on cardiac function by sensitizing the heart to injury during acute cardiac stress. In the following section, I have highlighted several key points of significance of my thesis work.

1) Identified a novel, pro-survival function for Bid

   In addition to its function as a pro-apoptotic BH3-only member of the Bcl-2 family of proteins, Bid has also been shown to have additional, non-apoptotic functions in certain contexts. My studies reveal a novel function for Bid in maintaining the structure, function, and lipid composition of the mitochondria, which is critical for regulating normal cellular physiology, especially in highly energetic tissues such as the heart. Ultimately, Bid is required to maintain efficient oxygen utilization by the mitochondria and to decrease the apoptotic threshold. Therefore, loss of Bid increases basal cell death signaling and results in hypersensitivity to cell death stimuli such as IL-3 withdrawal. My studies demonstrate that Bid is essential to maintain normal

mitochondrial function and viability, demonstrating a previously unrecognized role for Bid in promoting cell survival and homeostasis.

2) Established Bid as a regulator of CL homeostasis

The mechanisms controlling CL synthesis and remodeling have been studied extensively. CL composition is regulated through a combination of synthesis, CL fatty acid remodeling, and degradation. CL synthesis is catalyzed by enzymes such as CLS in the matrix leaflet of the IMM and is dependent upon trafficking of precursor lipids from the ER (140). Remodeling of CL is a complex process which also occurs in the IMM and is mediated by enzymes such as Tafazzin, MLCLAT, and ALCAT. CL degradation is mediated through enzymes such as iPLA$_2\gamma$. Despite our current knowledge, it remains unclear how these processes are regulated to maintain and dynamically modify CL composition to maintain mitochondrial structure and physiology (141).

My studies reveal Bid as a previously unrecognized regulator of CL homeostasis. Though the detailed mechanism remains elusive, I have demonstrated that Bid regulates CL composition independent of its BH3 domain and its apoptotic function. Though not directly demonstrated in my studies, my data also raise the possibility that M148 of Bid may be necessary for CL homeostasis, as it was required for normal mitochondrial respiration. Considering the many essential roles for CL in mitochondrial physiology (139), these findings suggest Bid may have many diverse effects on mitochondrial function through altering CL composition. Thus, my findings underscore a novel and unique role for Bid as a regulator of CL homeostasis and contribute new insight into the processes involved in CL regulation.

3) Implicated CL in Bcl-2 family mediated modulation of mitochondrial homeostasis.

Bcl-2 family proteins are essential regulators of apoptosis signaling at the mitochondria (39), but their role is not limited to apoptotic function alone. Members of the Bcl-2 family have been implicated in regulating mitochondrial dynamics (101, 102, 106), IMM structure (106), respiration (103-106), the DNA damage response (1-5), glucose metabolism (110-112), NOD signaling (108), insulin secretion (110, 111), calcium signaling (107), and autophagy (107). In light of my studies, it is possible that Bid may not be the only Bcl-2 family member with a functional link to CL.

Many of the functions of Bcl-2 family members have significant overlap with processes regulated by CL. For example, Bax has been shown to regulate mitochondrial fusion through interaction with Mfn1 (101, 102) and also may regulate mitochondrial fission in co-operation with Drp1 (204). CL can modify membrane structure by forming hexagonal structures, which may facilitate membrane fusion (302), and CL is required for proper function of both Drp1 (163, 165) in the OMM as well as Opa1 (303), which mediates IMM fusion. These findings raise the possibility that Bax and CL cooperate to regulate mitochondrial dynamics.

Bcl-xL also displays functional overlap with CL. By interacting with ATP synthase, Bcl-xL blocks leakage of protons across the IMM to improve efficiency of oxidative phosphorylation (103-105). CL also associates with ATP synthase to facilitate the formation of ATP synthase oligomers (144, 147) which is important for maintaining cristae morphology (149) and ATP synthase efficiency (148). CL also functions as a proton trap to further increase ATP synthase efficiency (159). Thus, CL and Bcl-xL may function together to regulate ATP synthase efficiency and regulate cristae morphology.

Mcl-1 may be the most likely candidate for having a functional relationship with CL. A matrix localized splice variant of Mcl-1 facilitates formation of ATP synthase oligomers, positively regulates respiration, maintains cristae structure, and regulates mitochondrial dynamics (106). CL also regulates these same mitochondrial features, and cells lacking matrix localized Mcl-1 display a similar phenotype to CL deficient cells (106, 139, 160). Furthermore, a recent study demonstrates that Mcl-1 is essential for normal cardiac function as Mcl-1 deletion in the heart results in dilated cardiomyopathy characterized by mitochondrial structural defects (213). While mostly mediated by an anti-apoptotic mechanism, the effect of Mcl-1 on heart function appears to be partially due to a respiratory defect (213). Disruption of CL composition is well established to accompany many types of cardiac disease, and is especially well known to contribute to dilated cardiomyopathy in Barth's syndrome (139, 233). The precise mechanism by which Mcl-1 affects mitochondrial structure and function is currently undetermined. Since nascent CL synthesis occurs on the matrix leaflet of the IMM (304), it is plausible that matrix localized Mcl-1 splice variant could regulate CL homeostasis by association with and/or regulation of the CL synthesis machinery, thus facilitating normal mitochondrial structure and physiology.

My findings clearly establish a role for Bid in regulating CL homeostasis and suggest that CL is at least partially responsible for the mitochondrial defects observed in the absence of Bid. Thus, my thesis work raises many interesting questions regarding the relationship between CL and other Bcl-2 family members. Further work will be required to determine how Bid impacts CL, how CL contributes to Bid's role in regulating

mitochondrial homeostasis, and whether this effect is specific to Bid alone among the Bcl-2 family.

4) Revealed a role for Bid in stress induced cardiac dysfunction and myocardial infarction.

Bid is linked to a wide variety of pathologies, however, in almost all cases these pathologies are mediated through either aberrant activation or inhibition of cell death. In this thesis, I have demonstrated that Bid is required for the tolerance of increased cardiac stress *in vivo* and that Bid SNPs associate with MI in humans. While Bid has been implicated in mediating cardiomyocyte apoptosis during ischemia/reperfusion in the heart (121, 211, 212), my findings are the first report that Bid is essential to maintain normal cardiac function, and that Bid may contribute to the susceptibility to MI in humans.

MI is among the most prevalent causes of death in the US (305). Fundamentally, MI occurs when there is an imbalance between myocardial oxygen supply and demand (306). Under conditions of increased cardiac stress or workload, maintenance of cardiac function and contractility requires an increased oxygen demand. By reducing the efficiency of oxygen utilization in cardiomyocytes, loss or alteration of Bid function could result in an impaired capacity to meet increased oxygen demand during cardiac stress or could result in a decreased ability to maintain cardiac function during ischemia. Thus, the functional status of Bid may be an important determinant of susceptibility to cardiac stress and MI. My studies suggest that *BID* SNPs, particularly those within the MBD, may serve as a useful clinical marker of susceptibility to MI or alternatively may help in determining outcome following MI in human patients. In particular, my findings suggest that M148, and perhaps helix 6 as a whole, is of critical importance to Bid's effect on cardiac function.

Bid's effect on CL may contribute to its role on cardiac stress tolerance. CL dysregulation is linked to multiple pathologies; however one of the strongest links is to Barth's syndrome (139). Barth's syndrome is primarily characterized by a dilated cardiomyopathy that ultimately progresses to heart failure and death (233). CL is also well established to be dysregulated in a variety of other cardiac pathologies including pressure overload-induced cardiac hypertrophy (235, 236), hypertension-induced heart failure (234), and ischemic and dilated cardiomyopathies (unrelated to Barth syndrome) (237, 238). Therefore, Bid's effect on CL composition may contribute to the susceptibility of *Bid -/-* hearts to cardiac stress and may also be a factor in the susceptibility of patients harboring Bid SNPs to MI. However, determining a causal role for CL in disease has proven to be difficult in most cases due to the complex relationship between CL homeostasis and mitochondrial physiology. Indeed, there is significant interdependence between mitochondrial function and CL composition. Thus it is currently not possible to discern whether CL dysregulation is a cause or consequence of altered mitochondrial physiology or cardiac dysfunction in *Bid -/-* mice. Nevertheless, even if CL dysregulation is not a primary cause of heart diseases, it is generally considered to at least contribute to the pathogenesis of such conditions. Further studies into how CL regulates cardiac biology, as well as investigations into how Bid regulates CL composition will be essential to understanding the contribution of CL to Bid's effect on cardiac stress tolerance and to the relationship between Bid and MI.

In this thesis, I have identified a novel role for Bid in regulating cardiac function, I have established an association between genetic variants of Bid and MI in human patients, and I have implicated a specific structural domain of Bid in regulating its respiratory and cardiac function.

In the long-term, these findings could impact our understanding of cardiac disease and could help identify patients that are susceptible to cardiac diseases such as MI. Furthermore, these findings also suggest that it will be important to consider alternative functions for Bid and other Bcl-2 family members when treating patients with Bcl-2 family inhibitors as they may have unforeseen cardiac toxicity. It is also feasible that Bid may contribute to other pathologies through its effects on mitochondrial function since mitochondria are essential for many cellular processes in multiple tissues and organs. Thus, investigating the role of Bid in cardiac disease and the precise mechanisms by which Bid regulates respiration warrants further study.

My studies add a novel element to the emerging paradigm of alternative functions for Bcl-2 family members. Although the Bcl-2 family is critical for the control of apoptosis, it is essential that ongoing studies consider that the Bcl-2 family is not restricted to regulating only a single process. The work presented in this thesis is one of only a few studies that has investigated Bid function outside the context of apoptosis. Indeed, very few studies assess how the absence of Bid impacts mitochondrial and cellular physiology. In addition, many *in vitro* studies of Bid are only performed in the context of tBid, and do not consider whether full length Bid has a biochemical or physiological function in the process being investigated. This principal should also apply to other Bcl-2 family members. While non-apoptotic functions are emerging for Bcl-2 family members, it is likely that many remain unrecognized. Therefore, it is important that research into the function of the Bcl-2 family is rigorous and critically evaluated with a consideration for how alternative functions for Bcl-2 family members may influence experimental interpretation. Identifying novel Bcl-2 functions will allow for improved understanding of how the Bcl-2 family regulates multiple cellular processes, how cell fate decisions are made, and how to best exploit these functions for therapeutic purposes.

Future Directions

How does Bid localization and phosphorylation regulate the DNA damage response?

Here, I have provided evidence that the sub-cellular localization of Bid is regulated by DNA damage and that phosphorylated Bid is enriched at the chromatin during DNA damage. In addition, my data indicates that Bid localization is regulated in a Crm1 dependent manner. However, as summarized above, it currently remains unclear how Bid localization is controlled by the DDR. It is also unknown how Bid phosphorylation regulates Bid function in the DNA damage response. In the following section, I discuss possible mechanisms by which Bid localization and phosphorylation may regulate its function in apoptosis and the DDR.

My findings indicate that Bid localization is regulated by DNA damage which is, at least in part, mediated by Crm1-mediated nuclear export. Following short term treatment with HU, Bid localizes to the nucleus in nuclear foci but later relocalizes to the mitochondria. However, it is unclear how this nuclear enrichment occurs and how the shuttling of Bid between cytosol, nucleus, and mitochondria is regulated. Given our current knowledge, there are two possible mechanisms by which the Bid trafficking may occur. First, it is possible that the nuclear accumulation of Bid is a passive process. This is possible since Bid is small enough to diffuse through the nuclear pore without active transport mechanisms (307). In this model, Bid may diffuse into the nucleus and accumulate at sites of DNA lesions through its association with the DNA damage sensing complex, thus resulting in an increased affinity of Bid for chromatin and shifting the equilibrium of Bid localization within the cell into the nucleus. This model would imply that the Crm1 mediated export of Bid is not required for nuclear accumulation, but is

instead only required for nuclear export following commitment of the cell to DNA damage induced apoptosis. This export would facilitate Bid's association with the mitochondria and thus promote apoptosis. Alternatively, Bid localization may be actively regulated through the DNA damage mediated regulation of Crm1 function. In this model, Bid may normally be excluded from the nucleus by Crm1, but upon DNA damage, Crm1 mediated export of Bid is inhibited, thus increasing the nuclear localization of Bid to the nucleus and facilitating its association with DNA lesions. Upon commitment to DNA damage induced apoptosis, inhibition of Crm1 mediated export of Bid is relieved, resulting in rapid export of Bid to the cytosol where it can translocate to the mitochondria and activate apoptosis. It is worth noting that these two models anre not mutually exclusive. In other words, the shift in Bid localization may be through a combination of both mechanisms.

One seemingly simple way in which to differentiate between these two models is by inhibition of Crm1 function and observing the effect on Bid localization. However, this strategy is flawed since inhibition of Crm1 may disrupt the normal function of the DDR through impacting other DDR effectors and therefore could interfere with accurate interpretation of results. Indeed, multiple proteins involved in DDR signaling are shuttled through Crm1 mediated export including Brca1 (308) and p53 (309). Thus, to determine how Crm1 affects Bid localization it is critical to better understand the mechanistic relationship between Bid and Crm1. Bid contains no recognizable nuclear localization sequence or functional nuclear export signal, suggesting that it does not directly interact with components of nuclear trafficking machinery. Thus, it is likely that the Crm1 mediated transport of Bid is indirect, potentially mediated by association with a "carrier protein" that is trafficked through Crm1. This association would also likely be regulated by the DDR since Bid localization changes between early and late stages of

DNA damage. Interestingly, p53 can repress the transcription of Crm1 during DNA damage, suggesting a potential mechanism by which nuclear export during the DDR may be regulated (309).

To determine how Bid localization is regulated by Crm1, future experiments would need to be directed at identifying Bid interaction partners in the nucleus that are induced by DNA damage. This approach would identify candidates for proteins that could facilitate nucleocytoplasmic trafficking of Bid which could then be validated by siRNA mediated knockdown and analysis of Bid localization. Structural analysis of the interaction between Bid and any validated candidates would allow the generation of Bid mutants that could be used for structure/function studies. This would allow for disruption of Crm1 dependent trafficking of Bid and provide mechanistic insight into the contribution of Crm1 to the role of Bid in the DDR and DNA damage induced apoptosis.

In addition to the role of Crm1 on Bid localization, it is likely that post-translational modification of Bid could affect its nucleocytoplasmic shuttling and the function of Bid in the DDR. The transport of Bid to the mitochondria following long exposure to HU could be regulated, in part, through the cleavage of Bid by the DNA damage induced nuclear caspase, Caspase-2. Indeed, Caspase-2 has been proposed to promote DNA damage induced apoptosis through Bid cleavage (256). Thus, it is possible that this cleavage may facilitate Crm1-dependent export of Bid to the cytoplasm in order to activate apoptosis. If this is true, a non-cleavable Bid mutant (such as the D59A Bid mutant) would likely be resistant to nuclear export during long term exposure to DNA damage.

Phosphorylation may also impact the DDR function and localization of Bid. For example, phosphorylation could inhibit Caspase-2 mediated Bid cleavage. Bid phosphorylation has been

demonstrated to inhibit its caspase mediated cleavage, thus preventing its apoptotic function (86). Alternatively, phosphorylation could influence the stability of Bid at sites of DNA damage. Consistent with this, I have observed a loss of Bid upon PP1 treatment of Bid immunoprecipitates from isolated chromatin fractions. This could be explained as a result of Bid degradation by chromatin associated components of the ubiquitin proteasome system which are known to be directly involved in regulating components of the DDR (301). To determine if the loss of Bid following PP1 treatment is indeed mediated by the ubiquitin proteasome system, treatment of chromatin associated Bid immunoprecipitates with proteasome inhibitors should block Bid degradation and inhibit signal loss by PP1. In addition, phosphorylation could promote the interaction of Bid with ATRIP and/or RPA. Indeed, we have previously demonstrated that the HU induced association of a non-phosphorylatable Bid mutant with ATRIP is blunted compared to WT Bid (4). Overall, my findings indicate that both the localization and phosphorylation of Bid play a key role in its function in the DDR and in DNA damage induced apoptosis. Thus, further studies into the processes regulating Bid localization and phosphorylation will provide valuable insight into how Bid regulates the DDR.

How does Bid Regulate Mitochondrial Physiology and Cardiac Function?

My studies indicate that Bid regulates mitochondrial cristae structure, respiratory efficiency, cell viability, and CL composition to ultimately reduce the tolerance of the heart to cardiac stress. The precise mechanism by which Bid regulates mitochondrial structure and physiology remains undetermined. In addition, several questions remain regarding how Bid modulates cardiac function *in vivo*. Below, I discuss how Bid could regulate these processes and what will be required to address these questions.

Based on our current findings as well as other data present in the literature, I propose two possible models to explain how Bid influences mitochondrial structure and function. In the first model (Fig. 5-1A), the primary effect of Bid on mitochondria is through regulating cristae structure, which in turn maintains Cytochrome *c* distribution to the IMM and efficient respiration, thus preventing aberrant ROS production and CL peroxidation/degradation. Alternatively, Bid's primary function may be to regulate CL composition (Fig. 5-1B), which in turn maintains cristae structure, respiratory efficiency, and inhibits Cytochrome *c* mobilization. Although both models are possible, I favor the former model in which the primary function of Bid is to regulate cristae structure since tBid has previously been shown to regulate cristae structure. Indeed, tBid induces significant remodeling of the IMM, resulting in disruption of cristae structure and mobilization of Cytochrome *c* (182). Cristae shape is critical for the organization of the complexes of the ETC into respiratory chain supercomplexes, which is required for efficient respiration (150). The remodeling of cristae by tBid is mediated through the disruption of Opa1 oligomerization, which normally acts as a tether to keep the cristae junctions closed and maintain cristae shape (270). Therefore, by disrupting Opa1 oligomers, tBid mediates cristae remodeling, induces respiratory dysfunction, promotes Cytochrome *c* mobilization, and facilitates apoptotic signaling. Although it is clear that tBid regulates cristae remodeling via Opa1, the precise mechanism by which tBid regulates Opa1 remains unclear. Thus, future investigation into this mechanism may provide insight into how tBid causes cristae remodeling.

A.

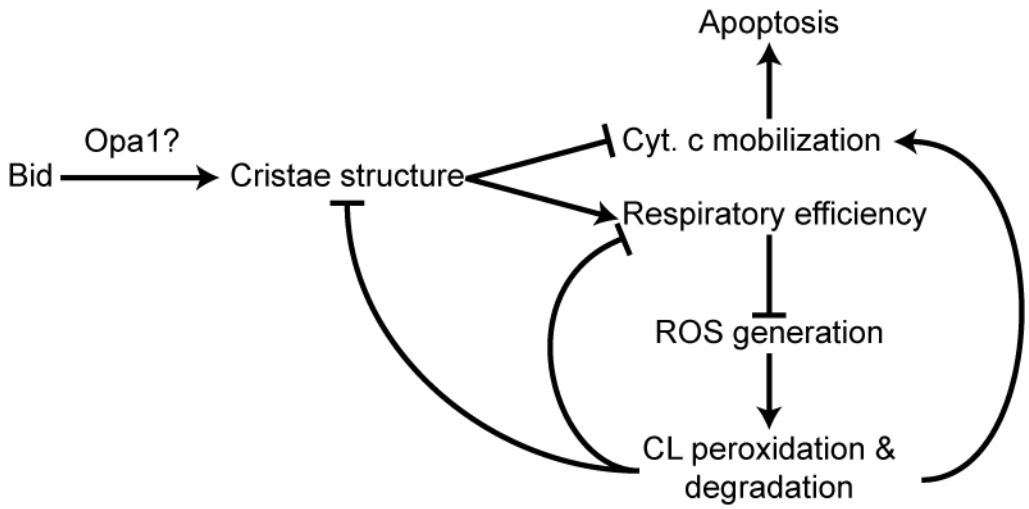
Apoptosis
Opa1?
Bid
Cristae structure
Cyt. c mobilization
Respiratory efficiency
ROS generation
CL peroxidation &
degradation

B.

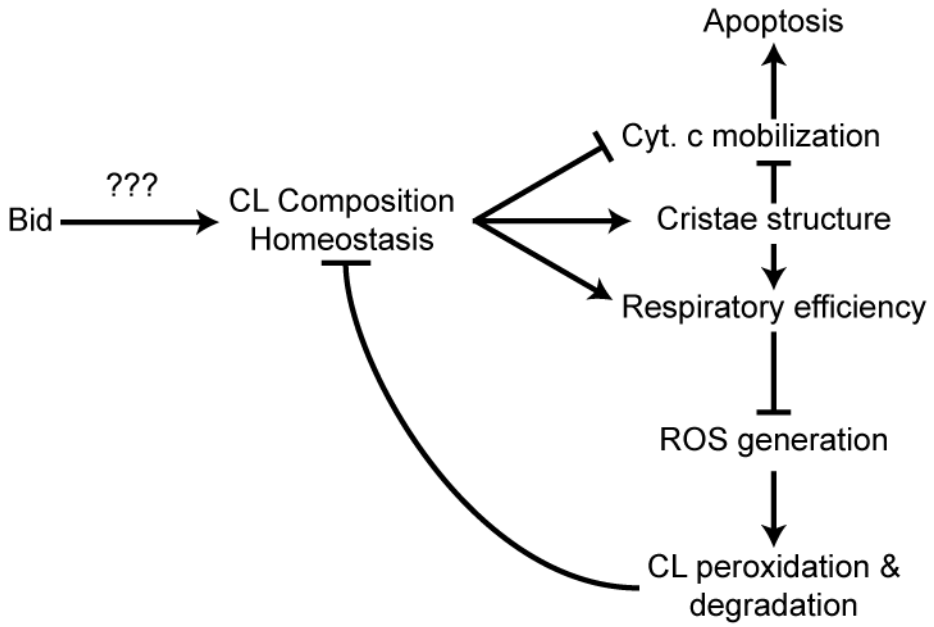
Apoptosis
???
Bid
CL Composition
Homeostasis
Cyt. c mobilization
Cristae structure
Respiratory efficiency
ROS generation
CL peroxidation &
degradation

Figure 5-1. Potential models of Bid mediated maintenance of mitochondrial structure and function. A) One manner in which Bid may maintain mitochondrial physiology is through modulation of mitochondrial structure. This could be mediated through regulation of proteins involved in cristae formation or stability such as Opa1. By maintaining mitochondrial cristae structure, Bid would promote the sequestration of proteins and complexes in the ETC to the cristae. This would have two major effects. First, the cristae are important in maintaining a diffusion barrier to proteins such as Cytochrome *c*. This would prevent Cytochrome *c* mobilization, ultimately maintaining the apoptotic threshold and preventing aberrant apoptosis. Second, cristae shape is essential for efficient respiration by facilitating the formation and stabilization of respiratory chain supercomplexes. Respiratory chain supercomplexes increase the efficiency of respiration and reducing ROS production. By preventing excess ROS production, CL peroxidation and degradation is reduced which further preserves cristae structure, respiratory function, and Cytochrome *c* localization to the IMM. In this model, Bid's primary homeostatic effect on the mitochondria is in preserving cristae structure, and CL composition homeostasis is a secondary effect. B) An alternative model is possible in which Bid maintains mitochondrial physiology is through modulation of CL composition in a more direct manner. It is currently unclear how Bid may regulate CL homeostasis. Nevertheless, by maintaining CL composition, Bid would also inhibit Cytochrome *c* mobilization, maintain cristae structure, and respiratory efficiency through many of the mechanisms described in (A) (see chapter I for detailed description of how CL regulates these processes). This would also inhibit excessive ROS generation and Cytochrome *c* mobilization, thus further preserving CL composition and preventing aberrant apoptotic signaling respectively.

In my studies, I observed disruption of cristae structure and respiratory function that is similar to that described in the context of tBid and apoptosis. However, in contrast to the above reports, my investigations demonstrated that cristae were disrupted by the loss of Bid and in non-apoptotic conditions. This data suggests that, while tBid can disrupt cristae, Bid must be present to maintain cristae structure in the absence of a death stimulus. Given the role of Opa1 in maintaining cristae structure, it is possible that Bid could maintain mitochondrial physiology through facilitating or stabilizing Opa1 oligomerization. This would require that Bid regulates Opa1 differently under apoptotic and non-apoptotic conditions (e.g. full length Bid maintains Opa1 oligomerization while tBid disrupts Opa1 oligomers). Regardless, whether Bid regulates cristae structure through Opa1 or through another mechanism, Bid does not have direct access to the IMM or to IMM proteins and thus would require signal transduction across the OMM to influence IMM structure. While there are many ways this could happen, a likely means by which Bid may influence the IMM is through associating with mitochondrial contact sites, where the IMM and OMM interface. Indeed, tBid has been shown to preferentially localize to these sites during apoptosis (184). Thus, investigating both the submitochondrial localization of full length Bid under non-apoptotic conditions, as well as the proteins it binds to at the membrane, may provide insight into how it influences cristae structure.

In addition to regulating mitochondrial structure and respiration, Bid also regulates the levels of L_4CL. Restoration of L_4CL levels was sufficient to restore normal mitochondrial structure and function, indicating that it is downstream of Bid and that its loss contributes to the altered morphology and function of *Bid -/-* mitochondria. CL is well established to be essential for efficient respiration and for mitochondrial structure (310) and CL composition is also known to be altered in many cardiac diseases (310). Despite this, it is currently unclear how CL

contributes to the phenotype of *Bid -/-* MPCs and its involvement in cardiac disease is not well understood.

Because CL and mitochondrial physiology are interdependent, it is challenging to differentiate whether CL is a primary cause or a downstream effect of mitochondrial dysfunction. The reality may be more complex in that CL alterations may be both a cause and effect of mitochondrial dysfunction. In other words, while disruptions to CL mass or composition may be downstream of the initiating event, it also may be a key factor in causing the downstream consequences. In light of my studies and other work in the field, I predict that this is the case in the context of Bid deficiency. I propose that the primary cause of mitochondrial dysfunction in *Bid -/-* cells is disruption of mitochondrial cristae structure. As a result, respiratory efficiency is reduced as a consequence of respiratory chain supercomplex disruption. A consequence of respiratory chain supercomplex disruption is an increase in ROS production. Current evidence suggests that respiratory supercomplexes facilitate efficient transfer of electrons between respiratory complexes and prevent the generation of ROS (311, 312). As discussed above, CL peroxidation by ROS is thought to promote the degradation of CL (139). Thus, as a consequence of Bid deficiency CL could be peroxidized and degraded. This would create a self-perpetuating cycle in which the degradation of CL leads to further dysfunction since CL is required for normal mitochondrial structure and respiratory function (310). Furthermore, this CL loss could also contribute to Cytochrome *c* mobilization and cell death sensitivity since CL is required for Cytochrome *c* localization to the IMM (144). This model would suggest that, while CL dysregulation is an effect of cristae malformation due to Bid deficiency, it also is a cause of perpetuating further mitochondrial dysfunction. Thus, although not the primary effect of Bid

deficiency, CL dysregulation is essential to establishing the mitochondrial phenotype observed in *Bid -/-* cells by mediating a pathological feed forward pathway of mitochondrial dysfunction.

While the above model seems most likely based on our findings and other studies in the field, I cannot currently exclude the alternative model described above (Fig. 5-1B). It remains possible that the cristae disruption is secondary to an effect that Bid has on CL. Bid could regulate enzymes that mediate cardiolipin degradation, remodeling, or synthesis. Alternatively, it is also possible that Bid influences the availability of substrates for CL synthesis in the mitochondria by influencing lipid trafficking or through globally affecting lipid metabolism. However, there is little evidence or indication that Bid is involved in such processes. Thus, I suggest that it is more likely that CL composition is affected by Bid as a secondary effect to a change in mitochondrial structure and function as described above. Future studies will be required to understand how Bid regulates CL biology. However, if the above model is correct, it is likely that investigating the manner in which Bid regulates mitochondrial structure and respiration will address many of the questions regarding how Bid influences CL composition.

In this thesis, I have initiated some early investigations into how Bid may regulate mitochondrial physiology through structure/function studies of known functional domains in Bid. In particular, I have shown that Bid does not require the BH3 domain to maintain mitochondrial structure and function. This suggests that Bid maintains mitochondrial physiology independent of its interaction with other Bcl-2 family members. However, Bid does require M148 in helix 6 to maintain efficient respiration. Since helix 6 is important for the binding of Bid to membranes and for Bid function (127, 129, 150, 283), the inability of M148T to maintain efficient respiration is suggestive that membrane binding is a pre-requisite to regulating mitochondrial function. However, our results do not exclude the possibility that M148 is

necessary for protein-protein interactions required for Bid's function in maintaining mitochondrial physiology. Analyzing the effect of M148 (using the M148T Bid mutant) on membrane/lipid binding as well as protein-protein interactions will help in establishing a mechanism for how Bid regulates mitochondrial structure and physiology. It is also possible that the M148T mutation could be used to identify binding partners of Bid that are specific to its role in regulating mitochondrial homeostasis.

In addition to disrupting mitochondrial structure and respiratory efficiency, loss of Bid also sensitized MPCs to apoptosis. *Bid -/-* cells not only proved to be more sensitive to an apoptotic stimulus (IL-3 withdrawal) but also displayed a higher rate of basal cell death in the absence of an overt cellular stress. This result was intriguing as it suggests that despite being a pro-apoptotic protein, Bid also maintains viability. One of the functions of the cristae is to restrict the diffusion and local concentrations of ions, metabolites, and proteins involved in respiration to the same space, which can dramatically influence the efficiency of oxidative phosphorylation (313, 314). Cytochrome *c*, which is among the proteins restricted to the cristae, is also crucial to apoptotic signaling. The cristae are thought to serve as a barrier to the free diffusion of Cytochrome *c* into the intermembrane space (313, 314). Thus, cristae disruption could contribute to mobilization of Cytochrome *c,* which is a precursor to Cytochrome *c* release (168). I found that *Bid -/-* mitochondria had an increased fraction of Cytochrome *c* mobilized to the intermembrane space. This mobilization could prime mitochondria for execution of apoptosis by increasing the kinetics of Cytochrome *c* release in the presence of a death stimulus. The finding that *Bid -/-* MPCs have an increased rate of basal cell death suggests that even in the absence of a cell death stimulus, Cytochrome *c* mobilization can sensitize cells to death under conditions that normally would be insufficient for initiation of apoptosis. Though it is unclear

how this occurs, it is possible that the aberrant mobilization of Cytochrome *c* could promote Cytochrome *c* leakage from the mitochondria. Cytochrome *c* leakage could potentially occur through the permeability transition pore, through transient permeabilization of the OMM, or due to physical damage to the OMM. Although not significantly different, I did observe a slightly higher level of release of Cytochrome *c* from *Bid -/-* mitochondria even before the addition of digitonin, which could indicate a low level of leakage. Using a combination of fluorescently labeled Cytochrome *c* and inhibitors of the MPTP and/or MOMP (such as cyclosporin A or Bcl-XL overexpression, respectively) it may be possible to determine how Cytochrome *c* release occurs in *Bid -/-* cells to increase the basal cell death rate.

Bid's effects on mitochondria are typically studied in the context of tBid and apoptotic signaling. However, my investigations suggest that Bid impacts the mitochondria in non-apoptotic contexts as well. I have also observed that even in the absence of apoptosis, Bid co-localizes with mitochondria via confocal immunofluorescence microscopy. These findings raise an interesting question regarding Bid's function in maintaining mitochondrial structure and respiration: Is Bid able to bind mitochondria without being cleaved? While my findings regarding Bid localization do not differentiate between tBid and full length Bid, tBid is a highly potent apoptotic protein and it is unlikely that the cells displaying such co-localization of tBid and mitochondria could remain viable. Nevertheless, current models suggest that cleavage is an integral part of Bid's association with membranes (127). However, the binding of full length Bid to mitochondria has not been rigorously evaluated. Furthermore, even full length Bid has been suggested to bind membranes or to lipids such as CL, albeit at a reduced efficiency compared to tBid (129, 185, 186). Thus, it is possible that full length Bid can associate with mitochondria to regulate their function. Alternatively, it is possible that the co-localization observed in my

studies is not in fact localized to the mitochondria directly but rather is peripherally associated with the mitochondria through interacting with mitochondrial proteins. Another possibility is that Bid is localized to other membranes that are closely associated with mitochondria such as the ER. Differentiating between these possibilities may prove to be critical in understanding how Bid regulates mitochondrial structure and function. Using high resolution microscopy and biochemical fractionation of cells to determine Bid's precise localization, and what interaction partners it may have at these locations, could provide valuable mechanistic insight.

In addition to investigating the role of Bid in regulating mitochondria, I also demonstrated that Bid has broader implications for cardiac function. In mice, Bid deficiency sensitized mice to cardiac dysfunction following acute cardiac stress induced by epinephrine. In humans, Bid SNPs (particularly SNPs present in the MBD of Bid) significantly associate with MI. Furthermore, I demonstrated that while BH3 mutant Bid rescues respiration in *Bid -/-* MPCs, a double mutant of the BH3 domain and M148T (one of the MBD SNPs) does not. Altogether these findings suggest that the mitochondrial phenotype of *Bid -/-* cells has significant consequences for cardiac function, especially during acute cardiac stress such as during increased workload or during reduced oxygen availability. These data are consistent with other findings in the literature that establish a critical importance of mitochondrial respiratory function for cardiac function (293). Nevertheless, there are several additional questions that remain. For example, as discussed above, *Bid -/-* MPCs are sensitized to basal and stimuli induced apoptosis. This suggests the possibility that *Bid -/-* cardiomyocytes may also be sensitized to stress-induced apoptosis. While the reduced respiratory efficiency will cause reduced cardiomyocyte (and reduced overall cardiac) function, it is also possible that *Bid -/-* hearts experience greater cardiomyocyte dropout due to sensitization to apoptosis. The combined effects of decreased

respiratory efficiency and increased susceptibility to cardiomyocyte death would be consistent with an overall decrease in cardiac function during stress. This could also suggest that loss of Bid or disruption of Bid function in maintaining mitochondrial homeostasis may impact the progression of, or recovery from, cardiac injury. Thus, a rigorous analysis of *Bid -/-* hearts following acute stress may provide greater information about exactly how Bid regulates heart function.

While my results indicate that Bid deficient hearts are sensitized to acute cardiac stress, we did not evaluate the long-term implications through inducing a chronic stress. For example, it is possible that, *Bid -/-* mice would be predisposed to developing cardiac hypertrophy or cardiomyopathy if exposed to chronic cardiac stress. Given our findings that *Bid -/-* cardiomyocytes have reduced respiratory efficiency, it would be logical that *Bid -/-* hearts would be unable to function properly during chronic stress and thus develop chronic heart conditions. Such chronic heart diseases often progress into heart failure, thus we may also expect an increased incidence of heart failure as an outcome to extended cardiac stress in *Bid -/-* mice. The effect of chronic cardiac stress could be established by performing aortic constriction or repeated exercise-induced cardiac stress experiments (such as the forced swim test). These findings could provide further insight into the consequences of Bid dysfunction and potentially extend into human studies.

One limitation to our investigation into human Bid SNP associations was that, due to the low minor allele frequency of Bid SNPs (0.0004% to 2.1%), we had a limited number of subjects for our study (1,033 for any Bid variant, 62 for MBD variant). Thus, while we were able to establish associations with MI by analyzing SNPs as groups, we did not have sufficient statistical power to establish associations with individual SNPs. Extending our analysis to larger cohorts, or

to different populations, may provide greater statistical power and reveal additional associations to other cardiac diseases. Such investigations could also serve to corroborate or inform additional mouse studies.

In my thesis, I focused specifically on how Bid impacts heart function. However, it is important to note that Bid deficiency may impact other tissues and organs. Mitochondrial function is essential for many basic cellular processes and thus could have diverse effects on physiology and viability of many different cell types. Indeed, mitochondrial dysfunction contributes to many different pathologies such as diabetes, Alzheimer's disease, Parkinson's disease, cardiovascular disease, and cancer (315). Thus, further studies into the effects of Bid deficiency could potentially reveal a role in pathologies in addition to cardiac diseases.

REFERENCES

1. **Zinkel SS, Hurov KE, Ong C, Abtahi FM, Gross A, Korsmeyer SJ.** 2005. A role for proapoptotic BID in the DNA-damage response. Cell **122:**579-591.
2. **Kamer I, Sarig R, Zaltsman Y, Niv H, Oberkovitz G, Regev L, Haimovich G, Lerenthal Y, Marcellus RC, Gross A.** 2005. Proapoptotic BID is an ATM effector in the DNA-damage response. Cell **122:**593-603.
3. **Liu Y, Aiello A, Zinkel SS.** 2012. Bid protects the mouse hematopoietic system following hydroxyurea-induced replicative stress. Cell Death Differ **19:**1602-1612.
4. **Liu Y, Bertram CC, Shi Q, Zinkel SS.** 2011. Proapoptotic Bid mediates the ATR-directed DNA damage response to replicative stress. Cell Death Differ **18:**841-852.
5. **Liu Y, Vaithiyalingam S, Shi Q, Chazin WJ, Zinkel SS.** 2011. BID binds to replication protein A and stimulates ATR function following replicative stress. Mol Cell Biol **31:**4298-4309.
6. **Danial NN, Korsmeyer SJ.** 2004. Cell death: critical control points. Cell **116:**205-219.
7. **Fuchs Y, Steller H.** 2011. Programmed cell death in animal development and disease. Cell **147:**742-758.
8. **Vaux DL, Korsmeyer SJ.** 1999. Cell death in development. Cell **96:**245-254.
9. **Agostini M, Tucci P, Melino G.** 2011. Cell death pathology: perspective for human diseases. Biochem Biophys Res Commun **414:**451-455.
10. **Avila J.** 2010. Alzheimer disease: caspases first. Nat Rev Neurol **6:**587-588.
11. **Sassone J, Colciago C, Marchi P, Ascardi C, Alberti L, Di Pardo A, Zippel R, Sipione S, Silani V, Ciammola A.** 2010. Mutant Huntingtin induces activation of the Bcl-2/adenovirus E1B 19-kDa interacting protein (BNip3). Cell Death Dis **1:**e7.
12. **Cheng J, Zhou T, Liu C, Shapiro JP, Brauer MJ, Kiefer MC, Barr PJ, Mountz JD.** 1994. Protection from Fas-mediated apoptosis by a soluble form of the Fas molecule. Science **263:**1759-1762.
13. **Gatenby PA, Irvine M.** 1994. The bcl-2 proto-oncogene is overexpressed in systemic lupus erythematosus. J Autoimmun **7:**623-631.
14. **Liu H, Pope RM.** 2003. The role of apoptosis in rheumatoid arthritis. Curr Opin Pharmacol **3:**317-322.
15. **Lee SC, Pervaiz S.** 2007. Apoptosis in the pathophysiology of diabetes mellitus. Int J Biochem Cell Biol **39:**497-504.
16. **Cummins NW, Badley AD.** 2010. Mechanisms of HIV-associated lymphocyte apoptosis: 2010. Cell Death Dis **1:**e99.
17. **Broughton BR, Reutens DC, Sobey CG.** 2009. Apoptotic mechanisms after cerebral ischemia. Stroke **40:**e331-339.
18. **Krijnen PA, Nijmeijer R, Meijer CJ, Visser CA, Hack CE, Niessen HW.** 2002. Apoptosis in myocardial ischaemia and infarction. J Clin Pathol **55:**801-811.
19. **Hanahan D, Weinberg RA.** 2011. Hallmarks of cancer: the next generation. Cell **144:**646-674.
20. **Zipp F.** 2000. Apoptosis in multiple sclerosis. Cell Tissue Res **301:**163-171.
21. **Tan W, Pasinelli P, Trotti D.** 2014. Role of mitochondria in mutant SOD1 linked amyotrophic lateral sclerosis. Biochim Biophys Acta **1842:**1295-1301.

22. **Engel T, Henshall DC.** 2009. Apoptosis, Bcl-2 family proteins and caspases: the ABCs of seizure-damage and epileptogenesis? Int J Physiol Pathophysiol Pharmacol **1:**97-115.
23. **Sancho-Pelluz J, Arango-Gonzalez B, Kustermann S, Romero FJ, van Veen T, Zrenner E, Ekstrom P, Paquet-Durand F.** 2008. Photoreceptor cell death mechanisms in inherited retinal degeneration. Mol Neurobiol **38:**253-269.
24. **Wang K.** 2014. Molecular mechanisms of hepatic apoptosis. Cell Death Dis **5:**e996.
25. **Tsujimoto Y, Shimizu S.** 2005. Another way to die: autophagic programmed cell death. Cell Death Differ **12 Suppl 2:**1528-1534.
26. **Liu Y, Shoji-Kawata S, Sumpter RM, Jr., Wei Y, Ginet V, Zhang L, Posner B, Tran KA, Green DR, Xavier RJ, Shaw SY, Clarke PG, Puyal J, Levine B.** 2013. Autosis is a Na+,K+-ATPase-regulated form of cell death triggered by autophagy-inducing peptides, starvation, and hypoxia-ischemia. Proc Natl Acad Sci U S A **110:**20364-20371.
27. **Edinger AL, Thompson CB.** 2004. Death by design: apoptosis, necrosis and autophagy. Curr Opin Cell Biol **16:**663-669.
28. **Linkermann A, Green DR.** 2014. Necroptosis. N Engl J Med **370:**455-465.
29. **Kerr JF, Wyllie AH, Currie AR.** 1972. Apoptosis: a basic biological phenomenon with wide-ranging implications in tissue kinetics. Br J Cancer **26:**239-257.
30. **Scaffidi C, Fulda S, Srinivasan A, Friesen C, Li F, Tomaselli KJ, Debatin KM, Krammer PH, Peter ME.** 1998. Two CD95 (APO-1/Fas) signaling pathways. EMBO J **17:**1675-1687.
31. **Barnhart BC, Alappat EC, Peter ME.** 2003. The CD95 type I/type II model. Semin Immunol **15:**185-193.
32. **Luo X, Budihardjo I, Zou H, Slaughter C, Wang X.** 1998. Bid, a Bcl2 interacting protein, mediates cytochrome c release from mitochondria in response to activation of cell surface death receptors. Cell **94:**481-490.
33. **Li H, Zhu H, Xu CJ, Yuan J.** 1998. Cleavage of BID by caspase 8 mediates the mitochondrial damage in the Fas pathway of apoptosis. Cell **94:**491-501.
34. **Wang K, Yin XM, Chao DT, Milliman CL, Korsmeyer SJ.** 1996. BID: a novel BH3 domain-only death agonist. Genes Dev **10:**2859-2869.
35. **Roos WP, Kaina B.** 2006. DNA damage-induced cell death by apoptosis. Trends Mol Med **12:**440-450.
36. **Sano R, Reed JC.** 2013. ER stress-induced cell death mechanisms. Biochim Biophys Acta **1833:**3460-3470.
37. **Brumatti G, Salmanidis M, Ekert PG.** 2010. Crossing paths: interactions between the cell death machinery and growth factor survival signals. Cell Mol Life Sci **67:**1619-1630.
38. **Circu ML, Aw TY.** 2010. Reactive oxygen species, cellular redox systems, and apoptosis. Free Radic Biol Med **48:**749-762.
39. **Danial NN.** 2007. BCL-2 family proteins: critical checkpoints of apoptotic cell death. Clin Cancer Res **13:**7254-7263.
40. **Susin SA, Lorenzo HK, Zamzami N, Marzo I, Snow BE, Brothers GM, Mangion J, Jacotot E, Costantini P, Loeffler M, Larochette N, Goodlett DR, Aebersold R, Siderovski DP, Penninger JM, Kroemer G.** 1999. Molecular characterization of mitochondrial apoptosis-inducing factor. Nature **397:**441-446.
41. **Li LY, Luo X, Wang X.** 2001. Endonuclease G is an apoptotic DNase when released from mitochondria. Nature **412:**95-99.

42. **Parrish J, Li L, Klotz K, Ledwich D, Wang X, Xue D.** 2001. Mitochondrial endonuclease G is important for apoptosis in C. elegans. Nature **412:**90-94.
43. **Du C, Fang M, Li Y, Li L, Wang X.** 2000. Smac, a mitochondrial protein that promotes cytochrome c-dependent caspase activation by eliminating IAP inhibition. Cell **102:**33-42.
44. **Verhagen AM, Ekert PG, Pakusch M, Silke J, Connolly LM, Reid GE, Moritz RL, Simpson RJ, Vaux DL.** 2000. Identification of DIABLO, a mammalian protein that promotes apoptosis by binding to and antagonizing IAP proteins. Cell **102:**43-53.
45. **Van Loo G, Demol H, van Gurp M, Hoorelbeke B, Schotte P, Beyaert R, Zhivotovsky B, Gevaert K, Declercq W, Vandekerckhove J, Vandenabeele P.** 2002. A matrix-assisted laser desorption ionization post-source decay (MALDI-PSD) analysis of proteins released from isolated liver mitochondria treated with recombinant truncated Bid. Cell Death Differ **9:**301-308.
46. **Liu X, Kim CN, Yang J, Jemmerson R, Wang X.** 1996. Induction of apoptotic program in cell-free extracts: requirement for dATP and cytochrome c. Cell **86:**147-157.
47. **Deveraux QL, Reed JC.** 1999. IAP family proteins--suppressors of apoptosis. Genes Dev **13:**239-252.
48. **van Loo G, van Gurp M, Depuydt B, Srinivasula SM, Rodriguez I, Alnemri ES, Gevaert K, Vandekerckhove J, Declercq W, Vandenabeele P.** 2002. The serine protease Omi/HtrA2 is released from mitochondria during apoptosis. Omi interacts with caspase-inhibitor XIAP and induces enhanced caspase activity. Cell Death Differ **9:**20-26.
49. **Daugas E, Susin SA, Zamzami N, Ferri KF, Irinopoulou T, Larochette N, Prevost MC, Leber B, Andrews D, Penninger J, Kroemer G.** 2000. Mitochondrio-nuclear translocation of AIF in apoptosis and necrosis. FASEB J **14:**729-739.
50. **Joza N, Susin SA, Daugas E, Stanford WL, Cho SK, Li CY, Sasaki T, Elia AJ, Cheng HY, Ravagnan L, Ferri KF, Zamzami N, Wakeham A, Hakem R, Yoshida H, Kong YY, Mak TW, Zuniga-Pflucker JC, Kroemer G, Penninger JM.** 2001. Essential role of the mitochondrial apoptosis-inducing factor in programmed cell death. Nature **410:**549-554.
51. **Enari M, Sakahira H, Yokoyama H, Okawa K, Iwamatsu A, Nagata S.** 1998. A caspase-activated DNase that degrades DNA during apoptosis, and its inhibitor ICAD. Nature **391:**43-50.
52. **Leung AW, Halestrap AP.** 2008. Recent progress in elucidating the molecular mechanism of the mitochondrial permeability transition pore. Biochim Biophys Acta **1777:**946-952.
53. **Pastorino JG, Chen ST, Tafani M, Snyder JW, Farber JL.** 1998. The overexpression of Bax produces cell death upon induction of the mitochondrial permeability transition. J Biol Chem **273:**7770-7775.
54. **Narita M, Shimizu S, Ito T, Chittenden T, Lutz RJ, Matsuda H, Tsujimoto Y.** 1998. Bax interacts with the permeability transition pore to induce permeability transition and cytochrome c release in isolated mitochondria. Proc Natl Acad Sci U S A **95:**14681-14686.
55. **Marzo I, Brenner C, Zamzami N, Jurgensmeier JM, Susin SA, Vieira HL, Prevost MC, Xie Z, Matsuyama S, Reed JC, Kroemer G.** 1998. Bax and adenine nucleotide translocator cooperate in the mitochondrial control of apoptosis. Science **281:**2027-2031.

56. **Zamzami N, Brenner C, Marzo I, Susin SA, Kroemer G.** 1998. Subcellular and submitochondrial mode of action of Bcl-2-like oncoproteins. Oncogene **16:**2265-2282.
57. **Crompton M.** 1999. The mitochondrial permeability transition pore and its role in cell death. Biochem J **341 (Pt 2):**233-249.
58. **Halestrap AP, Richardson AP.** 2015. The mitochondrial permeability transition: A current perspective on its identity and role in ischaemia/reperfusion injury. J Mol Cell Cardiol **78C:**129-141.
59. **Grimm S, Brdiczka D.** 2007. The permeability transition pore in cell death. Apoptosis **12:**841-855.
60. **Pop C, Salvesen GS.** 2009. Human caspases: activation, specificity, and regulation. J Biol Chem **284:**21777-21781.
61. **Riedl SJ, Salvesen GS.** 2007. The apoptosome: signalling platform of cell death. Nat Rev Mol Cell Biol **8:**405-413.
62. **Timmer JC, Salvesen GS.** 2007. Caspase substrates. Cell Death Differ **14:**66-72.
63. **Fischer U, Janicke RU, Schulze-Osthoff K.** 2003. Many cuts to ruin: a comprehensive update of caspase substrates. Cell Death Differ **10:**76-100.
64. **Sulston JE.** 1976. Post-embryonic development in the ventral cord of Caenorhabditis elegans. Philos Trans R Soc Lond B Biol Sci **275:**287-297.
65. **Ellis HM, Horvitz HR.** 1986. Genetic control of programmed cell death in the nematode C. elegans. Cell **44:**817-829.
66. **Hengartner MO, Horvitz HR.** 1994. Activation of C. elegans cell death protein CED-9 by an amino-acid substitution in a domain conserved in Bcl-2. Nature **369:**318-320.
67. **Conradt B, Horvitz HR.** 1998. The C. elegans protein EGL-1 is required for programmed cell death and interacts with the Bcl-2-like protein CED-9. Cell **93:**519-529.
68. **Tsujimoto Y, Finger LR, Yunis J, Nowell PC, Croce CM.** 1984. Cloning of the chromosome breakpoint of neoplastic B cells with the t(14;18) chromosome translocation. Science **226:**1097-1099.
69. **Cleary ML, Smith SD, Sklar J.** 1986. Cloning and structural analysis of cDNAs for bcl-2 and a hybrid bcl-2/immunoglobulin transcript resulting from the t(14;18) translocation. Cell **47:**19-28.
70. **Graninger WB, Seto M, Boutain B, Goldman P, Korsmeyer SJ.** 1987. Expression of Bcl-2 and Bcl-2-Ig fusion transcripts in normal and neoplastic cells. J Clin Invest **80:**1512-1515.
71. **Vaux DL, Cory S, Adams JM.** 1988. Bcl-2 gene promotes haemopoietic cell survival and cooperates with c-myc to immortalize pre-B cells. Nature **335:**440-442.
72. **McDonnell TJ, Deane N, Platt FM, Nunez G, Jaeger U, McKearn JP, Korsmeyer SJ.** 1989. bcl-2-immunoglobulin transgenic mice demonstrate extended B cell survival and follicular lymphoproliferation. Cell **57:**79-88.
73. **Hockenbery D, Nunez G, Milliman C, Schreiber RD, Korsmeyer SJ.** 1990. Bcl-2 is an inner mitochondrial membrane protein that blocks programmed cell death. Nature **348:**334-336.
74. **Oltvai ZN, Milliman CL, Korsmeyer SJ.** 1993. Bcl-2 heterodimerizes in vivo with a conserved homolog, Bax, that accelerates programmed cell death. Cell **74:**609-619.
75. **Datta SR, Katsov A, Hu L, Petros A, Fesik SW, Yaffe MB, Greenberg ME.** 2000. 14-3-3 proteins and survival kinases cooperate to inactivate BAD by BH3 domain phosphorylation. Mol Cell **6:**41-51.

76. **Zha J, Harada H, Yang E, Jockel J, Korsmeyer SJ.** 1996. Serine phosphorylation of death agonist BAD in response to survival factor results in binding to 14-3-3 not BCL-X(L). Cell **87:**619-628.
77. **Pinon JD, Labi V, Egle A, Villunger A.** 2008. Bim and Bmf in tissue homeostasis and malignant disease. Oncogene **27 Suppl 1:**S41-52.
78. **Akiyama T, Tanaka S.** 2011. Bim: guardian of tissue homeostasis and critical regulator of the immune system, tumorigenesis and bone biology. Arch Immunol Ther Exp (Warsz) **59:**277-287.
79. **Puthalakath H, Huang DC, O'Reilly LA, King SM, Strasser A.** 1999. The proapoptotic activity of the Bcl-2 family member Bim is regulated by interaction with the dynein motor complex. Mol Cell **3:**287-296.
80. **Han J, Flemington C, Houghton AB, Gu Z, Zambetti GP, Lutz RJ, Zhu L, Chittenden T.** 2001. Expression of bbc3, a pro-apoptotic BH3-only gene, is regulated by diverse cell death and survival signals. Proc Natl Acad Sci U S A **98:**11318-11323.
81. **Nakano K, Vousden KH.** 2001. PUMA, a novel proapoptotic gene, is induced by p53. Mol Cell **7:**683-694.
82. **Hikisz P, Kilianska ZM.** 2012. PUMA, a critical mediator of cell death--one decade on from its discovery. Cell Mol Biol Lett **17:**646-669.
83. **Ploner C, Kofler R, Villunger A.** 2008. Noxa: at the tip of the balance between life and death. Oncogene **27 Suppl 1:**S84-92.
84. **Sandow JJ, Jabbour AM, Condina MR, Daunt CP, Stomski FC, Green BD, Riffkin CD, Hoffmann P, Guthridge MA, Silke J, Lopez AF, Ekert PG.** 2012. Cytokine receptor signaling activates an IKK-dependent phosphorylation of PUMA to prevent cell death. Cell Death Differ **19:**633-641.
85. **Yin XM, Wang K, Gross A, Zhao Y, Zinkel S, Klocke B, Roth KA, Korsmeyer SJ.** 1999. Bid-deficient mice are resistant to Fas-induced hepatocellular apoptosis. Nature **400:**886-891.
86. **Desagher S, Osen-Sand A, Montessuit S, Magnenat E, Vilbois F, Hochmann A, Journot L, Antonsson B, Martinou JC.** 2001. Phosphorylation of bid by casein kinases I and II regulates its cleavage by caspase 8. Mol Cell **8:**601-611.
87. **Oda E, Ohki R, Murasawa H, Nemoto J, Shibue T, Yamashita T, Tokino T, Taniguchi T, Tanaka N.** 2000. Noxa, a BH3-only member of the Bcl-2 family and candidate mediator of p53-induced apoptosis. Science **288:**1053-1058.
88. **Villunger A, Michalak EM, Coultas L, Mullauer F, Bock G, Ausserlechner MJ, Adams JM, Strasser A.** 2003. p53- and drug-induced apoptotic responses mediated by BH3-only proteins puma and noxa. Science **302:**1036-1038.
89. **Kim JY, Ahn HJ, Ryu JH, Suk K, Park JH.** 2004. BH3-only protein Noxa is a mediator of hypoxic cell death induced by hypoxia-inducible factor 1alpha. J Exp Med **199:**113-124.
90. **Chi X, Kale J, Leber B, Andrews DW.** 2014. Regulating cell death at, on, and in membranes. Biochim Biophys Acta **1843:**2100-2113.
91. **Lindsten T, Ross AJ, King A, Zong WX, Rathmell JC, Shiels HA, Ulrich E, Waymire KG, Mahar P, Frauwirth K, Chen Y, Wei M, Eng VM, Adelman DM, Simon MC, Ma A, Golden JA, Evan G, Korsmeyer SJ, MacGregor GR, Thompson CB.** 2000. The combined functions of proapoptotic Bcl-2 family members bak and bax are essential for normal development of multiple tissues. Mol Cell **6:**1389-1399.

92. **Shamas-Din A, Kale J, Leber B, Andrews DW.** 2013. Mechanisms of action of Bcl-2 family proteins. Cold Spring Harb Perspect Biol **5:**a008714.
93. **Letai A, Bassik MC, Walensky LD, Sorcinelli MD, Weiler S, Korsmeyer SJ.** 2002. Distinct BH3 domains either sensitize or activate mitochondrial apoptosis, serving as prototype cancer therapeutics. Cancer Cell **2:**183-192.
94. **Terradillos O, Montessuit S, Huang DC, Martinou JC.** 2002. Direct addition of BimL to mitochondria does not lead to cytochrome c release. FEBS Lett **522:**29-34.
95. **Chen L, Willis SN, Wei A, Smith BJ, Fletcher JI, Hinds MG, Colman PM, Day CL, Adams JM, Huang DC.** 2005. Differential targeting of prosurvival Bcl-2 proteins by their BH3-only ligands allows complementary apoptotic function. Mol Cell **17:**393-403.
96. **Gallenne T, Gautier F, Oliver L, Hervouet E, Noel B, Hickman JA, Geneste O, Cartron PF, Vallette FM, Manon S, Juin P.** 2009. Bax activation by the BH3-only protein Puma promotes cell dependence on antiapoptotic Bcl-2 family members. J Cell Biol **185:**279-290.
97. **Kim H, Rafiuddin-Shah M, Tu HC, Jeffers JR, Zambetti GP, Hsieh JJ, Cheng EH.** 2006. Hierarchical regulation of mitochondrion-dependent apoptosis by BCL-2 subfamilies. Nat Cell Biol **8:**1348-1358.
98. **Kuwana T, Bouchier-Hayes L, Chipuk JE, Bonzon C, Sullivan BA, Green DR, Newmeyer DD.** 2005. BH3 domains of BH3-only proteins differentially regulate Bax-mediated mitochondrial membrane permeabilization both directly and indirectly. Mol Cell **17:**525-535.
99. **Ren D, Tu HC, Kim H, Wang GX, Bean GR, Takeuchi O, Jeffers JR, Zambetti GP, Hsieh JJ, Cheng EH.** 2010. BID, BIM, and PUMA are essential for activation of the BAX- and BAK-dependent cell death program. Science **330:**1390-1393.
100. **Moldoveanu T, Follis AV, Kriwacki RW, Green DR.** 2014. Many players in BCL-2 family affairs. Trends Biochem Sci **39:**101-111.
101. **Karbowski M, Norris KL, Cleland MM, Jeong SY, Youle RJ.** 2006. Role of Bax and Bak in mitochondrial morphogenesis. Nature **443:**658-662.
102. **Hoppins S, Edlich F, Cleland MM, Banerjee S, McCaffery JM, Youle RJ, Nunnari J.** 2011. The soluble form of Bax regulates mitochondrial fusion via MFN2 homotypic complexes. Mol Cell **41:**150-160.
103. **Alavian KN, Li H, Collis L, Bonanni L, Zeng L, Sacchetti S, Lazrove E, Nabili P, Flaherty B, Graham M, Chen Y, Messerli SM, Mariggio MA, Rahner C, McNay E, Shore GC, Smith PJ, Hardwick JM, Jonas EA.** 2011. Bcl-xL regulates metabolic efficiency of neurons through interaction with the mitochondrial F1FO ATP synthase. Nat Cell Biol **13:**1224-1233.
104. **Chen YB, Aon MA, Hsu YT, Soane L, Teng X, McCaffery JM, Cheng WC, Qi B, Li H, Alavian KN, Dayhoff-Brannigan M, Zou S, Pineda FJ, O'Rourke B, Ko YH, Pedersen PL, Kaczmarek LK, Jonas EA, Hardwick JM.** 2011. Bcl-xL regulates mitochondrial energetics by stabilizing the inner membrane potential. J Cell Biol **195:**263-276.
105. **Vander Heiden MG, Chandel NS, Schumacker PT, Thompson CB.** 1999. Bcl-xL prevents cell death following growth factor withdrawal by facilitating mitochondrial ATP/ADP exchange. Mol Cell **3:**159-167.
106. **Perciavalle RM, Stewart DP, Koss B, Lynch J, Milasta S, Bathina M, Temirov J, Cleland MM, Pelletier S, Schuetz JD, Youle RJ, Green DR, Opferman JT.** 2012.

Anti-apoptotic MCL-1 localizes to the mitochondrial matrix and couples mitochondrial fusion to respiration. Nat Cell Biol **14:**575-583.

107. **Hardwick JM, Soane L.** 2013. Multiple functions of BCL-2 family proteins. Cold Spring Harb Perspect Biol **5**.
108. **Yeretssian G, Correa RG, Doiron K, Fitzgerald P, Dillon CP, Green DR, Reed JC, Saleh M.** 2011. Non-apoptotic role of BID in inflammation and innate immunity. Nature **474:**96-99.
109. **Seo SY, Chen YB, Ivanovska I, Ranger AM, Hong SJ, Dawson VL, Korsmeyer SJ, Bellows DS, Fannjiang Y, Hardwick JM.** 2004. BAD is a pro-survival factor prior to activation of its pro-apoptotic function. J Biol Chem **279:**42240-42249.
110. **Danial NN, Gramm CF, Scorrano L, Zhang CY, Krauss S, Ranger AM, Datta SR, Greenberg ME, Licklider LJ, Lowell BB, Gygi SP, Korsmeyer SJ.** 2003. BAD and glucokinase reside in a mitochondrial complex that integrates glycolysis and apoptosis. Nature **424:**952-956.
111. **Danial NN, Walensky LD, Zhang CY, Choi CS, Fisher JK, Molina AJ, Datta SR, Pitter KL, Bird GH, Wikstrom JD, Deeney JT, Robertson K, Morash J, Kulkarni A, Neschen S, Kim S, Greenberg ME, Corkey BE, Shirihai OS, Shulman GI, Lowell BB, Korsmeyer SJ.** 2008. Dual role of proapoptotic BAD in insulin secretion and beta cell survival. Nat Med **14:**144-153.
112. **Lowman XH, McDonnell MA, Kosloske A, Odumade OA, Jenness C, Karim CB, Jemmerson R, Kelekar A.** 2010. The proapoptotic function of Noxa in human leukemia cells is regulated by the kinase Cdk5 and by glucose. Mol Cell **40:**823-833.
113. **Gross A, Yin XM, Wang K, Wei MC, Jockel J, Milliman C, Erdjument-Bromage H, Tempst P, Korsmeyer SJ.** 1999. Caspase cleaved BID targets mitochondria and is required for cytochrome c release, while BCL-XL prevents this release but not tumor necrosis factor-R1/Fas death. J Biol Chem **274:**1156-1163.
114. **Chou JJ, Li H, Salvesen GS, Yuan J, Wagner G.** 1999. Solution structure of BID, an intracellular amplifier of apoptotic signaling. Cell **96:**615-624.
115. **McDonnell JM, Fushman D, Milliman CL, Korsmeyer SJ, Cowburn D.** 1999. Solution structure of the proapoptotic molecule BID: a structural basis for apoptotic agonists and antagonists. Cell **96:**625-634.
116. **Hinds MG, Smits C, Fredericks-Short R, Risk JM, Bailey M, Huang DC, Day CL.** 2007. Bim, Bad and Bmf: intrinsically unstructured BH3-only proteins that undergo a localized conformational change upon binding to prosurvival Bcl-2 targets. Cell Death Differ **14:**128-136.
117. **Billen LP, Shamas-Din A, Andrews DW.** 2008. Bid: a Bax-like BH3 protein. Oncogene **27 Suppl 1:**S93-104.
118. **Lovell JF, Billen LP, Bindner S, Shamas-Din A, Fradin C, Leber B, Andrews DW.** 2008. Membrane binding by tBid initiates an ordered series of events culminating in membrane permeabilization by Bax. Cell **135:**1074-1084.
119. **Slee EA, Keogh SA, Martin SJ.** 2000. Cleavage of BID during cytotoxic drug and UV radiation-induced apoptosis occurs downstream of the point of Bcl-2 action and is catalysed by caspase-3: a potential feedback loop for amplification of apoptosis-associated mitochondrial cytochrome c release. Cell Death Differ **7:**556-565.

120. **Heibein JA, Goping IS, Barry M, Pinkoski MJ, Shore GC, Green DR, Bleackley RC.** 2000. Granzyme B-mediated cytochrome c release is regulated by the Bcl-2 family members bid and Bax. J Exp Med **192:**1391-1402.
121. **Chen M, He H, Zhan S, Krajewski S, Reed JC, Gottlieb RA.** 2001. Bid is cleaved by calpain to an active fragment in vitro and during myocardial ischemia/reperfusion. J Biol Chem **276:**30724-30728.
122. **Mandic A, Viktorsson K, Strandberg L, Heiden T, Hansson J, Linder S, Shoshan MC.** 2002. Calpain-mediated Bid cleavage and calpain-independent Bak modulation: two separate pathways in cisplatin-induced apoptosis. Mol Cell Biol **22:**3003-3013.
123. **Stoka V, Turk B, Schendel SL, Kim TH, Cirman T, Snipas SJ, Ellerby LM, Bredesen D, Freeze H, Abrahamson M, Bromme D, Krajewski S, Reed JC, Yin XM, Turk V, Salvesen GS.** 2001. Lysosomal protease pathways to apoptosis. Cleavage of bid, not pro-caspases, is the most likely route. J Biol Chem **276:**3149-3157.
124. **Reiners JJ, Jr., Caruso JA, Mathieu P, Chelladurai B, Yin XM, Kessel D.** 2002. Release of cytochrome c and activation of pro-caspase-9 following lysosomal photodamage involves Bid cleavage. Cell Death Differ **9:**934-944.
125. **Cirman T, Oresic K, Mazovec GD, Turk V, Reed JC, Myers RM, Salvesen GS, Turk B.** 2004. Selective disruption of lysosomes in HeLa cells triggers apoptosis mediated by cleavage of Bid by multiple papain-like lysosomal cathepsins. J Biol Chem **279:**3578-3587.
126. **Zha J, Weiler S, Oh KJ, Wei MC, Korsmeyer SJ.** 2000. Posttranslational N-myristoylation of BID as a molecular switch for targeting mitochondria and apoptosis. Science **290:**1761-1765.
127. **Shamas-Din A, Bindner S, Zhu W, Zaltsman Y, Campbell C, Gross A, Leber B, Andrews DW, Fradin C.** 2013. tBid undergoes multiple conformational changes at the membrane required for Bax activation. J Biol Chem **288:**22111-22127.
128. **Zaltsman Y, Shachnai L, Yivgi-Ohana N, Schwarz M, Maryanovich M, Houtkooper RH, Vaz FM, De Leonardis F, Fiermonte G, Palmieri F, Gillissen B, Daniel PT, Jimenez E, Walsh S, Koehler CM, Roy SS, Walter L, Hajnoczky G, Gross A.** 2010. MTCH2/MIMP is a major facilitator of tBID recruitment to mitochondria. Nat Cell Biol **12:**553-562.
129. **Lutter M, Fang M, Luo X, Nishijima M, Xie X, Wang X.** 2000. Cardiolipin provides specificity for targeting of tBid to mitochondria. Nat Cell Biol **2:**754-761.
130. **Kuwana T, Mackey MR, Perkins G, Ellisman MH, Latterich M, Schneiter R, Green DR, Newmeyer DD.** 2002. Bid, Bax, and lipids cooperate to form supramolecular openings in the outer mitochondrial membrane. Cell **111:**331-342.
131. **Wei MC, Lindsten T, Mootha VK, Weiler S, Gross A, Ashiya M, Thompson CB, Korsmeyer SJ.** 2000. tBID, a membrane-targeted death ligand, oligomerizes BAK to release cytochrome c. Genes Dev **14:**2060-2071.
132. **Yethon JA, Epand RF, Leber B, Epand RM, Andrews DW.** 2003. Interaction with a membrane surface triggers a reversible conformational change in Bax normally associated with induction of apoptosis. J Biol Chem **278:**48935-48941.
133. **Eskes R, Desagher S, Antonsson B, Martinou JC.** 2000. Bid induces the oligomerization and insertion of Bax into the outer mitochondrial membrane. Mol Cell Biol **20:**929-935.

134. **Plesnila N, Zinkel S, Le DA, Amin-Hanjani S, Wu Y, Qiu J, Chiarugi A, Thomas SS, Kohane DS, Korsmeyer SJ, Moskowitz MA.** 2001. BID mediates neuronal cell death after oxygen/ glucose deprivation and focal cerebral ischemia. Proc Natl Acad Sci U S A **98:**15318-15323.
135. **Zinkel SS, Ong CC, Ferguson DO, Iwasaki H, Akashi K, Bronson RT, Kutok JL, Alt FW, Korsmeyer SJ.** 2003. Proapoptotic BID is required for myeloid homeostasis and tumor suppression. Genes Dev **17:**229-239.
136. **Maryanovich M, Oberkovitz G, Niv H, Vorobiyov L, Zaltsman Y, Brenner O, Lapidot T, Jung S, Gross A.** 2012. The ATM-BID pathway regulates quiescence and survival of haematopoietic stem cells. Nat Cell Biol **14:**535-541.
137. **Green DR, Galluzzi L, Kroemer G.** 2014. Cell biology. Metabolic control of cell death. Science **345:**1250256.
138. **Lin MT, Beal MF.** 2006. Mitochondrial dysfunction and oxidative stress in neurodegenerative diseases. Nature **443:**787-795.
139. **Chicco AJ, Sparagna GC.** 2007. Role of cardiolipin alterations in mitochondrial dysfunction and disease. Am J Physiol Cell Physiol **292:**C33-44.
140. **Osman C, Voelker DR, Langer T.** 2011. Making heads or tails of phospholipids in mitochondria. J Cell Biol **192:**7-16.
141. **Schlame M.** 2013. Cardiolipin remodeling and the function of tafazzin. Biochim Biophys Acta **1831:**582-588.
142. **Beranek A, Rechberger G, Knauer H, Wolinski H, Kohlwein SD, Leber R.** 2009. Identification of a cardiolipin-specific phospholipase encoded by the gene CLD1 (YGR110W) in yeast. J Biol Chem **284:**11572-11578.
143. **Malhotra A, Edelman-Novemsky I, Xu Y, Plesken H, Ma J, Schlame M, Ren M.** 2009. Role of calcium-independent phospholipase A2 in the pathogenesis of Barth syndrome. Proc Natl Acad Sci U S A **106:**2337-2341.
144. **Houtkooper RH, Vaz FM.** 2008. Cardiolipin, the heart of mitochondrial metabolism. Cell Mol Life Sci **65:**2493-2506.
145. **Schwall CT, Greenwood VL, Alder NN.** 2012. The stability and activity of respiratory Complex II is cardiolipin-dependent. Biochim Biophys Acta **1817:**1588-1596.
146. **Paradies G, Paradies V, De Benedictis V, Ruggiero FM, Petrosillo G.** 2014. Functional role of cardiolipin in mitochondrial bioenergetics. Biochim Biophys Acta **1837:**408-417.
147. **Acehan D, Malhotra A, Xu Y, Ren M, Stokes DL, Schlame M.** 2011. Cardiolipin affects the supramolecular organization of ATP synthase in mitochondria. Biophys J **100:**2184-2192.
148. **Strauss M, Hofhaus G, Schroder RR, Kuhlbrandt W.** 2008. Dimer ribbons of ATP synthase shape the inner mitochondrial membrane. EMBO J **27:**1154-1160.
149. **Paumard P, Vaillier J, Coulary B, Schaeffer J, Soubannier V, Mueller DM, Brethes D, di Rago JP, Velours J.** 2002. The ATP synthase is involved in generating mitochondrial cristae morphology. EMBO J **21:**221-230.
150. **Cogliati S, Frezza C, Soriano ME, Varanita T, Quintana-Cabrera R, Corrado M, Cipolat S, Costa V, Casarin A, Gomes LC, Perales-Clemente E, Salviati L, Fernandez-Silva P, Enriquez JA, Scorrano L.** 2013. Mitochondrial cristae shape determines respiratory chain supercomplexes assembly and respiratory efficiency. Cell **155:**160-171.

151. **Zhang M, Mileykovskaya E, Dowhan W.** 2002. Gluing the respiratory chain together. Cardiolipin is required for supercomplex formation in the inner mitochondrial membrane. J Biol Chem **277:**43553-43556.
152. **Zhang M, Mileykovskaya E, Dowhan W.** 2005. Cardiolipin is essential for organization of complexes III and IV into a supercomplex in intact yeast mitochondria. J Biol Chem **280:**29403-29408.
153. **Pfeiffer K, Gohil V, Stuart RA, Hunte C, Brandt U, Greenberg ML, Schagger H.** 2003. Cardiolipin stabilizes respiratory chain supercomplexes. J Biol Chem **278:**52873-52880.
154. **Wenz T, Hielscher R, Hellwig P, Schagger H, Richers S, Hunte C.** 2009. Role of phospholipids in respiratory cytochrome bc(1) complex catalysis and supercomplex formation. Biochim Biophys Acta **1787:**609-616.
155. **Bazan S, Mileykovskaya E, Mallampalli VK, Heacock P, Sparagna GC, Dowhan W.** 2013. Cardiolipin-dependent reconstitution of respiratory supercomplexes from purified Saccharomyces cerevisiae complexes III and IV. J Biol Chem **288:**401-411.
156. **Hoffmann B, Stockl A, Schlame M, Beyer K, Klingenberg M.** 1994. The reconstituted ADP/ATP carrier activity has an absolute requirement for cardiolipin as shown in cysteine mutants. J Biol Chem **269:**1940-1944.
157. **Epand RF, Schlattner U, Wallimann T, Lacombe ML, Epand RM.** 2007. Novel lipid transfer property of two mitochondrial proteins that bridge the inner and outer membranes. Biophys J **92:**126-137.
158. **Epand RF, Tokarska-Schlattner M, Schlattner U, Wallimann T, Epand RM.** 2007. Cardiolipin clusters and membrane domain formation induced by mitochondrial proteins. J Mol Biol **365:**968-980.
159. **Haines TH, Dencher NA.** 2002. Cardiolipin: a proton trap for oxidative phosphorylation. FEBS Lett **528:**35-39.
160. **Ha EE, Frohman MA.** 2014. Regulation of mitochondrial morphology by lipids. Biofactors **40:**419-424.
161. **DeVay RM, Dominguez-Ramirez L, Lackner LL, Hoppins S, Stahlberg H, Nunnari J.** 2009. Coassembly of Mgm1 isoforms requires cardiolipin and mediates mitochondrial inner membrane fusion. J Cell Biol **186:**793-803.
162. **Joshi AS, Thompson MN, Fei N, Huttemann M, Greenberg ML.** 2012. Cardiolipin and mitochondrial phosphatidylethanolamine have overlapping functions in mitochondrial fusion in Saccharomyces cerevisiae. J Biol Chem **287:**17589-17597.
163. **Montessuit S, Somasekharan SP, Terrones O, Lucken-Ardjomande S, Herzig S, Schwarzenbacher R, Manstein DJ, Bossy-Wetzel E, Basanez G, Meda P, Martinou JC.** 2010. Membrane remodeling induced by the dynamin-related protein Drp1 stimulates Bax oligomerization. Cell **142:**889-901.
164. **Smirnova E, Griparic L, Shurland DL, van der Bliek AM.** 2001. Dynamin-related protein Drp1 is required for mitochondrial division in mammalian cells. Mol Biol Cell **12:**2245-2256.
165. **Bustillo-Zabalbeitia I, Montessuit S, Raemy E, Basanez G, Terrones O, Martinou JC.** 2014. Specific interaction with cardiolipin triggers functional activation of Dynamin-Related Protein 1. PLoS One **9:**e102738.
166. **Nakamura K, Nemani VM, Azarbal F, Skibinski G, Levy JM, Egami K, Munishkina L, Zhang J, Gardner B, Wakabayashi J, Sesaki H, Cheng Y,**

Finkbeiner S, Nussbaum RL, Masliah E, Edwards RH. 2011. Direct membrane association drives mitochondrial fission by the Parkinson disease-associated protein alpha-synuclein. J Biol Chem **286:**20710-20726.

167. **Ellis CE, Murphy EJ, Mitchell DC, Golovko MY, Scaglia F, Barcelo-Coblijn GC, Nussbaum RL.** 2005. Mitochondrial lipid abnormality and electron transport chain impairment in mice lacking alpha-synuclein. Mol Cell Biol **25:**10190-10201.
168. **Ott M, Robertson JD, Gogvadze V, Zhivotovsky B, Orrenius S.** 2002. Cytochrome c release from mitochondria proceeds by a two-step process. Proc Natl Acad Sci U S A **99:**1259-1263.
169. **Zamzami N, Marchetti P, Castedo M, Decaudin D, Macho A, Hirsch T, Susin SA, Petit PX, Mignotte B, Kroemer G.** 1995. Sequential reduction of mitochondrial transmembrane potential and generation of reactive oxygen species in early programmed cell death. J Exp Med **182:**367-377.
170. **Petrosillo G, Ruggiero FM, Pistolese M, Paradies G.** 2001. Reactive oxygen species generated from the mitochondrial electron transport chain induce cytochrome c dissociation from beef-heart submitochondrial particles via cardiolipin peroxidation. Possible role in the apoptosis. FEBS Lett **509:**435-438.
171. **Kagan VE, Tyurin VA, Jiang J, Tyurina YY, Ritov VB, Amoscato AA, Osipov AN, Belikova NA, Kapralov AA, Kini V, Vlasova, II, Zhao Q, Zou M, Di P, Svistunenko DA, Kurnikov IV, Borisenko GG.** 2005. Cytochrome c acts as a cardiolipin oxygenase required for release of proapoptotic factors. Nat Chem Biol **1:**223-232.
172. **Choi SY, Gonzalvez F, Jenkins GM, Slomianny C, Chretien D, Arnoult D, Petit PX, Frohman MA.** 2007. Cardiolipin deficiency releases cytochrome c from the inner mitochondrial membrane and accelerates stimuli-elicited apoptosis. Cell Death Differ **14:**597-606.
173. **Gonzalvez F, Schug ZT, Houtkooper RH, MacKenzie ED, Brooks DG, Wanders RJ, Petit PX, Vaz FM, Gottlieb E.** 2008. Cardiolipin provides an essential activating platform for caspase-8 on mitochondria. J Cell Biol **183:**681-696.
174. **Garcia Fernandez M, Troiano L, Moretti L, Nasi M, Pinti M, Salvioli S, Dobrucki J, Cossarizza A.** 2002. Early changes in intramitochondrial cardiolipin distribution during apoptosis. Cell Growth Differ **13:**449-455.
175. **Schlattner U, Tokarska-Schlattner M, Ramirez S, Bruckner A, Kay L, Polge C, Epand RF, Lee RM, Lacombe ML, Epand RM.** 2009. Mitochondrial kinases and their molecular interaction with cardiolipin. Biochim Biophys Acta **1788:**2032-2047.
176. **Liu J, Dai Q, Chen J, Durrant D, Freeman A, Liu T, Grossman D, Lee RM.** 2003. Phospholipid scramblase 3 controls mitochondrial structure, function, and apoptotic response. Mol Cancer Res **1:**892-902.
177. **Ndebele K, Gona P, Jin TG, Benhaga N, Chalah A, Degli-Esposti M, Khosravi-Far R.** 2008. Tumor necrosis factor (TNF)-related apoptosis-inducing ligand (TRAIL) induced mitochondrial pathway to apoptosis and caspase activation is potentiated by phospholipid scramblase-3. Apoptosis **13:**845-856.
178. **Imai H, Koumura T, Nakajima R, Nomura K, Nakagawa Y.** 2003. Protection from inactivation of the adenine nucleotide translocator during hypoglycaemia-induced apoptosis by mitochondrial phospholipid hydroperoxide glutathione peroxidase. Biochem J **371:**799-809.

179. **Paradies G, Petrosillo G, Paradies V, Ruggiero FM.** 2010. Oxidative stress, mitochondrial bioenergetics, and cardiolipin in aging. Free Radic Biol Med **48:**1286-1295.
180. **Petrosillo G, Casanova G, Matera M, Ruggiero FM, Paradies G.** 2006. Interaction of peroxidized cardiolipin with rat-heart mitochondrial membranes: induction of permeability transition and cytochrome c release. FEBS Lett **580:**6311-6316.
181. **Petrosillo G, Matera M, Moro N, Ruggiero FM, Paradies G.** 2009. Mitochondrial complex I dysfunction in rat heart with aging: critical role of reactive oxygen species and cardiolipin. Free Radic Biol Med **46:**88-94.
182. **Scorrano L, Ashiya M, Buttle K, Weiler S, Oakes Sa, Mannella Ca, Korsmeyer SJ.** 2002. A distinct pathway remodels mitochondrial cristae and mobilizes cytochrome c during apoptosis. Developmental cell **2:**55-67.
183. **Kroemer G, Reed JC.** 2000. Mitochondrial control of cell death. Nat Med **6:**513-519.
184. **Lutter M, Perkins GA, Wang X.** 2001. The pro-apoptotic Bcl-2 family member tBid localizes to mitochondrial contact sites. BMC Cell Biol **2:**22.
185. **Esposti MD, Cristea IM, Gaskell SJ, Nakao Y, Dive C.** 2003. Proapoptotic Bid binds to monolysocardiolipin, a new molecular connection between mitochondrial membranes and cell death. Cell Death Differ **10:**1300-1309.
186. **Liu J, Durrant D, Yang HS, He Y, Whitby FG, Myszka DG, Lee RM.** 2005. The interaction between tBid and cardiolipin or monolysocardiolipin. Biochem Biophys Res Commun **330:**865-870.
187. **Kim TH, Zhao Y, Ding WX, Shin JN, He X, Seo YW, Chen J, Rabinowich H, Amoscato AA, Yin XM.** 2004. Bid-cardiolipin interaction at mitochondrial contact site contributes to mitochondrial cristae reorganization and cytochrome C release. Mol Biol Cell **15:**3061-3072.
188. **Schafer B, Quispe J, Choudhary V, Chipuk JE, Ajero TG, Du H, Schneiter R, Kuwana T.** 2009. Mitochondrial outer membrane proteins assist Bid in Bax-mediated lipidic pore formation. Mol Biol Cell **20:**2276-2285.
189. **Schug ZT, Gonzalvez F, Houtkooper RH, Vaz FM, Gottlieb E.** 2011. BID is cleaved by caspase-8 within a native complex on the mitochondrial membrane. Cell Death Differ **18:**538-548.
190. **Esposti MD, Erler JT, Hickman JA, Dive C.** 2001. Bid, a widely expressed proapoptotic protein of the Bcl-2 family, displays lipid transfer activity. Mol Cell Biol **21:**7268-7276.
191. **Sorice M, Circella A, Cristea IM, Garofalo T, Di Renzo L, Alessandri C, Valesini G, Esposti MD.** 2004. Cardiolipin and its metabolites move from mitochondria to other cellular membranes during death receptor-mediated apoptosis. Cell Death Differ **11:**1133-1145.
192. **Lucken-Ardjomande S, Montessuit S, Martinou JC.** 2008. Contributions to Bax insertion and oligomerization of lipids of the mitochondrial outer membrane. Cell Death Differ **15:**929-937.
193. **Goping IS, Gross A, Lavoie JN, Nguyen M, Jemmerson R, Roth K, Korsmeyer SJ, Shore GC.** 1998. Regulated targeting of BAX to mitochondria. J Cell Biol **143:**207-215.
194. **Cartron PF, Priault M, Oliver L, Meflah K, Manon S, Vallette FM.** 2003. The N-terminal end of Bax contains a mitochondrial-targeting signal. J Biol Chem **278:**11633-11641.

195. **Sani MA, Dufourc EJ, Grobner G.** 2009. How does the Bax-alpha1 targeting sequence interact with mitochondrial membranes? The role of cardiolipin. Biochim Biophys Acta **1788:**623-631.
196. **Iverson SL, Enoksson M, Gogvadze V, Ott M, Orrenius S.** 2004. Cardiolipin is not required for Bax-mediated cytochrome c release from yeast mitochondria. J Biol Chem **279:**1100-1107.
197. **Polcic P, Su X, Fowlkes J, Blachly-Dyson E, Dowhan W, Forte M.** 2005. Cardiolipin and phosphatidylglycerol are not required for the in vivo action of Bcl-2 family proteins. Cell Death Differ **12:**310-312.
198. **Ott M, Zhivotovsky B, Orrenius S.** 2007. Role of cardiolipin in cytochrome c release from mitochondria. Cell Death Differ **14:**1243-1247.
199. **Shamas-Din A, Satsoura D, Khan O, Zhu W, Leber B, Fradin C, Andrews DW.** 2014. Multiple partners can kiss-and-run: Bax transfers between multiple membranes and permeabilizes those primed by tBid. Cell Death Dis **5:**e1277.
200. **Epand RF, Martinou JC, Fornallaz-Mulhauser M, Hughes DW, Epand RM.** 2002. The apoptotic protein tBid promotes leakage by altering membrane curvature. J Biol Chem **277:**32632-32639.
201. **Nicolay K, van der Neut R, Fok JJ, de Kruijff B.** 1985. Effects of adriamycin on lipid polymorphism in cardiolipin-containing model and mitochondrial membranes. Biochim Biophys Acta **819:**55-65.
202. **Cullis PR, de Kruijff B, Hope MJ, Nayar R, Rietveld A, Verkleij AJ.** 1980. Structural properties of phospholipids in the rat liver inner mitochondrial membrane. Biochim Biophys Acta **600:**625-635.
203. **Brustovetsky T, Antonsson B, Jemmerson R, Dubinsky JM, Brustovetsky N.** 2005. Activation of calcium-independent phospholipase A (iPLA) in brain mitochondria and release of apoptogenic factors by BAX and truncated BID. J Neurochem **94:**980-994.
204. **Karbowski M, Lee YJ, Gaume B, Jeong SY, Frank S, Nechushtan A, Santel A, Fuller M, Smith CL, Youle RJ.** 2002. Spatial and temporal association of Bax with mitochondrial fission sites, Drp1, and Mfn2 during apoptosis. J Cell Biol **159:**931-938.
205. **Stanley WC, Chandler MP.** 2002. Energy metabolism in the normal and failing heart: potential for therapeutic interventions. Heart Fail Rev **7:**115-130.
206. **Lesnefsky EJ, Moghaddas S, Tandler B, Kerner J, Hoppel CL.** 2001. Mitochondrial dysfunction in cardiac disease: ischemia--reperfusion, aging, and heart failure. J Mol Cell Cardiol **33:**1065-1089.
207. **Lesnefsky EJ, Gudz TI, Moghaddas S, Migita CT, Ikeda-Saito M, Turkaly PJ, Hoppel CL.** 2001. Aging decreases electron transport complex III activity in heart interfibrillar mitochondria by alteration of the cytochrome c binding site. J Mol Cell Cardiol **33:**37-47.
208. **Fannin SW, Lesnefsky EJ, Slabe TJ, Hassan MO, Hoppel CL.** 1999. Aging selectively decreases oxidative capacity in rat heart interfibrillar mitochondria. Arch Biochem Biophys **372:**399-407.
209. **Huss JM, Kelly DP.** 2005. Mitochondrial energy metabolism in heart failure: a question of balance. J Clin Invest **115:**547-555.
210. **Fiedler LR, Maifoshie E, Schneider MD.** 2014. Mouse models of heart failure: cell signaling and cell survival. Curr Top Dev Biol **109:**171-247.

211. **Chen M, Won DJ, Krajewski S, Gottlieb RA.** 2002. Calpain and mitochondria in ischemia/reperfusion injury. J Biol Chem **277:**29181-29186.
212. **Scarabelli TM, Stephanou A, Pasini E, Comini L, Raddino R, Knight RA, Latchman DS.** 2002. Different signaling pathways induce apoptosis in endothelial cells and cardiac myocytes during ischemia/reperfusion injury. Circ Res **90:**745-748.
213. **Wang X, Bathina M, Lynch J, Koss B, Calabrese C, Frase S, Schuetz JD, Rehg JE, Opferman JT.** 2013. Deletion of MCL-1 causes lethal cardiac failure and mitochondrial dysfunction. Genes Dev **27:**1351-1364.
214. **Gustafsson AB, Gottlieb RA.** 2007. Bcl-2 family members and apoptosis, taken to heart. Am J Physiol Cell Physiol **292:**C45-51.
215. **Baldi A, Abbate A, Bussani R, Patti G, Melfi R, Angelini A, Dobrina A, Rossiello R, Silvestri F, Baldi F, Di Sciascio G.** 2002. Apoptosis and post-infarction left ventricular remodeling. J Mol Cell Cardiol **34:**165-174.
216. **Di Napoli P, Taccardi AA, Grilli A, Felaco M, Balbone A, Angelucci D, Gallina S, Calafiore AM, De Caterina R, Barsotti A.** 2003. Left ventricular wall stress as a direct correlate of cardiomyocyte apoptosis in patients with severe dilated cardiomyopathy. Am Heart J **146:**1105-1111.
217. **Latif N, Khan MA, Birks E, O'Farrell A, Westbrook J, Dunn MJ, Yacoub MH.** 2000. Upregulation of the Bcl-2 family of proteins in end stage heart failure. J Am Coll Cardiol **35:**1769-1777.
218. **Brocheriou V, Hagege AA, Oubenaissa A, Lambert M, Mallet VO, Duriez M, Wassef M, Kahn A, Menasche P, Gilgenkrantz H.** 2000. Cardiac functional improvement by a human Bcl-2 transgene in a mouse model of ischemia/reperfusion injury. J Gene Med **2:**326-333.
219. **Chen Z, Chua CC, Ho YS, Hamdy RC, Chua BH.** 2001. Overexpression of Bcl-2 attenuates apoptosis and protects against myocardial I/R injury in transgenic mice. Am J Physiol Heart Circ Physiol **280:**H2313-2320.
220. **Imahashi K, Schneider MD, Steenbergen C, Murphy E.** 2004. Transgenic expression of Bcl-2 modulates energy metabolism, prevents cytosolic acidification during ischemia, and reduces ischemia/reperfusion injury. Circ Res **95:**734-741.
221. **Huang J, Ito Y, Morikawa M, Uchida H, Kobune M, Sasaki K, Abe T, Hamada H.** 2003. Bcl-xL gene transfer protects the heart against ischemia/reperfusion injury. Biochem Biophys Res Commun **311:**64-70.
222. **Murriel CL, Churchill E, Inagaki K, Szweda LI, Mochly-Rosen D.** 2004. Protein kinase Cdelta activation induces apoptosis in response to cardiac ischemia and reperfusion damage: a mechanism involving BAD and the mitochondria. J Biol Chem **279:**47985-47991.
223. **Graham RM, Frazier DP, Thompson JW, Haliko S, Li H, Wasserlauf BJ, Spiga MG, Bishopric NH, Webster KA.** 2004. A unique pathway of cardiac myocyte death caused by hypoxia-acidosis. J Exp Biol **207:**3189-3200.
224. **Hamacher-Brady A, Brady NR, Logue SE, Sayen MR, Jinno M, Kirshenbaum LA, Gottlieb RA, Gustafsson AB.** 2007. Response to myocardial ischemia/reperfusion injury involves Bnip3 and autophagy. Cell Death Differ **14:**146-157.
225. **Regula KM, Ens K, Kirshenbaum LA.** 2002. Inducible expression of BNIP3 provokes mitochondrial defects and hypoxia-mediated cell death of ventricular myocytes. Circ Res **91:**226-231.

226. **Yussman MG, Toyokawa T, Odley A, Lynch RA, Wu G, Colbert MC, Aronow BJ, Lorenz JN, Dorn GW, 2nd.** 2002. Mitochondrial death protein Nix is induced in cardiac hypertrophy and triggers apoptotic cardiomyopathy. Nat Med **8:**725-730.
227. **Toth A, Jeffers JR, Nickson P, Min JY, Morgan JP, Zambetti GP, Erhardt P.** 2006. Targeted deletion of Puma attenuates cardiomyocyte death and improves cardiac function during ischemia-reperfusion. Am J Physiol Heart Circ Physiol **291:**H52-60.
228. **Condorelli G, Morisco C, Stassi G, Notte A, Farina F, Sgaramella G, de Rienzo A, Roncarati R, Trimarco B, Lembo G.** 1999. Increased cardiomyocyte apoptosis and changes in proapoptotic and antiapoptotic genes bax and bcl-2 during left ventricular adaptations to chronic pressure overload in the rat. Circulation **99:**3071-3078.
229. **Jung F, Weiland U, Johns RA, Ihling C, Dimmeler S.** 2001. Chronic hypoxia induces apoptosis in cardiac myocytes: a possible role for Bcl-2-like proteins. Biochem Biophys Res Commun **286:**419-425.
230. **Kirshenbaum LA, de Moissac D.** 1997. The bcl-2 gene product prevents programmed cell death of ventricular myocytes. Circulation **96:**1580-1585.
231. **Kang PM, Haunstetter A, Aoki H, Usheva A, Izumo S.** 2000. Morphological and molecular characterization of adult cardiomyocyte apoptosis during hypoxia and reoxygenation. Circ Res **87:**118-125.
232. **Zhu L, Yu Y, Chua BH, Ho YS, Kuo TH.** 2001. Regulation of sodium-calcium exchange and mitochondrial energetics by Bcl-2 in the heart of transgenic mice. J Mol Cell Cardiol **33:**2135-2144.
233. **Barth PG, Valianpour F, Bowen VM, Lam J, Duran M, Vaz FM, Wanders RJ.** 2004. X-linked cardioskeletal myopathy and neutropenia (Barth syndrome): an update. Am J Med Genet A **126A:**349-354.
234. **Sparagna GC, Chicco AJ, Murphy RC, Bristow MR, Johnson CA, Rees ML, Maxey ML, McCune SA, Moore RL.** 2007. Loss of cardiac tetralinoleoyl cardiolipin in human and experimental heart failure. J Lipid Res **48:**1559-1570.
235. **O'Rourke B, Reibel DK.** 1992. Effects of adrenoceptor blockade on cardiac hypertrophy and myocardial phospholipids. Proc Soc Exp Biol Med **200:**95-100.
236. **Reibel DK, O'Rourke B, Foster KA, Hutchinson H, Uboh CE, Kent RL.** 1986. Altered phospholipid metabolism in pressure-overload hypertrophied hearts. Am J Physiol **250:**H1-6.
237. **Okumura K, Yamada Y, Kondo J, Hashimoto H, Ito T, Kitoh J.** 1991. Decreased 1,2-diacylglycerol levels in myopathic hamster hearts during the development of heart failure. J Mol Cell Cardiol **23:**409-416.
238. **Heerdt PM, Schlame M, Jehle R, Barbone A, Burkhoff D, Blanck TJ.** 2002. Disease-specific remodeling of cardiac mitochondria after a left ventricular assist device. Ann Thorac Surg **73:**1216-1221.
239. **Ciccia A, Elledge SJ.** 2010. The DNA damage response: making it safe to play with knives. Mol Cell **40:**179-204.
240. **McGivern DR, Lemon SM.** 2011. Virus-specific mechanisms of carcinogenesis in hepatitis C virus associated liver cancer. Oncogene **30:**1969-1983.
241. **Marechal A, Zou L.** 2013. DNA damage sensing by the ATM and ATR kinases. Cold Spring Harb Perspect Biol **5**.
242. **Bakkenist CJ, Kastan MB.** 2003. DNA damage activates ATM through intermolecular autophosphorylation and dimer dissociation. Nature **421:**499-506.

243. **Lee JH, Paull TT.** 2005. ATM activation by DNA double-strand breaks through the Mre11-Rad50-Nbs1 complex. Science **308:**551-554.
244. **Cremona CA, Behrens A.** 2014. ATM signalling and cancer. Oncogene **33:**3351-3360.
245. **Reinhardt HC, Yaffe MB.** 2009. Kinases that control the cell cycle in response to DNA damage: Chk1, Chk2, and MK2. Curr Opin Cell Biol **21:**245-255.
246. **Nam EA, Cortez D.** 2011. ATR signalling: more than meeting at the fork. Biochem J **436:**527-536.
247. **Byun TS, Pacek M, Yee MC, Walter JC, Cimprich KA.** 2005. Functional uncoupling of MCM helicase and DNA polymerase activities activates the ATR-dependent checkpoint. Genes Dev **19:**1040-1052.
248. **Cimprich KA, Cortez D.** 2008. ATR: an essential regulator of genome integrity. Nat Rev Mol Cell Biol **9:**616-627.
249. **Ward IM, Chen J.** 2001. Histone H2AX is phosphorylated in an ATR-dependent manner in response to replicational stress. J Biol Chem **276:**47759-47762.
250. **Yoo HY, Kumagai A, Shevchenko A, Shevchenko A, Dunphy WG.** 2007. Ataxia-telangiectasia mutated (ATM)-dependent activation of ATR occurs through phosphorylation of TopBP1 by ATM. J Biol Chem **282:**17501-17506.
251. **Yoo HY, Kumagai A, Shevchenko A, Shevchenko A, Dunphy WG.** 2009. The Mre11-Rad50-Nbs1 complex mediates activation of TopBP1 by ATM. Mol Biol Cell **20:**2351-2360.
252. **Shieh SY, Ahn J, Tamai K, Taya Y, Prives C.** 2000. The human homologs of checkpoint kinases Chk1 and Cds1 (Chk2) phosphorylate p53 at multiple DNA damage-inducible sites. Genes Dev **14:**289-300.
253. **Norbury CJ, Zhivotovsky B.** 2004. DNA damage-induced apoptosis. Oncogene **23:**2797-2808.
254. **Moll UM, Wolff S, Speidel D, Deppert W.** 2005. Transcription-independent pro-apoptotic functions of p53. Curr Opin Cell Biol **17:**631-636.
255. **Konishi A, Shimizu S, Hirota J, Takao T, Fan Y, Matsuoka Y, Zhang L, Yoneda Y, Fujii Y, Skoultchi AI, Tsujimoto Y.** 2003. Involvement of histone H1.2 in apoptosis induced by DNA double-strand breaks. Cell **114:**673-688.
256. **Guo Y, Srinivasula SM, Druilhe A, Fernandes-Alnemri T, Alnemri ES.** 2002. Caspase-2 induces apoptosis by releasing proapoptotic proteins from mitochondria. J Biol Chem **277:**13430-13437.
257. **Biswas S, Shi Q, Wernick A, Aiello A, Zinkel SS.** 2013. The loss of the BH3-only Bcl-2 family member Bid delays T-cell leukemogenesis in ATM-/- mice. Cell Death Differ **20:**869-877.
258. **Nakatani Y, Ogryzko V.** 2003. Immunoaffinity purification of mammalian protein complexes. Methods Enzymol **370:**430-444.
259. **Ridler TW, Calvard S.** 1978. Picture Thresholding Using an Iterative Selection Method. Ieee Transactions on Systems Man and Cybernetics **8:**630-632.
260. **Brookes PS, Shiva S, Patel RP, Darley-Usmar VM.** 2002. Measurement of mitochondrial respiratory thresholds and the control of respiration by nitric oxide. Methods Enzymol **359:**305-319.
261. **Pallotti F, Lenaz G.** 2007. Isolation and subfractionation of mitochondria from animal cells and tissue culture lines. Methods Cell Biol **80:**3-44.

262. **Veksler VI, Kuznetsov AV, Sharov VG, Kapelko VI, Saks VA.** 1987. Mitochondrial respiratory parameters in cardiac tissue: a novel method of assessment by using saponin-skinned fibers. Biochim Biophys Acta **892:**191-196.
263. **Yin H, Vergeade A, Shi Q, Zackert WE, Gruenberg KC, Bokiej M, Amin T, Ying W, Masterson TS, Zinkel SS, Oates JA, Boutaud O, Roberts LJ, 2nd.** 2012. Acetaminophen inhibits cytochrome c redox cycling induced lipid peroxidation. Biochem Biophys Res Commun **423:**224-228.
264. **Gundersen HJ, Jensen EB.** 1987. The efficiency of systematic sampling in stereology and its prediction. J Microsc **147:**229-263.
265. **Roden DM, Pulley JM, Basford MA, Bernard GR, Clayton EW, Balser JR, Masys DR.** 2008. Development of a large-scale de-identified DNA biobank to enable personalized medicine. Clin Pharmacol Ther **84:**362-369.
266. **Denny JC, Ritchie MD, Basford MA, Pulley JM, Bastarache L, Brown-Gentry K, Wang D, Masys DR, Roden DM, Crawford DC.** 2010. PheWAS: demonstrating the feasibility of a phenome-wide scan to discover gene-disease associations. Bioinformatics **26:**1205-1210.
267. **Denny JC, Bastarache L, Ritchie MD, Carroll RJ, Zink R, Mosley JD, Field JR, Pulley JM, Ramirez AH, Bowton E, Basford MA, Carrell DS, Peissig PL, Kho AN, Pacheco JA, Rasmussen LV, Crosslin DR, Crane PK, Pathak J, Bielinski SJ, Pendergrass SA, Xu H, Hindorff LA, Li R, Manolio TA, Chute CG, Chisholm RL, Larson EB, Jarvik GP, Brilliant MH, McCarty CA, Kullo IJ, Haines JL, Crawford DC, Masys DR, Roden DM.** 2013. Systematic comparison of phenome-wide association study of electronic medical record data and genome-wide association study data. Nat Biotechnol **31:**1102-1110.
268. **Moreland JL, Gramada A, Buzko OV, Zhang Q, Bourne PE.** 2005. The Molecular Biology Toolkit (MBT): a modular platform for developing molecular visualization applications. BMC Bioinformatics **6:**21.
269. **Mootha VK, Wei MC, Buttle KF, Scorrano L, Panoutsakopoulou V, Mannella CA, Korsmeyer SJ.** 2001. A reversible component of mitochondrial respiratory dysfunction in apoptosis can be rescued by exogenous cytochrome c. EMBO J **20:**661-671.
270. **Frezza C, Cipolat S, Martins de Brito O, Micaroni M, Beznoussenko GV, Rudka T, Bartoli D, Polishuck RS, Danial NN, De Strooper B, Scorrano L.** 2006. OPA1 controls apoptotic cristae remodeling independently from mitochondrial fusion. Cell **126:**177-189.
271. **Schlame M, Brody S, Hostetler KY.** 1993. Mitochondrial cardiolipin in diverse eukaryotes. Comparison of biosynthetic reactions and molecular acyl species. Eur J Biochem **212:**727-735.
272. **Gorski PA, Ceholski DK, Hajjar RJ.** 2015. Altered Myocardial Calcium Cycling and Energetics in Heart Failure-A Rational Approach for Disease Treatment. Cell Metab **21:**183-194.
273. **Mason EF, Rathmell JC.** 2011. Cell metabolism: an essential link between cell growth and apoptosis. Biochim Biophys Acta **1813:**645-654.
274. **Broughton SE, Dhagat U, Hercus TR, Nero TL, Grimbaldeston MA, Bonder CS, Lopez AF, Parker MW.** 2012. The GM-CSF/IL-3/IL-5 cytokine receptor family: from ligand recognition to initiation of signaling. Immunological reviews **250:**277-302.

275. **Gottlieb E, Armour SM, Thompson CB.** 2002. Mitochondrial respiratory control is lost during growth factor deprivation. Proc Natl Acad Sci U S A **99:**12801-12806.
276. **Khaled AR, Reynolds DA, Young HA, Thompson CB, Muegge K, Durum SK.** 2001. Interleukin-3 withdrawal induces an early increase in mitochondrial membrane potential unrelated to the Bcl-2 family. Roles of intracellular pH, ADP transport, and F(0)F(1)-ATPase. J Biol Chem **276:**6453-6462.
277. **Rosca MG, Vazquez EJ, Kerner J, Parland W, Chandler MP, Stanley W, Sabbah HN, Hoppel CL.** 2008. Cardiac mitochondria in heart failure: decrease in respirasomes and oxidative phosphorylation. Cardiovasc Res **80:**30-39.
278. **Shen W, Asai K, Uechi M, Mathier MA, Shannon RP, Vatner SF, Ingwall JS.** 1999. Progressive loss of myocardial ATP due to a loss of total purines during the development of heart failure in dogs: a compensatory role for the parallel loss of creatine. Circulation **100:**2113-2118.
279. **Ide T, Tsutsui H, Hayashidani S, Kang D, Suematsu N, Nakamura K, Utsumi H, Hamasaki N, Takeshita A.** 2001. Mitochondrial DNA damage and dysfunction associated with oxidative stress in failing hearts after myocardial infarction. Circ Res **88:**529-535.
280. **Eirin A, Lerman A, Lerman LO.** 2014. Mitochondrial injury and dysfunction in hypertension-induced cardiac damage. Eur Heart J **35:**3258-3266.
281. **Khiati S, Dalla Rosa I, Sourbier C, Ma X, Rao VA, Neckers LM, Zhang H, Pommier Y.** 2014. Mitochondrial topoisomerase I (top1mt) is a novel limiting factor of doxorubicin cardiotoxicity. Clin Cancer Res **20:**4873-4881.
282. **Hickey AJ, Chai CC, Choong SY, de Freitas Costa S, Skea GL, Phillips AR, Cooper GJ.** 2009. Impaired ATP turnover and ADP supply depress cardiac mitochondrial respiration and elevate superoxide in nonfailing spontaneously hypertensive rat hearts. Am J Physiol Cell Physiol **297:**C766-774.
283. **Oh KJ, Barbuto S, Meyer N, Kim RS, Collier RJ, Korsmeyer SJ.** 2005. Conformational changes in BID, a pro-apoptotic BCL-2 family member, upon membrane binding. A site-directed spin labeling study. J Biol Chem **280:**753-767.
284. **Schwarz K, Siddiqi N, Singh S, Neil CJ, Dawson DK, Frenneaux MP.** 2014. The breathing heart - mitochondrial respiratory chain dysfunction in cardiac disease. Int J Cardiol **171:**134-143.
285. **Andersen JL, Kornbluth S.** 2013. The tangled circuitry of metabolism and apoptosis. Mol Cell **49:**399-410.
286. **Gilkerson RW, Selker JM, Capaldi RA.** 2003. The cristal membrane of mitochondria is the principal site of oxidative phosphorylation. FEBS Lett **546:**355-358.
287. **Chaban Y, Boekema EJ, Dudkina NV.** 2014. Structures of mitochondrial oxidative phosphorylation supercomplexes and mechanisms for their stabilisation. Biochim Biophys Acta **1837:**418-426.
288. **Robinson NC.** 1982. Specificity and binding affinity of phospholipids to the high-affinity cardiolipin sites of beef heart cytochrome c oxidase. Biochemistry **21:**184-188.
289. **Gomez B, Jr., Robinson NC.** 1999. Phospholipase digestion of bound cardiolipin reversibly inactivates bovine cytochrome bc1. Biochemistry **38:**9031-9038.
290. **Fry M, Green DE.** 1981. Cardiolipin requirement for electron transfer in complex I and III of the mitochondrial respiratory chain. J Biol Chem **256:**1874-1880.

291. **Beyer K, Klingenberg M.** 1985. ADP/ATP carrier protein from beef heart mitochondria has high amounts of tightly bound cardiolipin, as revealed by 31P nuclear magnetic resonance. Biochemistry **24:**3821-3826.
292. **Nicholls P.** 1974. Cytochrome c binding to enzymes and membranes. Biochim Biophys Acta **346:**261-310.
293. **Stanley WC, Recchia FA, Lopaschuk GD.** 2005. Myocardial substrate metabolism in the normal and failing heart. Physiol Rev **85:**1093-1129.
294. **Jamil S, Mojtabavi S, Hojabrpour P, Cheah S, Duronio V.** 2008. An essential role for MCL-1 in ATR-mediated CHK1 phosphorylation. Mol Biol Cell **19:**3212-3220.
295. **Jamil S, Stoica C, Hackett TL, Duronio V.** 2010. MCL-1 localizes to sites of DNA damage and regulates DNA damage response. Cell Cycle **9:**2843-2855.
296. **Zeman MK, Cimprich KA.** 2014. Causes and consequences of replication stress. Nat Cell Biol **16:**2-9.
297. **Oberkovitz G, Regev L, Gross A.** 2007. Nucleocytoplasmic shuttling of BID is involved in regulating its activities in the DNA-damage response. Cell Death Differ **14:**1628-1634.
298. **Kudo N, Wolff B, Sekimoto T, Schreiner EP, Yoneda Y, Yanagida M, Horinouchi S, Yoshida M.** 1998. Leptomycin B inhibition of signal-mediated nuclear export by direct binding to CRM1. Exp Cell Res **242:**540-547.
299. **Sachdev S, Hannink M.** 1998. Loss of IkappaB alpha-mediated control over nuclear import and DNA binding enables oncogenic activation of c-Rel. Mol Cell Biol **18:**5445-5456.
300. **la Cour T, Kiemer L, Molgaard A, Gupta R, Skriver K, Brunak S.** 2004. Analysis and prediction of leucine-rich nuclear export signals. Protein Eng Des Sel **17:**527-536.
301. **McCann TS, Tansey WP.** 2014. Functions of the proteasome on chromatin. Biomolecules **4:**1026-1044.
302. **Cullis PR, de Kruijff B.** 1979. Lipid polymorphism and the functional roles of lipids in biological membranes. Biochim Biophys Acta **559:**399-420.
303. **Ban T, Heymann JA, Song Z, Hinshaw JE, Chan DC.** 2010. OPA1 disease alleles causing dominant optic atrophy have defects in cardiolipin-stimulated GTP hydrolysis and membrane tubulation. Hum Mol Genet **19:**2113-2122.
304. **Schlame M, Haldar D.** 1993. Cardiolipin is synthesized on the matrix side of the inner membrane in rat liver mitochondria. J Biol Chem **268:**74-79.
305. **Kochanek KD, Murphy SL, Xu J.** 2015. Deaths: Final Data for 2011. Natl Vital Stat Rep **63:**1-120.
306. **Braunwald E.** 1971. Control of myocardial oxygen consumption: physiologic and clinical considerations. Am J Cardiol **27:**416-432.
307. **Wente SR, Rout MP.** 2010. The nuclear pore complex and nuclear transport. Cold Spring Harb Perspect Biol **2:**a000562.
308. **Yang ES, Xia F.** 2010. BRCA1 16 years later: DNA damage-induced BRCA1 shuttling. FEBS J **277:**3079-3085.
309. **Nguyen KT, Holloway MP, Altura RA.** 2012. The CRM1 nuclear export protein in normal development and disease. Int J Biochem Mol Biol **3:**137-151.
310. **Claypool SM, Koehler CM.** 2012. The complexity of cardiolipin in health and disease. Trends Biochem Sci **37:**32-41.

311. **Genova ML, Lenaz G.** 2014. Functional role of mitochondrial respiratory supercomplexes. Biochim Biophys Acta **1837:**427-443.
312. **Acin-Perez R, Enriquez JA.** 2014. The function of the respiratory supercomplexes: the plasticity model. Biochim Biophys Acta **1837:**444-450.
313. **Mannella CA.** 2008. Structural diversity of mitochondria: functional implications. Ann N Y Acad Sci **1147:**171-179.
314. **Mannella CA, Lederer WJ, Jafri MS.** 2013. The connection between inner membrane topology and mitochondrial function. J Mol Cell Cardiol **62:**51-57.
315. **Pieczenik SR, Neustadt J.** 2007. Mitochondrial dysfunction and molecular pathways of disease. Exp Mol Pathol **83:**84-92.